2007

Modulation of adult neural plasticity by proteolytic catabolism of lecticans

Joanne Mayer
University of South Florida

Modulation of Adult Neural Plasticity by Proteolytic Catabolism of Lecticans

by

Joanne Mayer

A dissertation in partial fulfillment
of the requirements for the degree of
Doctor of Philosophy
Department of Molecular Pharmacology & Physiology
College of Medicine
University of South Florida

Major Professor: Paul E. Gottschall, Ph.D.
John R. Hassell, Ph.D.
Dave G. Morgan, Ph.D.
Keith R. Pennypacker, Ph.D.
Alison E. Willing, Ph.D.

Date of Approval:
March 30, 2007

Keywords: proteoglycan, brevican, plasticity, ADAMTS, extracellular matrix

Note to reader: The original of this document contains color that is necessary for understanding the data. The original dissertation is on file with the USF library in Tampa, Florida.

DEDICATION

This dissertation is dedicated to the late Henry W. Mayer, who always wanted to see his little girl go to college.

ACKNOWLEDGEMENTS

Although this is an individual work, I could never have completed this endeavor without the help, support and guidance of many people. I would like to first and foremost thank my major professor, Dr. Paul Gottschall, for taking me into his laboratory and providing me with years of supplies, support and writing reviews along with my dissertation committee, who saw me through many meetings, seminars, project discussions and provided ideas and suggestions along the way. I could not have done this without the support of my family, my mother, Monika Mayer and my siblings, Luther C. James, Diane A. Remail and Laura R. Sosnowski and their loving families. I also thank my fiancé, Craig "Ted" Ajmo Jr. for always being there and his continued love and support. I also extend my gratitude to Dr. Pennypacker for the use of the Zeiss Axioscope, Drs. Morgan and Gordon for providing APPsw breeder mice, Dr. Carl Flannery from Wyeth-Ayerst for providing the human recombinant ADAMTS4, and Drs. Thirunavukkarasu from Eli Lilly Co., for making the ADAMTS1 knockout mice available to us. Autumn Eakin was instrumental in her help and involvement in these experiments, thank you. I would like to thank my colleagues and many lifetime friends I have made during my time here at USF for their unconditional friendship and support and finally, thank you to all of my professors and the office staff of the Department of Molecular Pharmacology & Physiology who have helped more than they realize.

TABLE OF CONTENTS

LIST OF TABLES iv

LIST OF FIGURES v

ABSTRACT viii

INTRODUCTION
- Proteoglycans 1
- Neural plasticity and CSPGs 3
- Distribution of brevican in the ECM 4
- The “substrate – protease pair” 6
- The entorhinal cortex, perforant pathway, and neural plasticity 9
- ECL model of neural plasticity 10
- Alzheimer’s disease & CSPGs 12
- The current study 13
- References 17

CHAPTER 1: Discordance in the localization of *wisteria floribunda* agglutinin and brevican immunoreactivity in the central nervous system of the rodent brain 23
- Abstract 24
- Introduction 25
- Materials & Methods 28
  - Animals 28
  - Western blotting 29
  - Isolation of membrane fractions 30
  - Immunohistochemistry 31
  - Cleavage of PGs with hRecADAMTS4 32
  - Microscopy and image acquisition 34
- Results 34
- Discussion 41
- References 66

CHAPTER 2: Evidence for proteolytic cleavage of brevican by the ADAMTSs in the dentate gyrus after excitotoxic lesion of the mouse entorhinal cortex 72
- Abstract 73

Introduction 74
Materials & Methods 77
Animals 77
Surgical procedures – the entorhinal cortex lesion (ECL) 78
Region isolation method 79
Immunohistochemistry 81
Western blotting 82
Antibody generation 82
Results 83
Expression of ADAMTS-derived, brevican fragment 83
Deafferentation and neural plasticity in the dentate gyrus 84
Abundance and proteolysis of brevican after ECL 86
Discussion 87
References 108

CHAPTER 3: Brevican processing and associated levels of synaptic markers in APPsw mice 113
Abstract 114
Introduction 115
Materials & Methods 117
Animals 117
Western blotting 117
Immunohistochemistry 118
ELISA 119
Antibody generation 121
Microscopy and image acquisition 121
Results 122
Discussion 126
References 141

CHAPTER 4: Characterization of lectican processing and synaptic markers in the brain of a mutant mouse deficient for the proteoglycanse, ADAMTS1 148
Abstract 149
Introduction 150
Materials & Methods 152
Animals 152
Surgical procedures – the entorhinal cortex lesion (ECL) 153
Tissue preparation 154
Western blotting 154
ELISA 155
Results 157
Discussion 160
References 178

CONCLUSIONS 175
References 192

ABOUT THE AUTHOR END PAGE

LIST OF TABLES

CHAPTER 1:

Table 1 Relative reactivity of *Wisteria floribunda* agglutinin (WFA), brevican, and the neoepitope of the ADAMTS-derived fragment of brevican, anti-EAVESE, in the adult rat. 62

Table 2 Relative reactivity of *Wisteria floribunda* agglutinin (WFA), brevican, and the neoepitope of the ADAMTS-derived fragment of brevican, anti-EAMESE, in the adult mouse. 64

CHAPTER 3:

Table 3 Relative immunoreactivity of brevican isoforms in brain regions of APPsw transgenic (+) mouse brain compared to littermate control (-). 136

CHAPTER 4:

Table 4 Relative immunoreactivity of brevican isoforms in brain regions of ADAMTS1 knockout (-/-) mouse brain compared to wild-type (+/+). 167

Table 5 Relative immunoreactivity of versican isoforms in brain regions of ADAMTS1 knockout (-/-) mouse brain compared to wild-type (+/+). 170

Table 6 Relative synaptophysin, SNAP-25 and PSD-95 levels as measured by ELISA in regions of ADAMTS1 knockout mice and (-/-) and wild-type (+/+) brain tissue. 171

CONCLUSIONS

Table 7 Summary of evidence found for models investigated, supporting proteolytic degradation of lecticans in ECM influence neural plasticity. 197

LIST OF FIGURES

INTRODUCTION

Figure 1 "HLT (hyaluronan, lectican, and tenascin) complex" in the extracellular matrix of the central nervous system 16

CHAPTER 1:

Figure 2 Schematic representation of brevican isoforms in brain ECM and their ADAMTS-derived proteolytic cleavage fragments. 47

Figure 3 Degradation assay of brevican by human recombinant ADAMTS4. 49

Figure 4 Western blot of brevican, EAV(M)ESE, and *Wisteria Floribunda* agglutinin (WFA) in rodent brain extracts before and after chondroitinase digestion. 51

Figure 5 Western blot of brevican, EAMESE, and *Wisteria floribunda* agglutinin (WFA) in extracts from various regions of mouse brain before and after chondroitinase digestion. 53

Figure 6 Binding of *Wisteria floribunda* agglutinin (WFA) lectin to fixed tissue sections of rodent brain: effect of chondroitinase ABC. 55

Figure 7 Localization of *Wisteria floribunda* agglutinin (WFA) and ADAMTS-derived fragment of brevican reactivity in rat and mouse brain. 57

Figure 8 Localization of WFA and the ADAMTS-derived fragment of brevican reactivity in perineuronal nets. 59

Figure 9 Localization of WFA and brevican reactivity in peri-neuronal nets. 61

CHAPTER 2:

Figure 10	Schematic representation of the micro-dissection of dentate gyrus and entorhinal cortex.	95
Figure 11	Schematic representation of brevican cleavage by the glutamyl-endopeptidases, the ADAMTSs.	97
Figure 12	Brevican and EAMESE Western blotting in regions of mouse brain.	99
Figure 13	Alterations in brevican levels in lesioned entorhinal cortex.	101
Figure 14	Denervation of the outer molecular layer of the dentate gyrus after entorhinal cortex lesion.	103
Figure 15	Brevican immunoreactivity in the dentate gyrus after entorhinal cortex lesion.	105
Figure 16	Apparent ADAMTS activity.	107

CHAPTER 3:

Figure 17	Detection of brevican isoforms and proteolytic degradation by endogenous proteases at specific cleavage sites.	133
Figure 18	Relative immunoreactivity of brevican isoforms in the hippocampus of APPsw transgenic mice compared to littermate non-transgenic mice.	135
Figure 19	Immunohistochemical localization of brevican, the proteolytically cleaved fragment of brevican and Aβ plaques in APPsw transgenic mice.	138
Figure 20	Synaptic markers as measured by ELISA in brain regions of APPsw and non-transgenic animals.	140

CHAPTER 4:

Figure 21	Brevican processing in the ADAMTS1 knockout compared to littermate control.	166

Figure 22 Versican processing in the ADAMTS1 knockout compared to littermate control. 169

Figure 23 Brevican immunoreactivity in the dentate gyrus of ADAMTS1 knockout and control animals after entorhinal cortex lesion. 173

Figure 24 Apparent ADAMTS activity seven and twenty-one days after ECL. 175

Figure 25 Synaptic marker levels as measured by ELISA seven and twenty-one days after ECL. 177

CONCLUSIONS

Figure 26 Summary schematic of the tertiary complex in the brain between a pre-synaptic neuron and a post-synaptic neuron (or glial cell) as it relates to the inhibition (-) of neural plasticity and the ability (+) to undergo neural plasticity. 196

Modulation of Adult Neural Plasticity by Proteolytic Catabolism of Lecticans

Joanne Mayer

ABSTRACT

The extracellular environment of the central nervous system (CNS) through which neuritic processes must traverse during development or after injury is complex, and may vary from stabile conditions to a milieu favorable for neural plasticity and growth. The extracellular space in the CNS accounts for about 20% of brain volume and is composed of aggregating complexes of several different extracellular matrix (ECM) molecules. The ECM supports neural networks and acts as a barrier for neurite extention, depending on the type of molecules involved and the various signals they induce. One mechansim that may produce an environment favoring plasticity is the proteolytic cleavage of ECM. Brevican belongs to the lectican family of aggregating, chondroitin sulfate-containing proteoglycans (CSPGs) and is abundant in brain ECM complexes. It is localized peri-synaptically, inhibits neurite outgrowth, and is thought to stabilize synaptic networks in the adult. Interestingly, a significant proportion of brevican in the CNS is observed as a fragment of the protein core formed by proteolytic cleavage. Endogenous matrix-degrading proteinases, such as the MMPs (matrix metalloproteinases) and ADAMTS (a disintegrin and metalloproteinase with

thrombospondin motifs), cleave brevican and other lecticans potentially promoting neural plasticity. Cleavage of brevican and similar lectican family members may "loosen" the aggregated complexes and change the extracellular environment to one that is more permissive toward neural plasticity. After injury, during inflammation or with disease, alterations in the ECM may influence development and/or progression of neurological disease. The purpose of these studies was to investigate the catabolism of brevican in the ECM and its potential role in neural plasticity under each of these influences, taking an in depth look at how brevican is processed after (1) undergoing a classical model of neural plasticity, the entorhinal cortex lesion (ECL); (2) a disease state that is thought to have dysregulated neural and synaptic plasticity; and (3) how brevican catabolism and neural plasticity is effected by deleting the protease responsible for the cleavage of lecticans in a mouse model. Overall, these experiments provide evidence that the proteolytic cleavage of brevican, and lecticans in general, may play an important role in the regulation of neural plasticity.

INTRODUCTION

Extracellular matrix (ECM) that surrounds neurons has become recognized as increasingly important as a modulator of neural plasticity that occurs after injury, with inflammation, prior to the end of developmental critical periods, and with aging and disease. Interactions between neurons (or glia) and molecules in the extracellular milieu initiate signals to regulate neurite outgrowth, neural migration, synaptogenesis, axonal guidance, and topographical mapping during development, after which the CNS loses its ability to rearrange synaptic networks in the healthy adult. Although it is clear that soluble signals in the extracellular space can induce signaling in neurons, it is becoming increasingly evident that extracellular matrix macromolecules impinge on this signaling process (Bruckner et al., 2003). Proteoglycans are a main component of brain ECM and may be involved in the modulation of adult neural plasticity.

Proteoglycans

The ECM is an interlocking network of aggregating macromolecules that are secreted by individual cells and composes the extracellular space. ECM is important for nutrition, support, stability, serves as a medium for cell-to-cell communication, acts as a biochemical barrier, and may be important in the repositioning of neurite outgrowth and synaptogenesis during cell development,

neural plasticity, and wound repair. Varieties of proteins in the ECM contain high molecular weight sugars. Proteoglycans are glycoproteins that are heavily glycosylated and found throughout the ECM forming complexes with hyaluronan and other matrix proteins.

These molecules contain one or more negatively charged long, linear chains of repeating disaccharides called glycosaminoglycan (GAG) chains attached to the core protein of proteoglycans. These GAG chains are covalently attached to the core protein in the endoplasmic reticulum by adding the reducing end of xylose to the serine residue of the core protein (Grebner et al., 1966; Kjellen and Lindahl, 1991). Next, via a series of transferases, two galactose molecules are added and then a glucuronic acid is transferred by glucuronyl-transferase (Helting and Roden, 1969). This pattern of reactions is the general structure of linkage region in chondroitin sulfate that helps make up the GAG attachments to proteoglycans. For the production of chondroitin sulfate proteoglycans (CSPGs), the long GAG chains are formed by the addition of one monosaccharide at a time in the Golgi apparatus, producing repeating disaccharide chains of glucuronic acid and N-acetylgalactosamine. The highly negative charge found in CSPGs comes from the sulfate and uronic acid groups within the GAG chains. These CS-containing chains can be enzymatically removed via degradation by a bacterial enzyme from *proteus vulgaris*, which can cleave all three isomeric forms of chondroitin sulfate and is commercially available as Chondroitinase ABC. The chondroitin sulfate (CS) chain additions are thought to be the main inhibitory / stability component of proteoglycans in the

ECM and may play a major role in the permissibility of neural plasticity in the brain.

Neural plasticity and CSPGs

This research refers to neural plasticity as changes in neurite outgrowth, guidance and synapse formation that occur in response to injury. A more encompassing, broader definition is the growth and neuronal alterations which occur throughout brain development, in learning and memory, and with recovery from injury. Neurites must extend and synapses form in an extracellular milieu that consists of soluble molecules in addition to the ECM. Chondroitin sulfate (CS) containing proteoglycans (PGs) are abundant ECM molecules in the brain and are thought to confer diverse functions on neural plasticity (for review see (Viapiano and Matthews, 2006). CSPGs inhibit neural plasticity in various models and a number of mechanisms have been proposed to explain these effects, such as 1) an increase in intracellular calcium when neurons contact CS (Snow et al., 1994); 2) inhibition of neurite extension due to binding highly negatively charged GAG side chains (Dillon et al., 2000); and 3) an inhibition of proteolysis of local ECM molecules (Reeves et al., 2003).

The ECM undergoes cell-dependent remodeling during development and after injury by structural organization and reorganization (Lander, 1993; Deller et al., 2000; Thon et al., 2000). After injury, axonal processes must penetrate the altered extracellular environment to facilitate reinnervation. More specifically, after injury in the CNS, new axons and dendrites must traverse a stable,

inhibitory extracellular environment in order to repair damaged neural circuits. The glial scar is formed by the induction of reactive microglia and astrocytes at different times after injury, making it an “evolving structure” (Fawcett and Asher, 1999). The failure of injured axons to regenerate within the CNS may be attributed to the presence of the glial scar, particularly its makeup of growth inhibitory, astrocyte-derived CS-containing PGs (Reier and Houle, 1988; Maxwell et al., 1990; Properzi et al., 2003). The most active component within this “barrier” appears to be the CS side chain, which can block advancing axons (Snow et al., 1990; Oakley and Tosney, 1991; Brittis et al., 1992). The presence of CS chains has been reported to be responsible for the neurite growth inhibitory action in the ECM (Yamada et al., 1997) and these chains create a net-like complex that prevents neurite outgrowth and other plastic changes in this environment. One of the most abundant CS-containing PGs in the brain is brevican.

Distribution of brevican in the ECM

One CS-containing PG up regulated in areas of brain damage, as well as areas denervated by a lesion, is brevican. This up regulation suggests a prominent role in reactive gliosis and possibly neural plasticity. In fact, in the rat, brevican expression is markedly increased in astrocytes after entorhinal cortex lesion (Thon et al., 2000). Brevican is the most abundant CSPG in the brain and, along with aggrecan, versican, and neurocan, is a member of the lectican family of aggregating PGs. Lecticans are a family of CS-containing PGs, which bear a

hyaluronan-binding domain and a C-type lectin domain in their core proteins, which enable interactions with carbohydrate and protein ligands in the extracellular matrix and act as linkers of these ECM molecules. Brevican is one component of a complex of brain ECM that is found in perineuronal nets (PNNs) and throughout the neuropil (Celio and Blumcke, 1994; Cahal, 1995; Yamaguchi, 2002). PNNs and matrix complexes are thought to stabilize or maintain synapses in neural networks (Hockfield et al., 1990; Yamaguchi, 1996, 2000) in addition to inhibiting neural plasticity.

It is less likely that neuritic or synaptic remodeling would occur in regions with intact and abundant matrix complexes because of the inhibitory environment that these molecules produce. When the matrix is broken down and interactions between these complexed molecules are disrupted, the matrix becomes “loose” or unfastened and moveable, producing a favorable environment for cell migration, axonal growth and synaptogenesis. The core proteins of the lecticans in the ECM have a common domain structure. In each case the N-terminal globular region (G1) binds to hyaluronate in a ternary complex with core protein. The central domain of brevican is short relative to the lecticans but does contain two other serine residues that can be substituted with chondroitin sulfate. The C-terminal, G3 region, contains a domain region (the complement binding regulatory) that binds another ECM protein called tenascin-R. These three ECM components form an “HLT complex” (hyaluronan, lectican and tenascin) in the matrix and therefore form the lattice in which soluble molecules must diffuse (figure 1, A). Proteolytic cleavage of brevican’s core protein would therefore be

expected to disrupt this lattice and promote plasticity (figure 1, B). Versican is a large CS-containing member of the lectican family and has been shown to play a role in cell adhesion, migration, and proliferation. Versican has been implicated in inflammation (Wight and Merrilees, 2004; Toeda et al., 2005) and is highly expressed in tumors (Paulus et al., 1996; Zheng et al., 2004; Miquel-Serra et al., 2006). Like brevican, versican can also inhibit axonal growth following an injury in the CNS (Morgenstern et al., 2002). These lecticans can be catabolized by endogenous proteases within the ECM.

The "substrate – protease pair"

Brevican is selectively expressed in the CNS and localized peri-synaptically, where it surrounds, but is not on or over the active site of the synapse (Hagihara et al., 1999). The secreted form of brevican that bears chondroitin sulfate, likely attaches to the cell surface via ECM aggregates and has a molecular weight of more than 145 kD, depending upon the number and length of CS chains (brevican = up to 3). A significant amount of brevican does not bear CS chains and exists as the core protein alone (MW 145 kD). Most interesting is that a 55 kD form of brevican representing the G1 domain only, is as abundant in the normal brain as the intact forms. This fragment is generated by specific proteases that are secreted into the extracellular space of brain. These proteinases are members of the family of the matrix metalloproteinase (MMPs, specifically MMP-1, -2, -3, -7, -8, -10, -13) and a related family called the ADAMTSs (a disintegrin and metalloproteinase with thrombospondin motifs;

specifically ADAMTS-1, -4 -5 & -9) which can bind to matrix and are active in the brain, both of which are responsible for lectican catabolism in the brain.

The MMPs are a class of zinc-dependent proteases that have the capacity to cleave ECM proteins. They are secreted as zymogens that are inactive and the pro-peptide domain must be cleaved for activation to occur. They have three homologous domains that include the pro-peptide domain, the catalytic domain and a haemopexin-like C-terminal domain. The pro-peptide domain contains the "cysteine-switch" (Van Wart and Birkedal-Hansen, 1990) that interacts with a zinc in the active zone and initially prevents binding to and the proteolysis of a substrate in its inactive form. The activated MMPs have been implicated in many processes including development, cell proliferation, cell migration and adhesion, angiogenesis, apoptosis, wound healing, and tumor progression.

The ADAMTSs, rather than the MMPs, are thought to be the prominent proteases involved in the cleavage of lecticans, particularly brevican, and are a relatively new family of ECM-degrading, zinc-dependent, metalloproteinases. They consist of a pre-pro-protease domain that contains a signal peptide for secretion as well as a pro-domain, that must be cleaved for the molecule to become activated. In addition, there is catalytic domain, a disintegrin domain that may have some adhesion properties and, unlike MMPs, the TS type 1 motif, a cysteine-rich domain and a Spacer region – most of which show significant homology among the family members. There is variability in the number of thrombospondin motifs associated with each of the members of this family, and the thrombospondin domain is thought to be crucial for binding to the ECM prior

to proteolytic action (for review see: Adams and Tucker, 2000; Bornstein et al., 2004).

ADAMTS4 is highly expressed in brain and is synthesized as a latent pro-protease. In this conformation, an unpaired cysteine in the pro-domain binds to zinc in the catalytic site causing the enzyme to fold back upon itself. This structure maintains the protease in its inactive form. A variety of mechanisms including cleavage of the pro-domain by glycoylated protease furin activates the protease resulting in the 68 kD isoform of ADAMTS4, a form that is further processed by C-terminal truncations to 53kD and 40kD activated isoforms. The subgroup including ADAMTSs, -1, -4, -5, -8, -9 & -15 are also known as the aggrecanases due to their ability to cleave the major cartilage proteoglycan (& lectican) aggrecan. They have also been shown to cleave other lectican family members (e.g., brevican and versican).

ADAMTS4 (Tortorella et al., 1999) is synthesized as a latent 100kD protein that is intracellularly processed by pro-protease convertases such as furin and further C-terminally truncated (Gao et al., 2002; Kashiwagi et al., 2004) into 68kD, 53kD and 40kD fragments (Flannery et al., 2002). ADAMTS4 is secreted by astrocytes and neurons (Yuan et al., 2002) and the little data that is available suggests that, in vivo, ADAMTS-1 and –4 are most highly expressed of the four ADAMTSs found in brain (Nakamura et al., 2000). ADAMTSs cleave brevican and results in the appearance of the 55 kD N-terminal and 80 kD C- fragments. The ADAMTS-derived N-terminal fragment can be distinguished from other small fragments by its unique C-terminal neoepitope, EAMESE. Antiserum that

selectively recognizes the neoepitope (EAMESE) that is formed after ADAMTS activity can be used to detect brevican catabolism. Brevican cleavage can also be detected with antiserum that selectively recognizes the neoepitope (SAHPSA) that is formed after MMP cleavage.

The development of an ADAMTS1 knockout animal has helped in the understanding of its role in matrix modulation. The ADAMTS1 deficient mouse undergoes abnormal growth and development, as well as matrix irregularities in ovulation, urogenital function and angiogenesis (Kuno et al., 1997; Shindo et al., 2000). There is no current literature that examines the CNS of the ADAMTS1 null mouse. These findings here suggest that ADAMTS1 may play an important role in matrix maintenance and regulation in the brain as well. In this knockout animal, it appears that versican, rather than brevican, processing is hindered, suggesting a preference for ADAMTS1 to cleave versican, ultimately suggesting a "protease-substrate pair".

The entorhinal cortex, perforant pathway, and neural plasticity

The entorhinal cortex (EC) provides input from the cerebral cortex to the dentate gyrus, and indirectly, it is the main source of afferents to the hippocampal formation. The EC neurons are unique because they send unilateral axonal projections to the outer two-thirds of the molecular layer of the dentate gyrus (Scheff, 1989) where they synapse on granule cell dendrites. The lateral EC neurons innervate the septal portion of the hippocampus, whereas medial EC neurons project to the temporal region of the dentate gyrus. This is the initial

synapse of a tri-synaptic pathway called the perforant path which begins with EC projection to the dentate gyrus – through the CA3 region (mossy fibers), into the CA1 region (Schaefer collaterals) eventually projecting from the subiculum, the major source of hippocampal output. The perforant path is believed to be crucial in learning and memory and involved in long-term potentiation (LTP) within the hippocampus. Interruption of the input to the dentate results in a sprouting of the remaining viable cells and has been used as a model of neural plasticity for many years.

Increased ADAMTS cleavage of brevican occurs early and is sustained in several brain regions after excitotoxin-induced lesion, mainly the outer molecular layer of the dentate gyrus, therefore, implicating this process in the initial loss of synapses or the regenerative response that occurs after injury (Yuan et al., 2002). Thus, in these experiments, a more selective lesion of the input into the molecular layer of the dentate is employed called the classical ECL model of neural plasticity. Others have shown that brevican remains elevated in the outer molecular layer for up to six months after such a lesion (Deller et al., 2000). Thus, brevican expression is altered in models of neuronal plasticity and this provides the basis for the investigation into the role of brevican-degrading proteases in the same process.

The ECL model of neural plasticity

Some experiments in this thesis will utilize an animal model of synaptic plasticity called the entorhinal cortex lesion (ECL) model. The entorhinal cortex

sends its axons to the septal portion of the hippocampus, innervating the outer molecular layer (OML) of the dentate gyrus (Scheff, 1989). By lesioning the entorhinal cortex with injected excitotoxin, one can explore the effect of the denervation of synapses in the outer molecular layer of the dentate gyrus. Surviving neurons sprout and regenerate in the entorhinal cortex along with neuritic growth and sprouting of contralateral neurons into the ipsilateral outer molecular layer. The three surviving afferent fiber systems that contribute to the reorganization of the OML of the dentate after ECL are: 1) crossed entorhinal-dentate fibers; 2) commissural and associational fibers to the inner molecular layer (IML); and 3) septo-hippocampal fibers (Deller and Frotscher, 1997). With this injury model, we can further investigate ECM molecules during reinnervation and repair.

The ECL is a classical model for denervation of the molecular layer of the dentate gyrus (Matthews et al., 1976; Steward et al., 1977; Ramirez and Stein, 1984; Deller and Frotscher, 1997). Temporal changes in the loss and reinnervation of the OML, as measured by the level of synaptic input, are well defined in this model in the rat. The ability to completely lesion the targeted area has also been intricately documented (Matthews et al., 1976; Phinney et al., 2004). Most importantly, this is a lesion of the initial synapse of the perforant path and is unidirectional in its projections; therefore, it allows investigation of effects that occur without a secondary input-output. As with any model there are a few disadvantages, for example the extent of and recovery from the lesion is often measured using relative optical density of an immunohistochemical signal,

which is not very quantitative, especially in mice, as we are dealing with a much smaller region than the rat. In addition, good behavioral correlates in animals that have undergone this procedure in the literature (pertaining to the mouse) are lacking. Nonetheless, the ECL has proven to be an efficient and well-characterized model of neural plasticity.

Alzheimer's' disease and CS-containing PGs.

One hallmark of Alzheimer's disease is the formation of Aβ-containing amyloid plaques in the extracellular space in the brain. Aβ is thought to interfere with neuronal function due to its stimulatory effect on free radical production resulting in oxidative stress and neuronal cell death as well as inducing the inflammatory response (McGeer et al., 1989; Giulian et al., 1995). Amyloid plaques consist of largely insoluble deposits of Aβ and various forms of Aβ may activate astrocytes and may be toxic to neurons. Aβ is a 39-42 amino acid peptide that is formed by the proteolytic cleavage of β-amyloid precursor protein (APP). APP has been shown to be anterogradely transported from the entorhinal cortex neuron cell body to axonal endings in the dentate gyrus via projections of the perforant path (Sheng et al., 2002). When these projections are severed by ECL, there is a reduction in amyloid burden in the dentate gyrus (Lazarov et al., 2002), suggesting that amyloid is deposited at the nerve terminal. Interestingly, one gene induced by Aβ in cultured rat astrocytes is ADAMTS4 (Satoh et al., 2000), indicating that in reactive astrocytes, that may be reactive due to the presence of Aβ, there is an increase in ADAMTS4 expression in the culture. In

addition, we have found that Aβ binds to and inhibits ADAMTS4 activity (unpublished observations, (Gottschall et al., 2003). Thus, this provides evidence that the inhibition of ADAMTSs by Aβ in the brain may be involved in the lack of injury response, further supporting a role of the ADAMTSs, and other endogenous proteases, in neural plasticity.

Transgenic mouse models of Alzheimer's disease, that over expresses human mutant APP, have been developed and mimic several aspects of human disease especially deposition of Aβ. Here, we investigate brevican processing by ADAMTSs and MMPs in a transgenic mouse model of AD that over expresses human mutant β-amyloid precursor protein (Hsiao et al., 1996) to examine expression of brevican and it catabolic fragments. This model is the most prevalent Aβ producing AD mouse model in the literature and has been shown to have the same characteristics as Aβ deposits in human AD (Terai et al., 2001).

The current study

The overall hypothesis is that the catabolism of brevican is prominent and facilitates plasticity. Evidence from the literature and data is presented, which supports the theory that CS containing ECM, especially brevican and its lectican relatives are effective inhibitors of neural plasticity. The data presented here a) defines the proteolytic fragment of brevican is abundant in regions capable of undergoing neural plasticity, b) increased ADAMTS activity in a classical model of neural plasticity, c) in a model thought to have dysregulated plasticity, such as Alzheimer's disease, brevican processing is altered, and d) by altering one of the

proteases responsible for the catabolism of brevican, pronounced changes in the levels of synaptic markers in regions involved in plasticity can be observed. Here, it is proposed that the proteolysis of the brevican core protein in the matrix, by endogenous proteases such as the ADAMTSs and the MMPs, allows and promotes neurite outgrowth and synaptogenesis to occur more readily in the brain in response to injury and during recovery. These experiments test this hypothesis in mouse models of neural plasticity.

Figure 1. **"**HLT (hyaluronan, lectican, and tenascin) complex" in the extracellular matrix of the central nervous system. ECM between a neuron or glial cell is stabile and inhibitory toward neurite outgrowth via the N-terminus of the lectican, brevican, binding to hyaluronan and the C-terminus of brevican binding to tenascin (A). Proteolytic modulation of the core protein by endogenous proteases, such as the MMPs and ADAMTSs, may allow for neural plasticity to occur. Modified and adapted from Yamaguchi, 2000.

Introduction, Figure 1

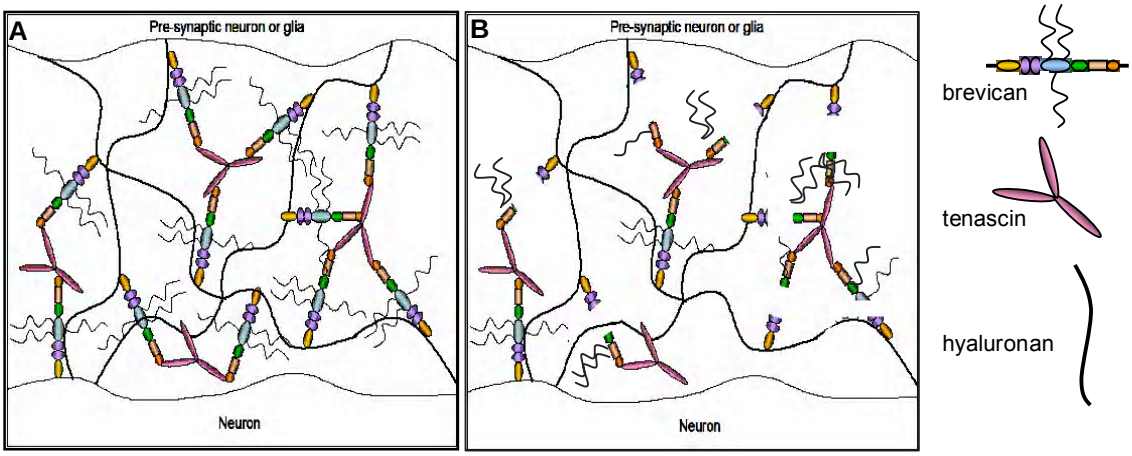

REFERENCES

Adams JC, Tucker RP (2000) The thrombospondin type 1 repeat (TSR) superfamily: diverse proteins with related roles in neuronal development. Dev Dyn 218:280-299.

Bornstein P, Agah A, Kyriakides TR (2004) The role of thrombospondins 1 and 2 in the regulation of cell-matrix interactions, collagen fibril formation, and the response to injury. Int J Biochem Cell Biol 36:1115-1125.

Brittis PA, Canning DR, Silver J (1992) Chondroitin sulfate as a regulator of neuronal patterning in the retina. Science 255:733-736.

Bruckner G, Grosche J, Hartlage-Rubasamen, Schmidt S, Schachner M (2003) Region and lamina-specific distribution of extracellular matrix proteoglycans, hyaluronan and tenascin-R in the mouse hippocampal formation. J Chem Neuroanat 26:37-50.

Cahal SRY (1995) Histology of the nervous system and vertebrates. . In: History of Neuroscience. New York: Oxford UP.

Celio MR, Blumcke I (1994) Perineuronal nets--a specialized form of extracellular matrix in the adult nervous system. Brain Res Brain Res Rev 19:128-145.

Deller T, Frotscher M (1997) Lesion-induced plasticity of central neurons: sprouting of single fibres in the rat hippocampus after unilateral entorhinal cortex lesion. Prog Neurobiol 53:687-727.

Deller T, Haas CA, Frotscher M (2000) Reorganization of the rat fascia dentata after a unilateral entorhinal cortex lesion. Role of the extracellular matrix. Ann N Y Acad Sci 911:207-220.

Dillon GP, Yu X, Bellamkonda RV (2000) The polarity and magnitude of ambient charge influences three-dimensional neurite extension from DRGs. J Biomed Mater Res 51:510-519.

Fawcett JW, Asher RA (1999) The glial scar and central nervous system repair. Brain Res Bull 49:377-391.

Flannery CR, Zeng W, Corcoran C, Collins-Racie LA, Chockalingam PS, Hebert T, Mackie SA, McDonagh T, Crawford TK, Tomkinson KN, LaVallie ER, Morris EA (2002) Autocatalytic cleavage of ADAMTS-4 (Aggrecanase-1) reveals multiple glycosaminoglycan-binding sites. J Biol Chem 277:42775-42780.

Gao G, Westling J, Thompson VP, Howell TD, Gottschall PE, Sandy JD (2002) Activation of the proteolytic activity of ADAMTS4 (aggrecanase-1) by C-terminal truncation. J Biol Chem 277:11034-11041.

Giulian D, Haverkamp LJ, Li J, Karshin WL, Yu J, Tom D, Li X, Kirkpatrick JB (1995) Senile plaques stimulate microglia to release a neurotoxin found in Alzheimer brain. Neurochem Int 27:119-137.

Gottschall PE, Yuan W, Muffly BG (2003) Attenuated Proteoglycanase activity in Alzheimer's Disease hippocampus: Associated with diminished synaptic density and inhibition of activity by abeta-amyloid. In: Society for Neuroscience. New Orleans, Louisiana: Abstarct Viewer / Itinerary Planner.

Grebner EE, Hall CW, Neufeld EF (1966) Glycosylation of serine residues by a uridine diphosphate-xylose: protein xylosyltransferase from mouse mastocytoma. Arch Biochem Biophys 116:391-398.

Hagihara K, Miura R, Kosaki R, Berglund E, Ranscht B, Yamaguchi Y (1999) Immunohistochemical evidence for the brevican-tenascin-R interaction: colocalization in perineuronal nets suggests a physiological role for the interaction in the adult rat brain. J Comp Neurol 410:256-264.

Helting T, Roden L (1969) Biosynthesis of chondroitin sulfate. I. Galactosyl transfer in the formation of the carbohydrate-protein linkage region. J Biol Chem 244:2790-2798.

Hockfield S, Kalb RG, Zaremba S, Fryer H (1990) Expression of neural proteoglycans correlates with the acquisition of mature neuronal properties in the mammalian brain. Cold Spring Harb Symp Quant Biol 55:505-514.

Hsiao K, Chapman P, Nilsen S, Eckman C, Harigaya Y, Younkin S, Yang F, Cole G (1996) Correlative memory deficits, Abeta elevation, and amyloid plaques in transgenic mice. Science 274:99-102.

Kashiwagi M, Enghild JJ, Gendron C, Hughes C, Caterson B, Itoh Y, Nagase H (2004) Altered proteolytic activities of ADAMTS-4 expressed by C-terminal processing. J Biol Chem 279:10109-10119.

Kjellen L, Lindahl U (1991) Proteoglycans: structures and interactions. Annu Rev Biochem 60:443-475.

Kuno K, Kanada N, Nakashima E, Fujiki F, Ichimura F, Matsushima K (1997) Molecular cloning of a gene encoding a new type of metalloproteinase-disintegrin family protein with thrombospondin motifs as an inflammation associated gene. J Biol Chem 272:556-562.

Lander AD (1993) Proteoglycans in the nervous system. Curr Opin Neurobiol 3:716-723.

Lazarov O, Lee M, Peterson DA, Sisodia SS (2002) Evidence that synaptically released beta-amyloid accumulates as extracellular deposits in the hippocampus of transgenic mice. J Neurosci 22:9785-9793.

Matthews DA, Cotman C, Lynch G (1976) An electron microscopic study of lesion-induced synaptogenesis in the dentate gyrus of the adult rat. II. Reappearance of morphologically normal synaptic contacts. Brain Res 115:23-41.

Maxwell WL, Follows R, Ashhurst DE, Berry M (1990) The response of the cerebral hemisphere of the rat to injury. I. The mature rat. Philos Trans R Soc Lond B Biol Sci 328:479-500.

McGeer PL, Akiyama H, Itagaki S, McGeer EG (1989) Immune system response in Alzheimer's disease. Can J Neurol Sci 16:516-527.

Miquel-Serra L, Serra M, Hernandez D, Domenzain C, Docampo MJ, Rabanal RM, de Torres I, Wight TN, Fabra A, Bassols A (2006) V3 versican isoform expression has a dual role in human melanoma tumor growth and metastasis. Lab Invest 86:889-901.

Morgenstern DA, Asher RA, Fawcett JW (2002) Chondroitin sulphate proteoglycans in the CNS injury response. Prog Brain Res 137:313-332.

Nakamura H, Fujii Y, Inoki I, Sugimoto K, Tanzawa K, Matsuki H, Miura R, Yamaguchi Y, Okada Y (2000) Brevican is degraded by matrix metalloproteinases and aggrecanase-1 (ADAMTS4) at different sites. J Biol Chem 275:38885-38890.

Oakley RA, Tosney KW (1991) Peanut agglutinin and chondroitin-6-sulfate are molecular markers for tissues that act as barriers to axon advance in the avian embryo. Dev Biol 147:187-206.

Paulus W, Baur I, Dours-Zimmermann MT, Zimmermann DR (1996) Differential expression of versican isoforms in brain tumors. J Neuropathol Exp Neurol 55:528-533.

Phinney AL, Calhoun ME, Woods AG, Deller T, Jucker M (2004) Stereological analysis of the reorganization of the dentate gyrus following entorhinal cortex lesion in mice. Eur J Neurosci 19:1731-1740.

Properzi F, Asher RA, Fawcett JW (2003) Chondroitin sulphate proteoglycans in the central nervous system: changes and synthesis after injury. Biochem Soc Trans 31:335-336.

Ramirez JJ, Stein DG (1984) Sparing and recovery of spatial alternation performance after entorhinal cortex lesions in rats. Behav Brain Res 13:53-61.

Reeves TM, Prins ML, Zhu J, Povlishock JT, Phillips LL (2003) Matrix metalloproteinase inhibition alters functional and structural correlates of deafferentation-induced sprouting in the dentate gyrus. J Neurosci 23:10182-10189.

Reier PJ, Houle JD (1988) The glial scar: its bearing on axonal elongation and transplantation approaches to CNS repair. Adv Neurol 47:87-138.

Satoh K, Suzuki N, Yokota H (2000) ADAMTS-4 (a disintegrin and metalloproteinase with thrombospondin motifs) is transcriptionally induced in beta-amyloid treated rat astrocytes. Neurosci Lett 289:177-180.

Scheff S (1989) Synaptic reorganization after injury: the hippocampus as a model system. In: Neuronal regeneration and transplantation, pp 137-156. New York: Liss.

Sheng JG, Price DL, Koliatsos VE (2002) Disruption of corticocortical connections ameliorates amyloid burden in terminal fields in a transgenic model of Abeta amyloidosis. J Neurosci 22:9794-9799.

Shindo T, Kurihara H, Kuno K, Yokoyama H, Wada T, Kurihara Y, Imai T, Wang Y, Ogata M, Nishimatsu H, Moriyama N, Oh-hashi Y, Morita H, Ishikawa T, Nagai R, Yazaki Y, Matsushima K (2000) ADAMTS-1: a metalloproteinase-disintegrin essential for normal growth, fertility, and organ morphology and function. J Clin Invest 105:1345-1352.

Snow DM, Lemmon V, Carrino DA, Caplan AI, Silver J (1990) Sulfated proteoglycans in astroglial barriers inhibit neurite outgrowth in vitro. Exp Neurol 109:111-130.

Snow DM, Atkinson PB, Hassinger TD, Letourneau PC, Kater SB (1994) Chondroitin sulfate proteoglycan elevates cytoplasmic calcium in DRG neurons. Dev Biol 166:87-100.

Steward O, Loesche J, Horton WC (1977) Behavioral correlates of denervation and reinnervation of the hippocampal formation of the rat: open field activity and cue utilization following bilateral entorhinal cortex lesions. Brain Res Bull 2:41-48.

Terai K, Iwai A, Kawabata S, Tasaki Y, Watanabe T, Miyata K, Yamaguchi T (2001) beta-amyloid deposits in transgenic mice expressing human beta-amyloid precursor protein have the same characteristics as those in Alzheimer's disease. Neuroscience 104:299-310.

Thon N, Haas CA, Rauch U, Merten T, Fassler R, Frotscher M, Deller T (2000) The chondroitin sulphate proteoglycan brevican is upregulated by astrocytes after entorhinal cortex lesions in adult rats. Eur J Neurosci 12:2547-2558.

Toeda K, Nakamura K, Hirohata S, Hatipoglu OF, Demircan K, Yamawaki H, Ogawa H, Kusachi S, Shiratori Y, Ninomiya Y (2005) Versican is induced in infiltrating monocytes in myocardial infarction. Mol Cell Biochem 280:47-56.

Tortorella MD, Burn TC, Pratta MA, Abbaszade I, Hollis JM, Liu R, Rosenfeld SA, Copeland RA, Decicco CP, Wynn R, Rockwell A, Yang F, Duke JL, Solomon K, George H, Bruckner R, Nagase H, Itoh Y, Ellis DM, Ross H, Wiswall BH, Murphy K, Hillman MC, Jr., Hollis GF, Newton RC, Magolda RL, Trzaskos JM, Arner EC (1999) Purification and cloning of aggrecanase-1: a member of the ADAMTS family of proteins. Science 284:1664-1666.

Van Wart HE, Birkedal-Hansen H (1990) The cysteine switch: a principle of regulation of metalloproteinase activity with potential applicability to the entire matrix metalloproteinase gene family. Proc Natl Acad Sci U S A 87:5578-5582.

Viapiano MS, Matthews RT (2006) From barriers to bridges: chondroitin sulfate proteoglycans in neuropathology. Trends Mol Med 12:488-496.

Wight TN, Merrilees MJ (2004) Proteoglycans in atherosclerosis and restenosis: key roles for versican. Circ Res 94:1158-1167.

Yamada H, Fredette B, Shitara K, Hagihara K, Miura R, Ranscht B, Stallcup WB, Yamaguchi Y (1997) The brain chondroitin sulfate proteoglycan brevican associates with astrocytes ensheathing cerebellar glomeruli and inhibits neurite outgrowth from granule neurons. J Neurosci 17:7784-7795.

Yamaguchi Y (1996) Brevican: a major proteoglycan in adult brain. Perspect Dev Neurobiol 3:307-317.

Yamaguchi Y (2000) Lecticans: organizers of the brain extracellular matrix. Cell Mol Life Sci 57:276-289.

Yamaguchi Y (2002) Glycobiology of the synapse: the role of glycans in the formation, maturation, and modulation of synapses. Biochim Biophys Acta 1573:369-376.

Yuan W, Matthews RT, Sandy JD, Gottschall PE (2002) Association between protease-specific proteolytic cleavage of brevican and synaptic loss in the dentate gyrus of kainate-treated rats. Neuroscience 114:1091-1101.

Zheng PS, Wen J, Ang LC, Sheng W, Viloria-Petit A, Wang Y, Wu Y, Kerbel RS, Yang BB (2004) Versican/PG-M G3 domain promotes tumor growth and angiogenesis. Faseb J 18:754-756.

CHAPTER 1

DISCORDANCE IN THE LOCALIZATION OF *WISTERIA FLORIBUNDA* AGGLUTININ AND BREVICAN IMMUNOREACTIVITY IN THE CENTRAL NERVOUS SYSTEM OF THE RODENT

Joanne Mayer, Autumn K. Eakin, Michelle G. Hamel, Paul E. Gottschall

Department of Molecular Pharmacology & Physiology, University of South Florida, Tampa, Florida, 33612

Acknowledgments: This work is supported in part by Alzheimer's Association (grant # IIRG-02-3758), Shriner's of North America (grant #8560), the American Heart Association (AHA, grant #0555216B) the National Institutes of Health (AG022101). The authors would like to thank Dr. Carl Flannery for providing human recombinant ADAMTS4 and Dr. Yu Yamaguchi for the brevican antibody, RB18.

ABSTRACT

The extracellular environment of the central nervous system (CNS) through which neuritic processes must traverse during development or after trauma or injury is complex, and may vary from conditions favorable for plasticity and growth to a milieu favorable for stabilization. The extracellular matrix (ECM) may act as a barrier for neurite extention in a growth tract, depending on the type of molecules involved, and the various signals they induce. One mechansim that may produce an environment that favors plasticity is the proteolytic cleavage of ECM. Brevican, a proteoglycan abundantly expressed in the adult CNS, belongs to the lectican family of aggregating chondroitin sulfate (CS)-bearing proteoglycans that can modulate neurite outgrowth and synaptogenesis. The ADAMTS (a disintegrin and metalloproteinase with thrombospondin motifs) family proteolytically cleave brevican, and could promote neural plasticity. The purpose of these studies was to compare the localization and abundance of the ADAMTS-derived fragment of brevican in the CNS, which would potentially identify regions of plasticty, with that of *Wisteria floribunda* agglutin (WFA) reactivity, a common method used to detect "perineuronal nets" (PNNs) of intact matrix which would identify stable regions. Although WFA reactivity was found primarily as PNNs, brevican and the ADAMTS-derived fragment of brevican were more broadly distributed to neuropil, yet in particular regions, they were also localzed to PNNs. In general, a discordance was observed between WFA and brevican or the N-terminal fragment of brevican. Functionally, this difference may correspond to regions of low and high neural plasticity, respectively.

Running Title: WFA and brevican immunoreactivity

Key words : extracellular matrix, synaptic plasticity, proteoglycan, ADAMTS, perineuronal nets

INTRODUCTION

Extracellular matrix (ECM) in the central nervous system (CNS) is deposited in the extracellular space of the neuropil and around a subset of neurons in the form of distinctive structures termed perineuronal nets (PNNs), coverings of matrix that ensheath perikarya, proximal dendrites and axon initial segments. The components of this matrix are aggregating proteoglycans (PGs), termed lecticans, that interact with tenascin and hyaluronan, to form complexes which maintain an anionic environment in the extracellular milieu of the CNS (Herndon and Lander, 1990; Lundell et al., 2004) (Fig. 2D). The core proteins of lecticans bear covalently-linked, highly negatively-charged, linear chondroitin sulfate (CS) chains that consist of glucuronic acid / N-acetylgalactosamine repeats, sulfated to varying extents at the 4 and 6 positions (Yamaguchi, 2000). Methods developed to detect the lecticans in fixed brain sections have employed: 1) antibodies that recognize CS epitopes of the lecticans, 2) antibodies that recognize initial disaccharides of CS chains exposed on the core protein after digestion with chondroitinase ABC (Ch'ase), and 3) labeled lectins derived from plants that recognize "selective" monosaccharide components of CS.

Wisteria floribunda agglutinin (WFA) is a lectin that binds to terminal N-acetylgalactosamine-containing residues (Young and Williams, 1985) and can decorate various structures in the CNS, especially PNNs where its reactivity has been well-documented (Brauer et al., 1993; Bruckner et al., 1994; Bruckner et al., 1996). Various layers of rostral-caudal rat cerebral cortex, and particularly the retrosplenial cortex, thalamus, cerebellum and brain stem are regions that contain numerous PNNs prominently labeled by WFA (Bruckner et al., 1996). In rat neocortex, several types of morphology are associated with WFA-reactive PNNs, (Brauer et al., 1993; Wegner et al., 2003). Other data indicate that the reactivity seen with WFA may be independent of the perineuronal proteoglycan, and that lectin binding identifies terminal N-acetylgalatosamines present on neuronal cell surface glycoproteins (Murakami et al., 1999). Importantly, WFA binding in nervous tissue co-localizes with signal from antibodies raised against CSs (Bruckner et al., 1998), and signal is lost when tissue sections are pre-treated with chondroitinase ABC (Koppe et al., 1997a), suggesting that WFA binds indirectly or directly to CS. Thus, WFA reactivity has become a standard method of identifying CS-containing subsets of neurons in the CNS that are surrounded by PNNs.

Brevican is a lectican highly expressed in the adult brain along with aggrecan and the V2 isoform of versican. The deposition of these lecticans is heterogeneous in the complex ECM of PNNs and in the neuropil (Yamaguchi, 2000) (Fig. 1D). Functionally, CS side chains of the lecticans inhibit neural plasticity and neurite extension and even may stabilize synapses in neural

networks (Hockfield et al., 1990; Bandtlow and Zimmermann, 2000; Yamaguchi, 2000). Various isoforms of brevican are found in the adult brain including > 145 kD molecule that carries 1-3 CS chains (Fig. 2A), the core 145 kD protein without CS, a 120 kD glycosylphosphatidylinositol-linked membrane bound form, and 55 kD N-terminal, and 80 kD C-terminal fragments (Fig. 2C) that are the result of endopeptidase action on the holoprotein. The proteases mainly responsible for cleavage of brevican are glutamyl endopeptidases, the ADAMTSs (a disintegrin and metalloproteinase with thrombospondin motifs) (Fig. 2D, E). Several of these multi-domain proteases (Porter et al., 2005) (ADAMTS-1, 4, 5, and 9) are expressed in brain (Sasaki et al., 2001; Yuan et al., 2002; Cross et al., 2006) (our unpublished observations) and are potent in cleaving aggrecan (Tortorella et al., 1999), versican (Westling et al., 2004) and brevican (Matthews et al., 2000) (for review, see Gottschall et al., 2005). ADAMTS-cleaved fragments of each lectican are found in untreated nervous tissue extracts (Matthews et al., 2000; Lemons et al., 2001; Yuan et al., 2002; Westling et al., 2004; Hamel et al., 2005; Mayer et al., 2005), indicating that ADAMTSs are active proteases capable of cleaving lecticans in a "normal" nervous system. The fragments of lecticans may be localized in brain tissue sections by using antibodies raised against the terminal, neoepitope sequences of the core protein that are exposed after ADAMTS cleavage (Gao et al., 2002; Westling et al., 2002; Gottschall et al., 2005). Using one of these antibodies that recognizes the C-terminal sequence of the N-terminal fragment of brevican that is uncovered after ADAMTS cleavage (Matthews et al., 2000), we noted that the distribution of this immunoreactivity in

rat hippocampus was markedly different from WFA reactivity in the same region. We expected that the distribution of the signal from both reagents would be similar, since fragments of brevican are stable after cleavage (Yamaguchi, 2000), and the preponderance of the C-terminal fragments bear CS chains. Thus, the purpose of this study was to describe the distribution and characteristic immunoreactivity for the ADAMTS-cleaved fragment of brevican, and compare this with WFA binding in the rodent CNS. The results show a marked discordance between the two, with the breadth of distribution of the ADAMTS-derived brevican fragment much greater than that of WFA reactivity.

MATERIALS & METHODS

Animals

All animal procedures described in this manuscript were approved by the Institutional Animal Care and Use Committee (IACUC) at the University of South Florida. Adult male C57BL/6 mice (23 g - 27 g; Harlan, Indianapolis, IN) and adult male Sprauge-Dawley rats (250 g - 300 g; Harlan, Indianapolis, IN) were housed under a 12 hour light cycle with regulated temperature and humidity. Mice were housed 3 to 4 per cage and rats were housed individually with both having free access to food and water. Brain tissue was collected from animals between 3 and 4 months of age: biochemical analysis n=4 and immunohistochemistry n=6.

Western Blotting

For collection of tissue for blotting with antibodies and biotin-WFA, animals were euthanatized by exposure to excess CO_2 until death and immediately decapitated. Various brain regions were rapidly dissected and extracted with a teflon-glass homogenizer in 5 volumes of Triton-X-100-containing buffer (20 mM Tris-HCl at pH 7.4, 10 mM EDTA, 1% Triton-X-100, and 1:100 protease inhibitor cocktail [Calbiochem type III, LaJolla, CA]) for 2 minutes. The homogenate was centrifuged in a microcentrifuge at 6800 x g for 5 minutes, and the isolated supernatant collected and stored at –80^{o}C.

In some experiments, brain tissue extract was treated with Ch'ase prior to Western blot to determine whether WFA recognized CS-containing proteins. Thus, 25 µl of sodium acetate buffer (50 mM sodium acetate, 1 M Tris, 10 mM EDTA) containing 10 mU of chondroitinase ABC (Sigma-Aldrich, St. Louis, MO) was added to 25 µl of brain tissue extract and incubated for 1.5 h at 37^{o}C. To determine whether there was protease contamination in the Ch'ase preparation, samples underwent Ch'ase digestion in the presence of a protease inhibitor cocktail. All samples were reduced (mercaptoethanol-containing, SDS-PAGE sample buffer), denatured for 4 minutes at 95^{o}C, and subjected to SDS-PAGE.

Tissue extracts were loaded (equal amounts of protein) onto pre-cast, 1.5 mm, 4-20% gradient SDS-PAGE gels (Novex gels, Invitrogen, Carlsbad, CA). Separated proteins were electrophoretically transferred to a polyvinylidine difluoride membrane (PVDF, Immobilon, Millipore, Billerica, MA). For brevican and EAV(M)ESE immunoblotting, the membranes were washed with Buffer B (10

mM phosphate buffered saline, pH 7.4 containing 0.05% Tween 20) for 5 minutes, blocked for 1 h in 5% non-fat dry milk diluted in Buffer B and probed for 2 hours using primary antibodies against mouse anti-brevican (1:1000, BD Transduction Labs, San Jose, CA), rabbit anti-EAMESE (1:1000) (Mayer et al., 2005), or rabbit anti-EAVESE (1:500) (Aya-ay et al., 2005; Hamel et al., 2005). For WFA blotting, the membranes were washed with Buffer B for 5 minutes, blocked in 1% bovine serum albumin diluted in Buffer B for 1 hour and probed for 2 hours using biotinylated *Wisteria floribunda* lectin (1:10,000 in 1% BSA, Vector Laboratories, Burlingame, CA) as the primary binding reagent. Primary antibodies and biotinylated *Wisteria floribunda* lectin were detected with corresponding secondary antibodies including anti-mouse, anti-rabbit and streptavidin conjugated to horse radish peroxidase (Chemicon, Temecula, CA), respectively. Antigens were visualized using a chemiluminescence developing system (SuperSignal, Pierce, Rockford, IL). It should be noted that ADAMTS-derived fragment antibodies were raised against the species-specific neoepitopes for rat and mouse, since they show limited cross-reactivity with one another, ie. anti-EAVESE (rat sequence) does not recognize the C-terminus of the N-terminal, ADAMTS-cleaved fragment EAMESE (murine sequence) of mouse brevican.

Isolation of Membrane Fractions

Whole rat brain was collected as descibed above and homogenized for one minute with a Glas-Col (Terre Haute, IN) motorized (low speed, 333 rpm),

teflon-glass homogenizer in 10 volumes of 50 mM Tris-HCl, pH 7.4, 1 mM EDTA, containing 1:100 protease inhibitor cocktail (Calbiochem type III, LaJolla, CA). The homogenate was centrifuged at 500 x g for 5 minutes and then the isolated supernatant was centrifuged at 40,000 x g to obtain soluble and insoluble fractions. The supernatant, "soluble" fraction, was removed immediately, aliquoted and stored at -80^{o}C. The insoluble "membrane" fraction was resuspended with buffer, centrifuged (40,000 x g for 30 min) and reconstituted in detergent-containing RIPA buffer (50mM Tris base, 150mM NaCl, 1mM EDTA, 1mM EGTA, 1% Triton-X-100, 1% sodium deoxycholate, 1% SDS, pH = 7.4), aliquoted and stored at -80^{o}C .

Immunohistochemistry

Rats and mice were euthanatized with excess Nembutal, and the brains fixed via cardiac perfusion as described (Aya-ay et al., 2005). The brains of the animals were cleared using phosphate buffered saline (PBS; pH 7.4), fixed with fresh 4% paraformaldehyde in 0.1M phosphate buffer (PB; pH 7.4), collected, post-fixed overnight in 4% paraformaldehyde and cryoprotected with 15% and 30% sucrose (in PBS) for 24 hours each. The individual brains were mounted on a cryostat chuck at –20^{o}C and sectioned at 30 µm. Sections were stored freely floating in antifreeze solution at –20^{o}C.

For Ch'ase treated tissue, matched sections were selected, washed three times with PBS and incubated in 500 mU of Ch'ase in 0.5 ml of sodium acetate buffer for 1.5 hours at 37^{o}C. Selected sections to be used for

immunohistochemistry were washed in PBS for 15 minutes, blocked and permeabilized in 10% normal goat serum, 3% 1 M lysine and 3% Triton-X-100 for 1h and incubated overnight in primary antibodies anti-EAMESE (1:1000) (Mayer et al., 2005), EAVESE (1:500) (Yuan et al., 2002; Aya-ay et al., 2005), brevican (1:1000, N-terminal (G1); Transduction Labs, San Jose, CA) and 1:500, C-terminal (G3) RB18, generous gift from Yu Yamaguchi, Burnham Institute, La Jolla, CA, (an antibody that recognizes a C-terminal region epitope of rat brevican) and *Wisteria floribunda* lectin (1:1000) at 4^{o}C. Doubly probed sections were washed and incubated in anti-rabbit IgG conjugated to Alexa-Fluor 488 (Molecular Probes, Eugene, OR) and streptavidin conjugated to Alexa-Fluor 594 (Molecular Probes, Eugene, OR) for 1 hr at room temperature. The sections were washed for 15 minutes, wet mounted on glass slides, and coverslipped with VectaShield mounting medium (Vector Labs, Burlingame, CA).

Cleavage of PGs with human recombinant ADAMTS4

PGs present in whole rat brain extracts were bound to and eluted from a DEAE Sepharose Fast Flow cation exchange matrix (Pharmacia, Pfizer, New York, NY) as described (Yamada et al., 1994) with modifications. All procedures were carried out at 4^{o}C unless otherwise stated. Briefly, rat brain tissue (1g) was placed in 10 ml, ice cold, 4 mM HEPES pH 8.0, 0.15 mM NaCl, 0.1% Triton-X-100 containing 2 mM 1,10 phenanthroline (Sigma, St. Louis, MO) and protease inhibitor cocktail (set III, Calbiochem, San Diego, CA). The tissue was disrupted in a Teflon-glass homogenizer and the extract centrifuged at 30,000 x g for 30

min. The supernatant was removed, diluted 1:1 with 50 mM Tris-HCl, 0.15 M NaCl, 0.1% Triton-X-100, and applied to a DEAE column pre-equilibrated with the same buffer at a flow rate of less than 0.5 ml per minute. The flow through was collected, passed over the column again, and bound proteins were eluted with 5 column volumes of consecutive buffers containing 50 mM Tris-HCl pH 8.2, 0.15 M NaCl, 0.1% Triton-X-100, then 50 mM Tris-HCl pH 8.2, 0.25 M NaCl, 6 M urea, 0.1% Triton-X-100, and fractions containing PGs were eluted with 50 mM Tris-HCl pH 8.2, 1.0 M NaCl. PG (protein)-containing fractions were dialyzed against water for 24 h in SpectraPor 6000-8000 MWCO (Millipore, Billerica, MA) membrane at 4^{o}C, the samples concentrated on a speed-vac and aliquoted. Total protein was measured in the samples (1.3 µg/µl). DEAE-purified PG samples were incubated with 25 nM human recombinant ADAMTS4, (a gift of Carl Flannery, Wyeth Pharmaceuticals, Collegeville, PA) diluted in 10 mM Tris-HCl, 0.15 M NaCl, and 10mM $CaCl_2$ for two hours at 37^{o}C. After the incubation period, beta-mercaptoethanol-containing, SDS-PAGE sample buffer was added to the samples, the samples were heated at 95˚C for 4 minutes, subjected to SDS-PAGE, and electrically transferred to Immobilon PVDF membrane (Millipore, Bedford, MA). Membranes were probed with mouse anti-brevican (BD Biosciences, San Jose, CA) at 1:1000 primary antibody detected with anti-mouse conjugated to horse-radish peroxidase (Chemicon, Temecula, CA), and signal detected using SuperSignal chemiluminescence substrate (Pierce, Rockford, IL). The membrane was probed a second time with anti-EAVESE (1:100) (Hamel et al., 2005), as described under the Western blot section above.

Microscopy and image acquisition

Single and multi-labeled, epifluorescent tissue sections were viewed using a Zeiss Axioskop microscope, interfaced with an Axiocam and images acquired with Openlab software. Confocal images (Fig. 8) were attained using a Leica SP-2 confocal microscope and Leica LCS software. Controls for each immunomarker included secondary antibody in the absence of a primary antibody, in which the staning in control sections was minimal to absent. Exposure times and aperture opening were constant for each magnification and antibody used. Some images were minimally and equally modified (contrast and brightness) using Abobe photoshop.

RESULTS

Brevican exists in rodent brain ECM as a holoprotein, in part, with a central region that bears CS chains and globular terminal domains which do not. When brevican is detected on Western blot using an N-terminal region antibody, a 55 kD, N-terminal fragment of brevican is prominent. The predominant protease activity responsible for this cleavage is ADAMTS-derived, glutamyl-endopeptidase activity. The neoepitope antibody(s) used in these experiments, anti-EAV(M)ESE, represents the C-terminal sequence exposed on the N-terminal, 55 kD fragment of brevican after ADAMTS cleavage (Matthews et al., 2000). To verify that this antibody recognizes ADAMTS-cleaved brevican, the CS-bearing form of brevican was partially purified on a DEAE anion exchange matrix, and the PG-containing eluant was incubated with active human

recombinant ADAMTS4. As shown in Fig. 3, when a Western blot of the DEAE extract was probed using an N-terminal region monoclonal, anti-brevican antibody, a smear >145 kD was observed (Fig. 3A). After digestion by ADAMTS4, the abundance of the holoprotein was markedly reduced with the appearance of a 55 kD N-terminal fragment (Fig. 3C). When probed with polyclonal anti-EAVESE, little or no anti-EAVESE immunoreactive fragment was present in the DEAE extract prior to digestion (since the fragment does not bind the column) (Fig. 3B), however, after cleavage of brevican by human recombinant ADAMTS4, the same 55 kD fragment was apparent (Fig. 3D). This indicates that ADAMTS-cleaved brevican is recognized by anti-EAVESE, as a 55 kD, N-terminal fragment, the same fragment detected using an N-terminal region anti-brevican antibody.

In an effort to identify the molecular species in rodent brain detected by the N-terminal region anti-brevican antibody, those detected by anti-EAV(M)ESE, and by biotin-WFA, cortical homogenates from rat and mouse brain that were either pre-treated with Ch'ase or were left untreated were subjected to SDS-PAGE and probed with the reagents (Fig. 4). When membranes containing soluble brain extract were probed with the N-terminal region anti-brevican antibody, the pattern of brevican immunoreactivity included a smear of immunoreactivity found at >145 kD, a distinct 145 kD band, and a 55 kD, N-terminal fragment of brevican (Fig. 4A). Ch'ase treatment eliminated the smear in the mouse sample with an associated marked increase in the 145 kD holoprotein without CS in both the mouse and rat samples (Fig 4A). Ch'ase

treatment did not alter the intensity of the 55 kD fragment, and this same N-terminal fragment was identified (alone) when the membrane was probed with anti-EAVESE (rat) or anti-EAMESE (mouse) (Fig. 4B). Interestingly, those signals observed with streptavidin-HRP to identify proteins that bind to biotin-WFA did not correspond to the molecular weight of any isoform of brevican (Fig. 4C). In fact, only the very high molecular weight smear observed in mouse cortical extract was diminished after incubation with Ch'ase. Two of the major bands seen in this blot, however, were non-specific binding signals that were present when membrane was probed with streptavidin-HRP alone (Fig. 4C, right lane, Ms). In addition, when brain homogenates were differentially centrifuged to obtain "membrane" and "soluble" fractions, the majority of brevican immunoreactivity was found in the soluble fraction (Fig. 4D, left panel, S), whereas, the major signals observed after probing with biotin-WFA were observed mainly in the “insoluble”, membrane fraction (Fig. 4D, right panel, I). These results suggest that few or none of the brevican isoforms are detected when probed with biotinylated WFA on membranes. To verify that the effect of Ch'ase on the high molecular weight, WFA reactive smear was due solely to degradation of polysaccharides (and not to proteolytic activity in the Ch'ase preparation), the samples were treated with Ch'ase in the absence and presence of protease inhibitor cocktail (Fig. 4E, left panel). In both rat and mouse samples, the pattern of WFA reactivity was identical, whether or not the samples contained protease inhibitor cocktail. These results suggest that WFA does indeed bind to a high molecular weight, CS moiety that is removed after Ch'ase treatment;

however the results suggest it may be a different CS-containing molecule other than brevican. To verify the effectiveness of Ch'ase digestion, the same membrane was probed with brevican and there was a complete removal of CS chains and a marked increase in the abundance of the core protein in Ch'ase-treated samples (Fig. 4E, right panel, rat only, mouse not shown) with no change in the abundance of fragment.

This discordance between biotin-WFA and anti-brevican reactivity was not region specific, because when cerebellum, brain stem, temporal lobe and diencephalon extracts were probed with anti-brevican, anti-EAMESE and biotin-WFA, similar results were observed (Fig. 4). Nonetheless, biotin-WFA was highly effective at identifying neurons in the CNS that were surrounded by PNNs, and minor reactivity was also found in the neuropil in both rat and mouse tissue sections (Fig. 6A, B). Note the abundant PNNs in retrosplenial cortex (arrows) and scattered PNNs in parietal cortex. The intense signal was nearly abolished by pre-incubating the tissue section with high concentrations of Ch'ase (Fig. 6 C, D). When streptavidin-Alexa 594 alone was used, the section was completely blank (not shown). In addition, immunoreactivity for anti-EAV(M)ESE was not influenced by Ch'ase pre-treatment of tissue (not shown). These results suggest that whatever moiety is bound by WFA is released upon treatment with Ch'ase, yet the N-terminal brevican fragment that does not bear CS chains is unaffected by Ch'ase.

There are several regions of the brain where there is distinctive and discordant reactivity between WFA and the ADAMTS-derived N-terminal

fragment of brevican. Particularly, the reticular thalamic nucleus shows prominent staining with WFA in both the rat and mouse (Fig. 7A, 7C, and 7D, 7F) whereas the barrels of the ventral posteriolateral and posteriomedial thalamic nuclei are most evident in the rat, compared to the mouse (Fig. 7A and 7C with 7D and 7F). In contrast, anti-EAV(M)ESE immunoreactivity is weak in the reticular thalamus, but highly prominent between the barrels in the posteriolateral and medial nuclei (Fig. 7B, 7C, 7E and 7F). There were striking differences seen in the hippocampus and surrounding cortex as well. Mostly the neuropil layers of the dorsal hippocampus contain weak to absent staining with WFA, the exceptions being the CA2-CA3 transition region, the molecular layer of the lateral blade and the polymorphic layer (especially in the mouse) of the dentate gyrus and the fasciaola cinera (Fig. 7G). However, clear PNNs were found in and just adjacent to the pyramidal cell layer in the stratum oriens in Ammon's horn (Bruckner et al., 2003). These hippocampal neurons containing PNNs appeared to be markedly more abundant in the mouse compared to the rat (Fig. 7G, 7J). The white matter regions of the corpus callosum, external capsule and alveus were all intensely stained by WFA; however, at least a portion of this staining was not eliminated after Ch'ase treatment of the sections. Staining by anti-EAV(M)ESE showed comparatively intense immunoreactivity in the hippocampal neuropil, especially the stratum oriens, and this staining reached the pyramidal cell layer (Fig. 7H, 7K) where there was a cobblestone appearance of this layer (not shown). Scattered PNNs were noted in and around the pyramidal cell layer, similar to WFA staining, and some of these appeared to co-localize with WFA

reactivity in the mouse (Fig. 7J, K, L). In the cerebellum, the lobular molecular layer was weakly stained by WFA, the granular layer contained heavily labeled neuropil and PNNs and lobule white matter (Fig. 7M, 7P). The white matter was completely negative for reaction product to EAV(M)ESE, however, marked immunoreactivity was observed in the granular layer, but especially as PNNs surrounding the aligned Purkinjie cells that make up the molecular-granular layer interface (Fig. 7N, 7O, 7Q, 7R). Interestingly, these aligned Purkinjie neurons have previously been shown to be labeled with parvalbumin but not by WFA (Corvetti and Rossi, 2005).

Neurons with PNNs that contain EAV(M)ESE are not quite as abundant as those identified by WFA, but they appear to have a broad distribution. PNNs and intense fiber-like staining were found in the horizontal limb of the diagonal band (Fig. 8A), the medial septum (Fig. 8B) and in piriform cortex (Fig. 8C). In addition, they were broadly distributed in cerebral cortex in layers distinct from PNNs surrounded by WFA reactivity, (Fig. 8D – 8F), and there was a low percent of cells that co-localize with WFA. In murine cerebral cortex, anti-EAMESE immunoreactivity was found mostly in deep cortical layer IV where sporadic neurons containing WFA-reactive PNNs were located. For WFA reactivity, an intensely-stained region was primary somatosensory cortex (Fig. 8E - 8F). However, most neurons with WFA reactive PNNs were found in layer III, and the superficial region of layer IV lacks many PNNs positive for WFA or anti-EAMESE (Fig. 8F). Both reagents show a similar distribution in the rat (data not shown). Another region of cortex that is intensely labeled by both WFA and anti-

EAV(M)ESE was retrosplenial cortex (not shown; at high magnification, see Fig. 7, G-L).

Immunoreactivity for brevican holoprotein, and not its proteolytic fragment, was distributed throughout the CNS neuropil and in PNNs as has been identified by others. Neurons with PNNs that contain brevican immunoreactivity are clearly more abundant than those identified by WFA. Brevican immunoreactivity was broadly distributed in cerebral cortex in layers distinct from PNNs surrounded by WFA reactivity, (Fig. 9A – 9C), although there was a higher percentage of brevican immunoreactive cells that co-localize with WFA compared to that of EAV(M)ESE immunoreactivity. In murine cerebral cortex, anti-brevican immunoreactivity was found in neuropil and PNNs of cortical layers II, III and deep layer IV and V, whereas the most abundant distribution of neurons containing WFA-reactive PNNs were found in layer III. Both reagents showed a similar distribution in the rat (data not shown). A higher magnification of cortex reveals PNNs that are positive for brevican and WFA reactivity (Fig. 9D - 9F). A confocal micrograph of retrosplenial cortex stained with anti-brevican, biotin-WFA and DAPI, demonstrated that there are clearly PNNs that co-localize and are reactive for both reagents (Fig. 9, G - denoted by arrows). While many PNNs were immunoreactive for brevican, other PNNs were reactive toward WFA alone, (Fig. 9, G - denoted by asterisk). PNNs reactive with WFA and not brevican, expressed other CS-containing PGs or N-acetylgalactosamine containing molecules. A complete localization of anti-brevican, anti-EAV(M)ESE, and biotinylated WFA PNNs and their reactivity in the neuropil of the CNS, with semi-

quantitation for both reagents may be found in supplemental Tables 1 (rat) and 2 (mouse).

DISCUSSION

Interactions between neurons and molecules in the extracellular milieu initiate signals that may regulate neurite outgrowth and targeting, neural migration and synaptogenesis, collectively a morphological measure of neural plasticity. Increasing evidence supports the concept that ECM molecules are important regulators of neural plasticity. The lectican brevican is abundant in brain ECM, is localized perisynaptically, inhibits neurite outgrowth (Yamada et al., 1997) and is thought to stabilize neural networks in the adult (Hockfield et al., 1990), whereas conditions that augment the proteolytic cleavage of brevican are associated with neural plasticity (Yuan et al., 2002; Phillips et al., 2004; Mayer et al., 2005) Here, we intended to compare the distribution of PNNs and neuropil stained by the classical reagent WFA and an antibody against a proteolytic cleavage fragment of brevican. We found a discordance in the deposition of classical PNNs and regions where the proteolytic fragment of brevican was observed. In particular, there appeared to be an association between regions with significant deposition of this fragment and areas known to be involved in neural plasticity, supporting the involvement of ADAMTSs in neural plasticity mechanisms (Yuan et al., 2002; Mayer et al., 200;, Gottschall et al., 2005).

Interestingly, a significant proportion of total brevican immunoreactivity in brain extracts was observed as a fragment formed by proteolytic cleavage of the

intact core protein. Proteolysis of lecticans may be an important mechanism by which the nervous system overcomes the inhibition exerted by PGs during periods of neural plasticity. After systemic injection of the excitotoxin, kainic acid (Yuan et al., 2002) or after targeted unilateral lesion of the entorhinal cortex (Mayer et al., 2005), there was an increase in the abundance of an ADAMTS-derived brevican fragment in the dentate gyrus terminals, a region where sprouting occurs in response to the lesion. Thus, proteolytic cleavage of PGs may be a key mechanism involved in neural plasticity, whereas intact PGs promote neural stabilization. Here we compared the localization of an ADAMTS-derived proteolytic fragment of brevican to the distribution of classically identified PNNs, as recognized by WFA reactivity. Assuming that WFA detected the N-aceylgalactosamine residue in the CS chains of brevican, the hypothesis was that areas of high PG deposition, as marked by WFA, may stabilize neural networks and provide an environment resistant to neural plasticity. Indeed, areas deficient in the proteolytically-derived fragment of brevican tended to have significant reactivity with WFA.

Localization of brevican with CNS immunohistochemistry (Yamaguchi, 1996; Bruckner et al., 2003) and *in situ* hybridization (Seidenbecher et al., 1998; Jaworski et al., 1999), revealed that brevican is highly expressed in cerebellar and cerebral cortex, hippocampus and thalamic nuclei and abundant in brain stem PNNs. Since molecular complexes that contain tenascin, hyaluronic acid and a lectican such as brevican are presumed to form the aggregates of deposited ECM, then the CS chains of the lecticans, whether the core protein is

cleaved or not, should exist in close proximity to each other (Fig. 2), and thus, we expected to observe co-localized reactivity between WFA and anti-EAV(M)ESE. In contrast to this notion, we observed marked differences in the distribution between these labels. In general, regions where the ADAMTS-derived fragment of brevican is abundant, maybe 20% of the neurons appear to co-localize with WFA. Where PNNs of WFA predominate, there was marked regional variability and co-localization with brevican and fragment immunoreactivity.

Since there is debate in the literature about which molecules in the CNS are labeled by WFA, we were interested in determining whether brevican, and its CS chains, was a binding partner for this lectin. WFA is a lectin that binds to N-acetylgalactosamine-linked α or β to the 3 or 6 position of galactose (Goldstein and Poretz, 1986). Often WFA is used as marker for PNNs that contain CS chains, and some believe that WFA binds directly to CS. Our data show that WFA clearly did not recognize CS-containing brevican on Western blot, although there was at least one high molecular weight WFA reactive band. No corresponding bands were seen at the molecular weights representing the isoforms of brevican. In addition, the preponderance of brevican was found in the soluble fraction of brain extract, whereas WFA reactivity was mainly located in the particulate, insoluble fraction after differential centrifugation of brain extract. As seen in whole rat tissue, none of the brevican isoforms corresponded to bands recognized by WFA lectin in the insoluble fraction. These results support the notion that WFA binds molecules that differ from the lectican, brevican. Significant evidence supports the concept that WFA-binding proteins

are cell surface glycoproteins as reported by Murakami et al. This group demonstrated (Murakami et al., 1999; Murakami et al., 2001) that terminal N-acetylgalactosamine residues, which are present on neuronal cell surface glycoproteins, are responsible for the PNN reactivity seen with WFA lectin binding. Based on a series of studies using degradative enzymes to define the presence or absence of polysaccharides bound to ECM proteins, their model suggests that perineuronal proteoglycans, such as brevican, bind to these cell surface glycoproteins. Ch'ase treatment removes the terminal N-acetylgalactosamine from these proteoglycans, thereby releasing the lectican from its binding partner on the cell surface. It is not surprising that polysaccharides contained within PNNs differ from those found in the more diffuse ECM neuropil (Deepa et al., 2006), since lecticans may bind to cell surface glycoproteins. This may, in part, account for the discordance in reactivity seen here between brevican and WFA.

High molecular weight isoforms of brevican, abundant on Western blot in all regions examined, contained CS chains since there was a marked reduction in molecular weight after enzymatic treatment of the brain extract with Ch'ase. Surprisingly, all bands that were reactive for biotin-WFA were unchanged after Ch'ase treatment, with the exception of a reduction in a high molecular weight smear found in brain extract. This, along with the discrepancies seen in histochemistry, prompted us to question whether WFA recognizes N-acetylgalactosamine residues present in the CS chains of brevican. To our knowledge, there is no direct evidence of WFA binding to any specific CS-

containing PG, including the lecticans. The most supportive data of such a concept is that reactivity observed with WFA and antibodies generated against CS chains are similarly distributed in rat brain (Wegner et al., 2003), such as in PNNs, although there may be a host of proteins present in these ECM complexes. In addition, many groups have shown that after Ch'ase digestion of fixed brain sections, binding of WFA is diminished (Bertolotto et al., 1995; Koppe et al., 1997b). However, it is possible, in fact likely, that WFA binds to a molecule that may be indirectly bound to CS. In any case, no biochemical evidence is available to show that WFA binds to large polymeric chains of repeating disaccharides that contain N-acetylgalactosamine.

Although WFA may not recognize brevican, the data presented here only begins to uncover the intricate molecular environment around individual neurons that may modulate its function and structure. The discordant distribution between these molecules may relate to the functional environment, i.e. more abundance of CS chains stained with WFA (defining a more stable environment) whereas an increase in proteolytic cleavage of ECM, stained with the fragement neoepitope (defining a more permissive environment), in regions that are capable of undergoing neural plasticity. These findings are intriguing since we observe intense immunoreactivity for the ADAMTS-derived brevican fragment in areas thought to be highly plastic such as the hippocampus. Therefore, the relative abundance of cleaved proteoglycans, such as brevican, in a particular region suggest a functional change in surrounding ECM complexes which may contribute to overall neural plasticity.

Figure2. Schematic representation of brevican isoforms in brain ECM and their ADAMTS-derived proteolytic cleavage fragments: Secreted brevican core protein that bears 1-3 chondroitin sulfate chains (A, MW > 145 kD). Secreted brevican core protein without chondroitin sulfate side chains (B, MW = 145 kD). When cleaved by extracellular glutamylendopeptidases, the ADAMTSs (denoted by arrows), a C-terminal fragment is formed together with a N-terminal, 55 kD fragment of brevican (C) that contains a unique C-terminal epitope murine (ms) sequence "EAMESE", homologous to the rat (rt) "EAVESE". Indicated here are the anti-EAV(M)ESE antibody recognition sites (C). The >145 kD and 145 kD isoforms of brevican or other lecticans in matrix form a tertiary complex with hyaluronan and tenascin (D) and when cleaved by ADAMTSs, the proteolytic degradation of brevican loosens the ECM complex and may promote plasticity (E).

Chapter 1, Figure 2

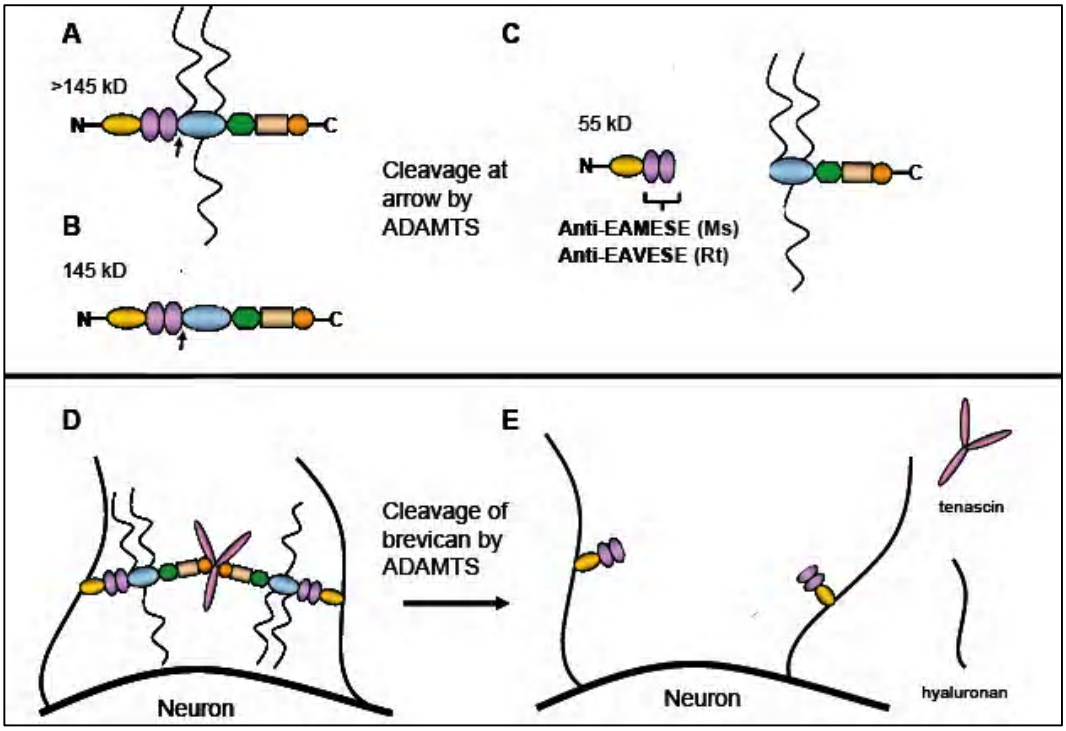

Figure 3. Degradation assay of brevican by human recombinant ADAMTS4: Purified rat brain proteoglycan, isolated on a DEAE cation exchange matrix, and probed with anti-brevican (A). Purified proteoglycan was probed for anti-EAVESE, an antibody raised against the C-terminal sequence of the ADAMTS-cleaved N-terminal fragment of brevican (B). Proteoglycan extract after incubation with human recombinant ADAMTS4 and probed with anti-brevican (C) and anti-EAVESE (D). After incubation with human recombinant ADAMTS4, brevican was proteolytically cleaved resulting in diminished full length brevican and the appearance of a 55 kD isoform.

Chapter 1, Figure 3

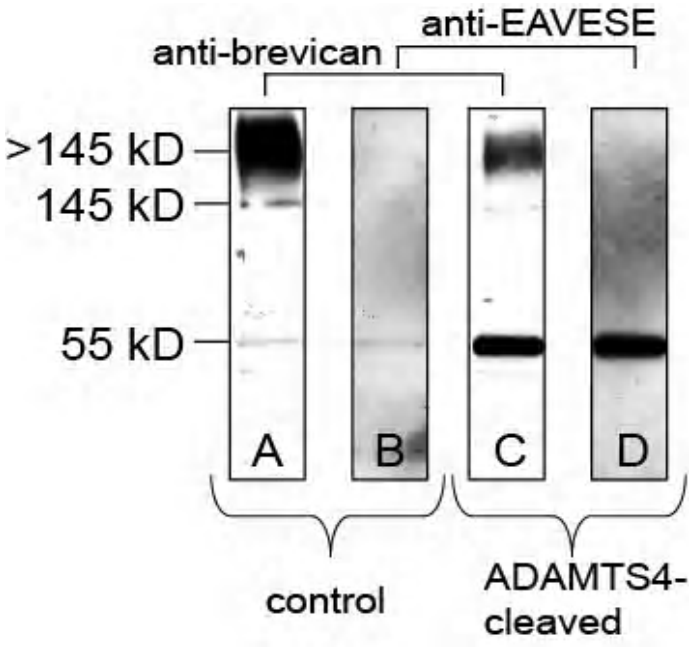

Figure 4. Western blot of brevican, EAV(M)ESE, and *Wisteria floribunda* agglutinin (WFA) in rodent brain extracts before and after chondroitinase digestion: Rat (rt) and mouse (ms) extracts were probed for anti-brevican (A), anti-EAVESE (B, left column) and anti-EAMESE (B, right column), and with biotinylated WFA (C): Samples were treated with (+) and without (-) chondroitinase (Ch'ase) ABC. The 145 kD core protein of brevican increased after chondroitinase treatment (A+ lanes), the proteolytic fragment remained unchanged (B+ lanes), and WFA was only slightly affected by this enzymatic process (C+ lanes). After probing with WFA, multiple unknown lower molecular weight bands were observed along with the classical high molecular weight sugar-containing moieties. The third column in (C) was probed with secondary, HRP-conjugated streptavidin alone, which revealed two, major non-specific bands. After differential centrifugation of rat brain tissue (D), brevican immunoreactivity (left panel) was predominately found in the soluble fraction (S), whereas most of the WFA reactivity (right panel) was observed in the membrane "insoluble" fraction (I) and EAVESE was evident in both fractions (middle panel). Rat and mouse samples were enzymatically-treated with chondroitinase (Ch'ase) in the absence or presence of a protease inhibitor cocktail (E, left panel). The high molecular weight smear is eliminated after treatment with chondroitinase. The same membrane was probed with anti-brevican where a complete removal of CS chains led to an increase in abundance of the core protein (E, right panel) with no change in the abundance of fragment.

Chapter 1, Figure 4

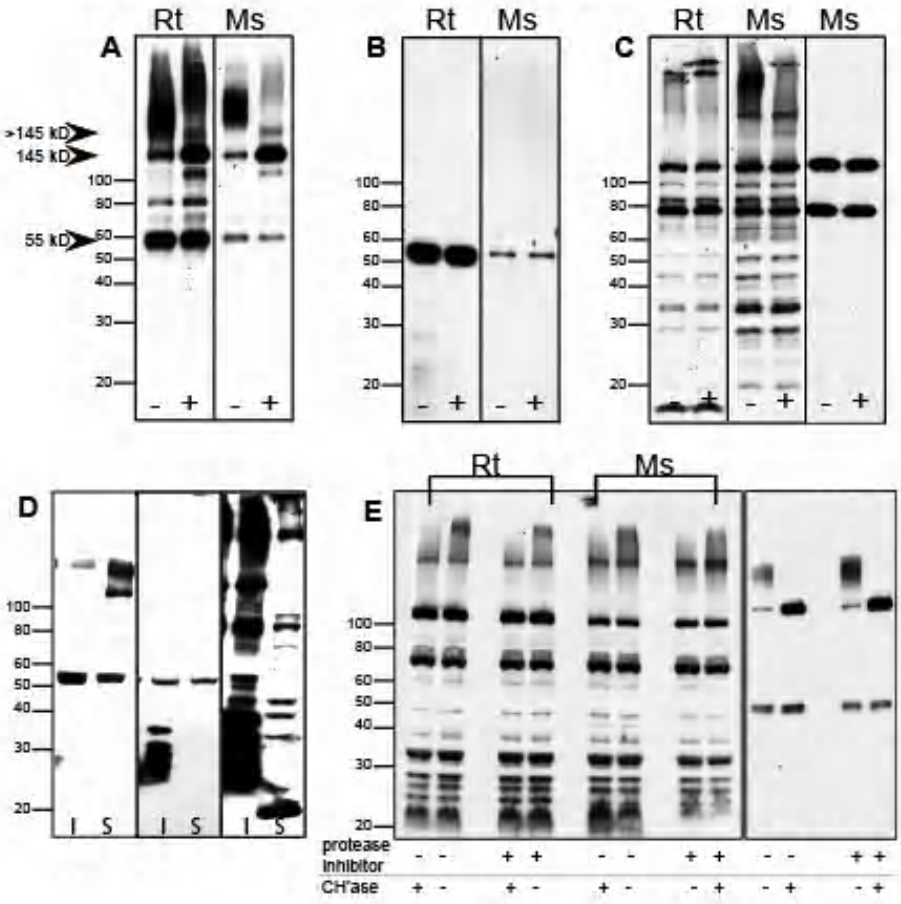

Figure 5. Western blot of brevican, EAMESE, and *Wisteria floribunda* agglutinin (WFA) in extracts from various regions of mouse brain before and after chondroitinase digestion: Several mouse brain regions (cerebellum (CB), hippocampus (HC), brain stem (BS), temporal lobe (TL) and diencephalon (DE) were probed for anti-brevican (A), anti-EAMESE (B) and WFA (C). Samples were treated with (+) and without (-) chondroitinase ABC. The 145 kD core protein of mouse brevican increased after chondroitinase treatment (A, +lanes), the proteolytic fragment remained unchanged (B, +lanes), and high molecular weight bands after biotinylated WFA were only slightly affected by this enzymatic process (C, +lanes). These effects were consistent in most regions examined.

Chapter 1, Figure 5

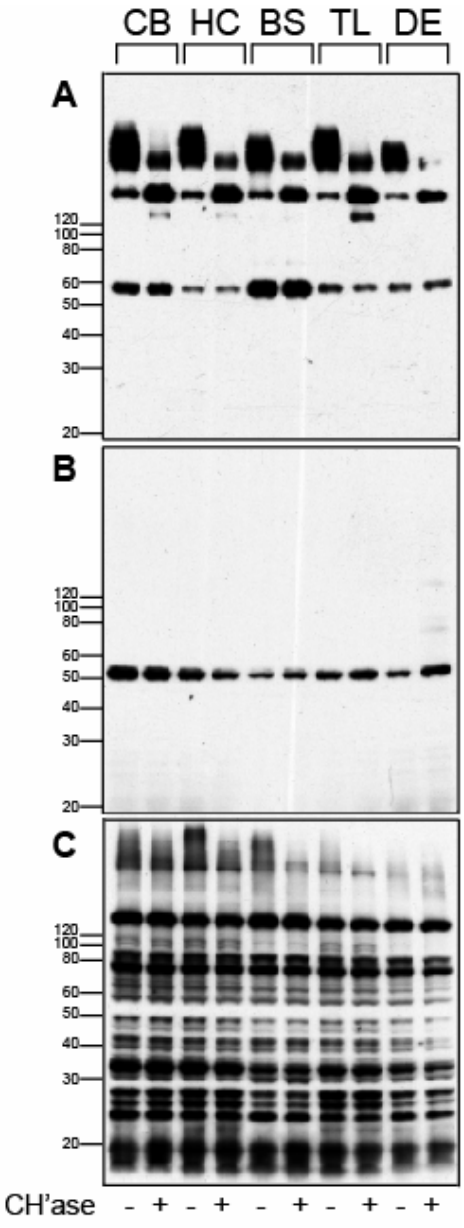

Figure 6. Binding of *Wisteria floribunda* agglutinin (WFA) lectin to fixed tissue sections of rodent brain: effect of chondroitinase ABC: Rat and mouse hippocampal fixed tissue sections reactive for biotinylated WFA before (A and B) and after (C and D) chondroitinase treatment. Arrow = retrosplenial cortex; arrow head = parietal cortex. Note the near elimination of reactivity after digestion. All images were captured at 25x magnification. Marker represents 100um.

Chapter 1, Figure 6

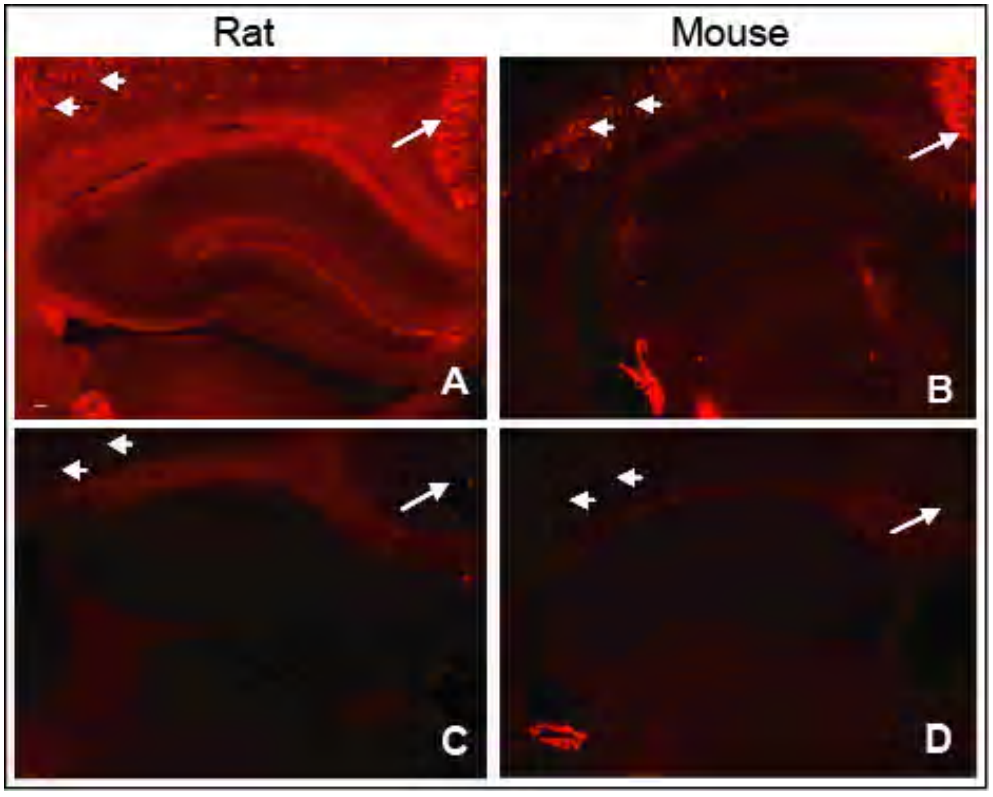

Figure 7. Localization of *Wisteria floribunda* agglutinin (WFA) and ADAMTS-derived fragment of brevican reactivity in rat and mouse brain: Reticular thalamic nuclei (A-F); Hippocampus (G-L); Cerebellum (M-R). Epifluorescent micrographs of WFA reactivity (A, D, G, J, M, and P), anti-EAVESE (rat) immunoreactivity (B, H, N), anti-EAMESE (mouse) immunoreactivity (E, K, Q) and merged composites of WFA and anti-EAVESE (C, I O), and WFA and anti-EAMESE (F, L, R) in fixed brain sections. Images A-L were captured at 25x magnification and M-R were captured at 100x magnification. Marker represents 100 μm.

Chapter 1, Figure 7

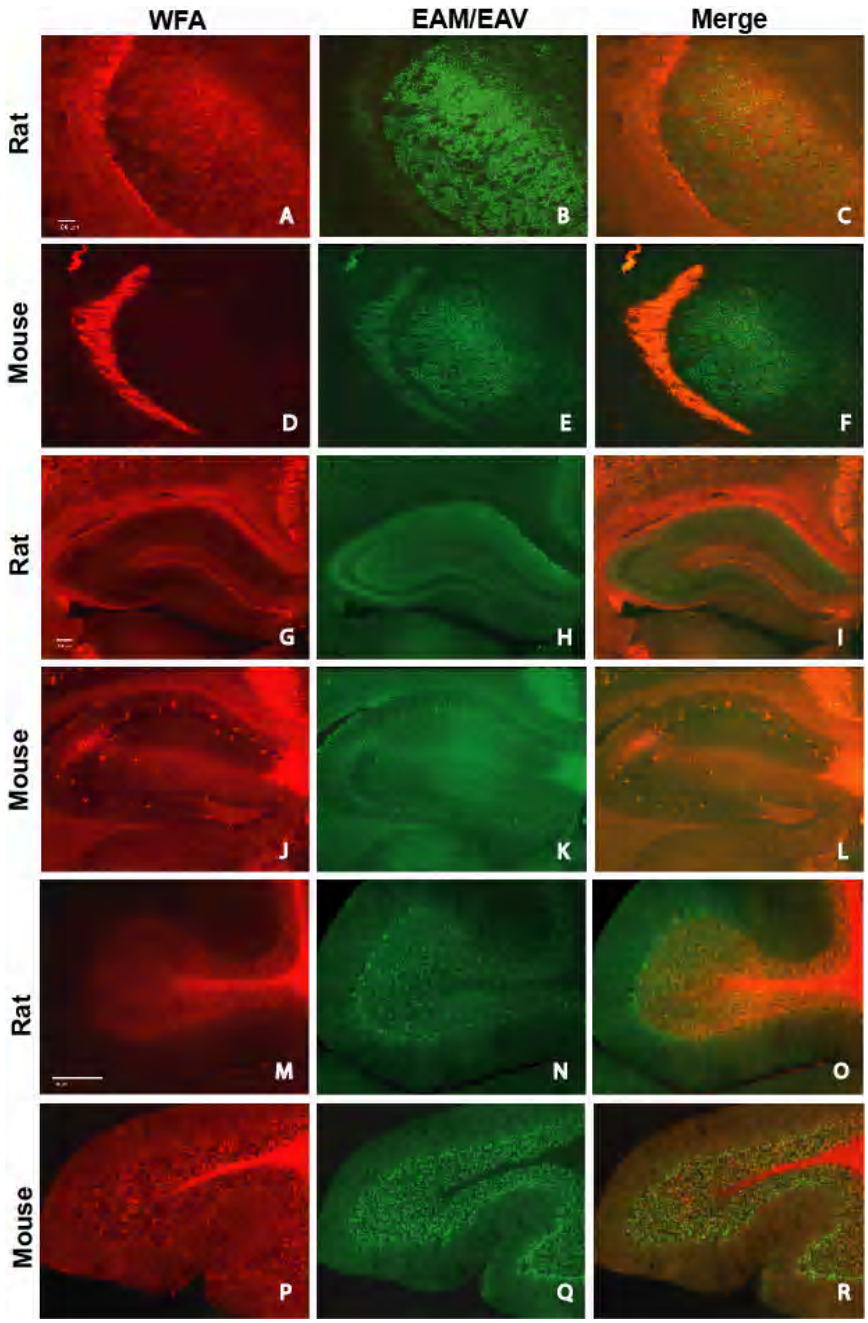

Figure 8. Localization of WFA and the ADAMTS-derived fragment of brevican reactivity in perineuronal nets: PNNs immunoreactive for the ADAMTS-derived fragment of brevican distinguished with anti-EAVESE were found in the horizontal limb of the diagonal band (A), the medial septum (B), and in piriform cortex (C). Immunoreactivity for anti-EAMESE in cerebral cortex (D) is broadly distributed, but especially prominent deep in cortical layer IV, which differs from the distinct pattern of WFA staining of PNNs (E). The most intense region of WFA reactivity appears in cortical layer III of primary somatosensory cortex (D-F). Scattered WFA positive PNNs are also found in layer V. Images A and C were captured at 400x magnification, B was captured at 200x magnification and D-F were captured at 100x magnification. Marker represents 100 μm.

Chapter 1, Figure 8

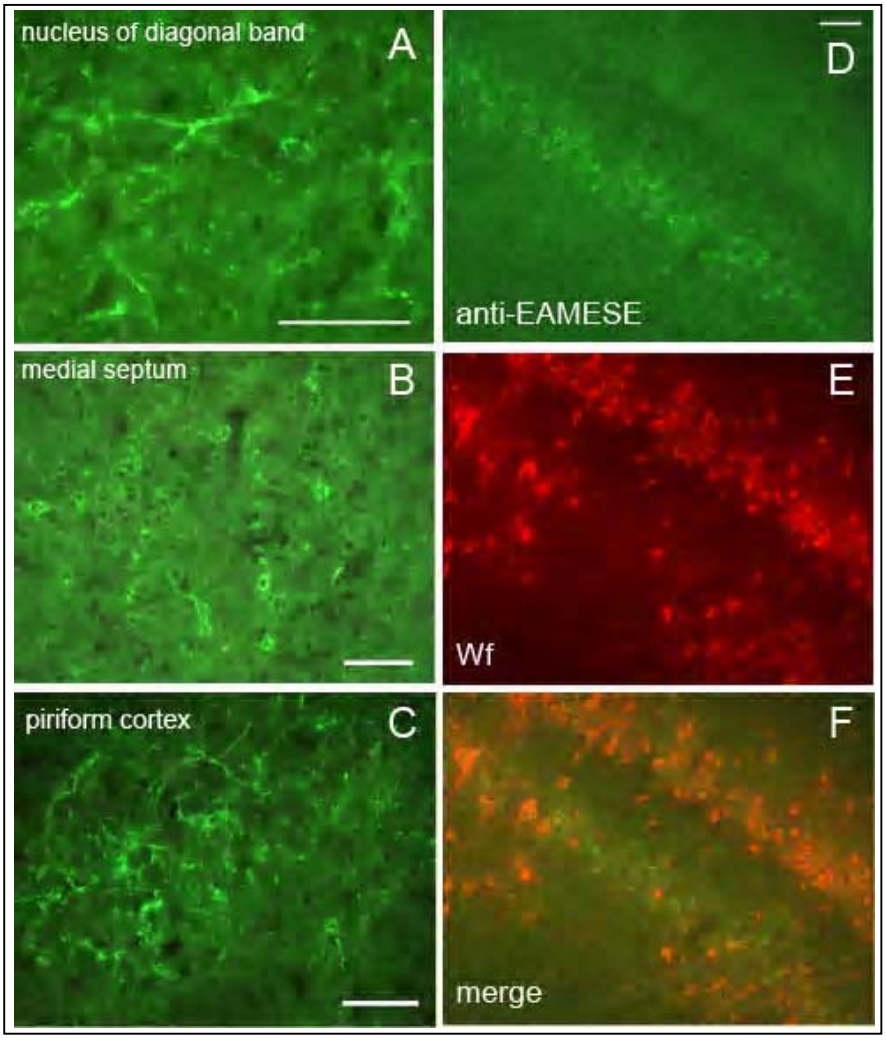

Figure 9. Localization of WFA and brevican reactivity in perineuronal nets: Brevican immunoreactivity was found in neuropil and PNNs of cortical layers II, III, deep layer IV and V (A and C). WFA immunoreactivity is predominant in PNNs of cortical layer III (B and C). A higher magnification of cortex reveals PNNs that are positive for brevican (D) and WFA reactivity (E). A confocal micrograph of retrosplenial cortex stained with anti-brevican, biotin-WFA and DAPI (G) demonstrates that there are clearly PNNs that co-localize and are reactive for both reagents (denoted by arrows). While the majority of these neurons appear PNN positive solely for brevican, it seems that neurons can also react with WFA binding moieties alone (denoted by asterisk). Images A-C were captured at 100x magnification, D-F were captured at 200x magnification and confocal image G was captured at 630x. Marker represents 100μm.

Chapter 1, Figure 9

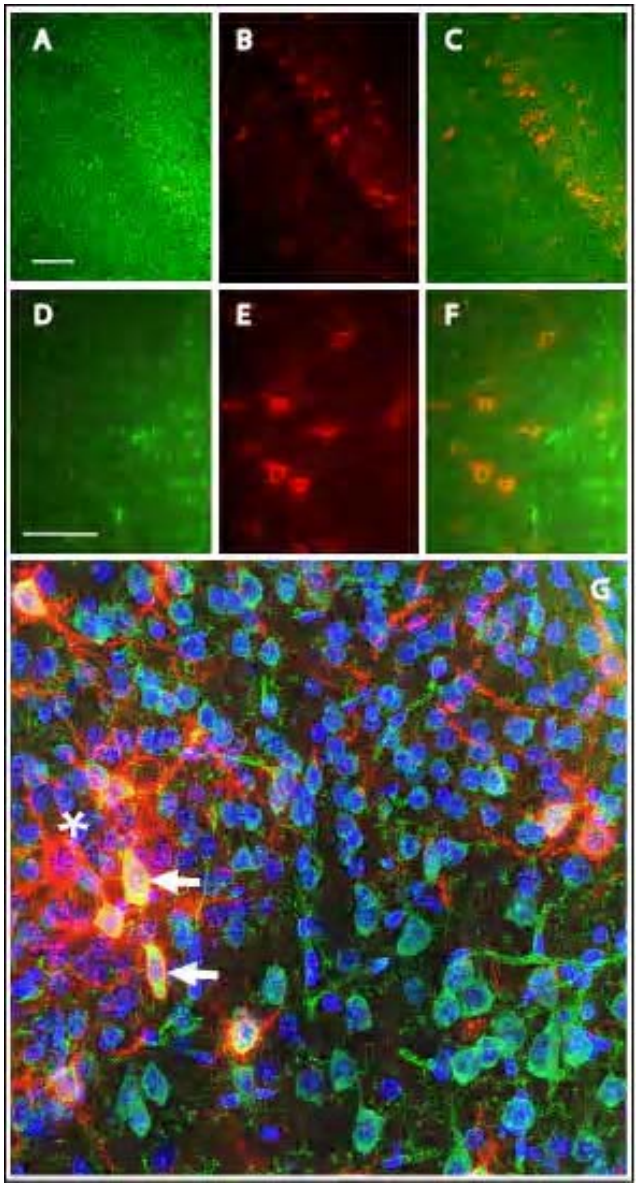

Table 1. Relative reactivity of *Wisteria floribunda* agglutinin (WFA), brevican, and the neoepitope of The ADAMTS-derived fragment of brevican, anti-EAVESE, in the adult rat [§ †].

	Wisteria	***floribunda***	**anti-**	**EAVESE**	**anti-**	**brevican**
	PNNs	neuropil	PNNs	neuropil	PNNs	neuropil
Thalamus						
Reticular nuc	++++	++++	-	+	+	+++
Ventral posterolateral nuc	+++	+++	+	+	+	+++
Ventral posteromedial nuc	+++	+++	++	++	+	++
Mammillo-tract-zona incerta	+	++++	+	++	+	++
Zona incerta	-	++	+	+	+	++
Lateral habenular nuc	-	++++	-	+	+	+
Hypothalamus						
Anterior hypothalamic area	+	+	-	-	-	++
Lateral hypothalamic area	-	+	-	+	+	++
Median eminence	NA	++	NA	+	NA	+
Anterior commissure	NA	++++	NA	+	NA	+
Fornix	NA	++++	NA	+	NA	++
Optic tract	NA	+++	NA	+++	NA	++
Dorsomedial nuc	++	+	+	+	+	+
Ventromedial nuc	++	++	+	+	+	+
Striatum						
Caudate putamen (striatal)	-	+++	+	+++	+	+++
Caudate putamen (hippocampal)	-	++	+	++	+	+++
Lateral globus pallidus	-	+	+	++	+	++
Medial globus pallidus	-	++	+	++	+	+++
Entopeduncular nuc	+	++++	-	+	-	+
Stria terminalis	-	+	-	-	-	+
Septal region						
Ventral limb of diag. band	++	+++	++	+	+	++
Medial septum	-	-	-	-	++	+
Lateral septum (dorsal)	+	++	++	+++	+	++
Lateral septum (intermediate)	+++	++	++	+	+	++
Lateral septum (ventral)	+	++	++	+++	+	++

Hippocampus						
Stratum oriens	-	++	++	+++	+++	+
CA1 pyramidal layer	+	NA	+	NA	+++	NA
CA2 pyramidal layer	++++	NA	++	NA	++	NA
CA3 pyramidal layer	++	NA	+	NA	+	NA
Stratum radiatum	-	-	+	++	+	+
Stratum lacunosum mol.	-	++	-	++	+	++
Dentate gyrus						
Outer molec. layer	-	+++	+	+	++	++
Middle molec. Layer	-	+	+	+	+	+
Inner molec. Layer	-	+++	+	++	-	+
Hilar interneurons	+	+	+	++	++	+
Granule neurons	++	NA	++	NA	+	NA
Hippocmapal fimbria	NA	+++	NA	-	NA	++
Cortex						
Retrospenial	++++	+	++	+++	+++	+++
Primary motor	+++	+	+	+	+	++
Somatosensory (parietal)	+++	++	++	+++	++	++
Piriform	-	+	-	++	+	++
Temporal	+++	+++	+	+	+	++
Perirhinial	+	+	-	+	+	++
Perirhinial (layer 1)	-	++++	+	-	+	++
Amygdala						
basolateral nuc	+	++	-	+	-	++
medial nuc	+	-	+	+++	+	+
lateral nuc	-	-	-	+	-	+
bed nuc-strial terminalis	+	++++	+	+++	+	+
entorhinal	+	++	+	+	++	++
corpus collosum	NA	++++	NA	-	NA	-
Cerebellum						
Folium						
Molecular Layer	NA	+	NA	+	NA	+
Purkinje cell layer	-	-	+	+++	+	++
Granule cell layer	++	+	+++	+	++	+
Deep white matter	NA	++++	NA	-	NA	+
Cerebellar Commissure						
Interposed nuc	+	+	++	++	++	++

Lateral (dentate) nuc	+	+	++	++	++	++
Medial (fastigial) nuc	+	+	++	+	++	++

§ All interpretations are within each individual reagent: [+] = 0-25%, [++] = 26-50%, [+++] = 51-75%, and [++++] = 76-100%.
† Brevican data is the result of the combined detection by the C-terminal and N-terminal globular domain recognizing antibodies.

Table 2. Relative reactivity of *Wisteria floribunda* agglutinin (WFA), brevican, and the neoepitope of the ADAMTS-derived fragment of brevican, anti-EAMESE, in the adult mouse § †.

	Wisteria	***floribunda***	**anti-**	**EAMESE**	**anti-**	**brevican**
	PNNs	neuropil	PNNs	neuropil	PNNs	neuropil
Thalamus						
Reticular nuc	++++	++++	-	-	++	-
Ventral posterolateral nuc	-	-	+++	+++	++	++
Ventral posteromedial nuc	-	+	+++	++	+++	+++
Mammillo-tract-zona incerta	-	++	-	-	-	+
Zona incerta	+	-	-	-	-	+
Lateral habenular nuc	+	+++	-	++	++	+
Hypothalamus						
Anterior hypothalamic area	+	+	-	-	-	+
Lateral hypothalamic area	++	-	+	++	+	++
Median eminence	NA	+	NA	-	NA	+
Anterior commissure	NA	+++	NA	-	NA	++
Fornix	NA	++	NA	-	NA	++
Optic tract	NA	+++	NA	+++	NA	++++
Dorsomedial nuc	++	-	-	-	++	+
Ventromedial nuc	-	++	-	-	++	+
Striatum						
Caudate putamen (striatal)	+	-	-	-	-	+
Caudate putamen (hippocampal)	+	++	+	+	-	+
Lateral globus pallidus	++	+	-	++	-	++
Medial globus pallidus	+	+++	-	++	-	++
Entopeduncular nuc	+	++	-	+	-	+
Stria terminalis	-	+	-	-	-	-
Septal region						

Ventral limb of diag. band	+	++	-	+	+	+
Medial septum	-	-	-	-	+	+
Lateral septum (dorsal)	+	-	+	-	++	+
Lateral septum (intermediate)	+++	+	+	-	++	+
Lateral septum (ventral)	+	-	-	-	++	+
Hippocampus						
Stratum oriens	-	++	-	-	-	+
CA1 pyramidal layer	++++	NA	-	NA	+	NA
CA2 pyramidal layer	+++	NA	+	NA	++	NA
CA3 pyramidal layer	+	NA	++	NA	+	NA
Stratum radiatum	+	+++	-	+	-	+
Stratum lacunosum mol.	-	+	-	+	-	++
Dentate gyrus						
Outer molec. layer	+	++	-	+	+	++
Middle molec. Layer	+	+	-	+	+	++
Inner molec. Layer	+	+	+	++	-	+
Hilar interneurons	++	++	++	+	+	++
Granule neurons	+	NA	+++	NA	-	NA
Hippocmapal fimbria	NA	+	NA	+	NA	++
Cortex						
Retrospenial	++++	++	++	+++	++	+++
Primary motor	+	-	-	+	-	+
Somatosensory (parietal)	++++	+++	+++	++	+++	++
Piriform	+	++	-	-	+	-
Temporal	+++	-	++	+	-	-
Perirhinial	+	-	-	+	+	++
Perirhinial (layer 1)	+	-	+	+	+	++
Amygdala						
basolateral nuc	-	+	-	+	-	+
medial nuc	++	+++	-	+	-	-
lateral nuc	-	-	-	-	-	+
bed nuc-strial terminalis	-	++	-	-	-	+
Entorhinal	+	+	+	++	++	++
Corpus collosum	NA	+++	NA	+++	NA	+
Cerebellum						
Folium						
Molecular Layer	NA	+	NA	+	NA	+
Purkinje cell layer	+	++	+	++	+	+
Granule cell layer	++	+	+++	+	++	+
Deep white matter	NA	++++	NA	-	NA	-
Cerebellar Commissure						

Interposed nuc	+	+	++	++	++	+
Lateral (dentate) nuc	+	+	++	++	+	+
Medial (fastigial) nuc	+	+	++	+	+	+

[§] All interpretations are within each individual reagent: [+] = 0-25%, [++] = 26-50%, [+++] = 51-75%, and [++++] = 76-100%.
[†] Brevican data is the result of the combined detection by the C-terminal and N-terminal globular domain recognizing antibodies.

REFERENCES CITED

Aya-ay J, Mayer J, Eakin AK, Muffly BG, Anello M, Sandy JD, Gottschall PE (2005) The effect of hypoxic-ischemic brain injury in perinatal rats on the abundance and proteolysis of brevican and NG2. Exp Neurol 193:149-162.

Bandtlow CE, Zimmermann DR (2000) Proteoglycans in the developing brain: new conceptual insights for old proteins. Physiol Rev 80:1267-1290.

Bertolotto A, Manzardo E, Iudicello M, Lovisetto C, Riccio A (1995) Disappearance of the Vicia villosa-positivity from the perineuronal net containing chondroitin proteoglycan after chondroitinase digestion. Brain Res 673:344-348.

Brauer K, Hartig W, Bigl V, Bruckner G (1993) Distribution of parvalbumin-containing neurons and lectin-binding perineuronal nets in the rat basal forebrain. Brain Res 631:167-170.

Bruckner G, Grosche J, Hartlage-Rubasamen, Schmidt S, Schachner M (2003) Region and lamina-specific distribution of extracellular matrix proteoglycans, hyaluronan and tenascin-R in the mouse hippocampal formation. J Chem Neuroanat 26:37-50.

Bruckner G, Seeger G, Brauer K, Hartig W, Kacza J, Bigl V (1994) Cortical areas are revealed by distribution patterns of proteoglycan components and parvalbumin in the Mongolian gerbil and rat. Brain Res 658:67-86.

Bruckner G, Hartig W, Kacza J, Seeger J, Welt K, Brauer K (1996) Extracellular matrix organization in various regions of rat brain gray matter. J Neurocytol 25:333-346.

Bruckner G, Bringmann A, Hartig W, Koppe G, Delpech B, Brauer K (1998) Acute and long-lasting changes in extracellular-matrix chondroitin-sulphate proteoglycans induced by injection of chondroitinase ABC in the adult rat brain. Exp Brain Res 121:300-310.

Corvetti L, Rossi F (2005) Degradation of chondroitin sulfate proteoglycan induces sprouting of intact Purkinjie axons in the cerebellum of hte adult rat. J Neurosci 25:7150-7158.

Cross AK, Haddock G, Surr J, Plumb J, Bunning RA, Buttle DJ, Woodroofe MN (2006) Differential expression of ADAMTS-1, -4, -5 and TIMP-3 in rat spinal cord at different stages of acute experimental autoimmune encephalomyelitis. J Autoimmun 26:16-23.

Deepa SS, Carulli D, Galtrey C, Rhodes K, Fukuda J, Mikami T, Sugahara K, Fawcett JW (2006) Composition of perineuronal net extracellular matrix in rat brain: a different disaccharide composition for the net-associated proteoglycans. J Biol Chem 281:17789-17800.

Gao G, Westling J, Thompson VP, Howell TD, Gottschall PE, Sandy JD (2002) Activation of the proteolytic activity of ADAMTS4 (aggrecanase-1) by C-terminal truncation. J Biol Chem 277:11034-11041.

Goldstein I, Poretz R (1986) Isolation, Physiochemical Characterization, and Carbohyfrate-Binding Specificity of Lectins. In: The Lectins: Properties, Functions, and Applications in Biology and Medicine (Liener I, Sharon N, Goldstein I, eds), pp 33-247. Orlando: Academic Press, Inc.

Gottschall PE, Sandy JD, Zimmermann DR (2005) Chapter 4: Substrates for metalloproteinases in the central nervous system. In: Matrix metalloproteinases in the central nervous system. (Conant K, Gottschall PE, eds), pp 87-118. London: Imperial College Press.

Hamel MG, Mayer J, Gottschall PE (2005) Altered production and proteolytic processing of brevican by transforming growth factor beta in cultured astrocytes. Journal of Neurochemistry 93:1533-1541.

Herndon ME, Lander AD (1990) A diverse set of developmentally regulated proteoglycans is expressed in the rat central nervous system. Neuron 4:949-961.

Hockfield S, Kalb RG, Zaremba S, Fryer H (1990) Expression of neural proteoglycans correlates with the acquisition of mature neuronal properties in the mammalian brain. Cold Spring Harb Symp Quant Biol 55:505-514.

Horn AK, Bruckner G, Hartig W, Messoudi A (2003) Saccadic omnipause and burst neurons in monkey and human are ensheathed by perineuronal nets but differ in their expression of calcium-binding proteins. J Comp Neurol 455:341-352.

Jaworski DM, Kelly GM, Hockfield S (1999) Intracranial injury acutely induces the expression of the secreted isoform of the CNS-specific hyaluronan-binding protein BEHAB/brevican. Exp Neurol 157:327-337.

Koppe G, Bruckner G, Hartig W, Delpech B, Bigl V (1997a) Characterization of proteoglycan-containing perineuronal nets by enzymatic treatments of rat brain sections. Histochem J 29:11-20.

Koppe G, Bruckner G, Brauer K, Hartig W, Bigl V (1997b) Developmental patterns of proteoglycan-containing extracellular matrix in perineuronal nets and neuropil of the postnatal rat brain. Cell Tissue Res 288:33-41.

Lemons ML, Sandy JD, Anderson DK, Howland DR (2001) Intact aggrecan and fragments generated by both aggrecanse and metalloproteinase-like activities are present in the developing and adult rat spinal cord and their relative abundance is altered by injury. J Neurosci 21:4772-4781.

Lemons ML, Barua S, Abanto ML, Halfter W, Condic ML (2005) Adaptation of sensory neurons to hyalectin and decorin proteoglycans. J Neurosci 25:4964-4973.

Lundell A, Olin AI, Morgelin M, al-Karadaghi S, Aspberg A, Logan DT (2004) Structural basis for interactions between tenascins and lectican C-type lectin domains: evidence for a crosslinking role for tenascins. Structure 12:1495-1506.

Matthews RT, Gary SC, Zerillo C, Pratta M, Solomon K, Arner EC, Hockfield S (2000) Brain-enriched hyaluronan binding (BEHAB)/brevican cleavage in a glioma cell line is mediated by a disintegrin and metalloproteinase with thrombospondin motifs (ADAMTS) family member. Journal of Biological Chemistry 275:22695-22703.

Mayer J, Hamel MG, Gottschall PE (2005) Evidence for proteolytic cleavage of brevican by the ADAMTSs in the dentate gyrus after excitotoxic lesion of the mouse entorhinal cortex. BMC Neurosci 6:52.

Murakami T, Murakami S, Fuyama Y, Taguchi T, Ohtsuka A (2001) The extracellular matrix in the mature brain: its reactions to endo-alpha-N-acetylgalactosaminidase and collagenase. Ital J Anat Embryol 106:475-480.

Murakami T, Ohtsuka A, Su WD, Taguchi T, Oohashi T, Murakami T, Abe K, Ninomiya Y (1999) The extracellular matrix in the mouse brain: its reactions to endo-alpha-N-acetylgalactosaminidase and certain other enzymes. Arch Histol Cytol 62:273-281.

Porter S, Clark IM, Kevorkian L, Edwards DR (2005) The ADAMTS metalloproteinases. Biochemical Journal 386:15-27.

Sasaki M, Seo-Kiryu S, Kato R, Kita S, Kiyama H (2001) A disintegrin and metalloprotease with thrombospondin type1 motifs (ADAMTS-1) and IL-1 receptor type 1 mRNAs are simultaneously induced in nerve injured motor neurons. Brain Research Molecular Brain Research 89:158-163.

Schmalfeldt M, Bandtlow CE, Dours-Zimmermann MT, Winterhalter KH, Zimmermann DR (2000) Brain derived versican V2 is a potent inhibitor of axonal growth. J Cell Sci 113 (Pt 5):807-816.

Seidenbecher CI, Gundelfinger ED, Bockers TM, Trotter J, Kreutz MR (1998) Transcripts for secreted and GPI-anchored brevican are differentially distributed in rat brain. Eur J Neurosci 10:1621-1630.

Tortorella MD, Burn TC, Pratta MA, Abbaszade I, Hollis JM, Liu R, Rosenfeld SA, Copeland RA, Decicco CP, Wynn R, Rockwell A, Yang F, Duke JL, Solomon K, George H, Bruckner R, Nagase H, Itoh Y, Ellis DM, Ross H, Wiswall BH, Murphy K, Hillman MC, Jr., Hollis GF, Newton RC, Magolda RL, Trzaskos JM, Arner EC (1999) Purification and cloning of aggrecanase-1: a member of the ADAMTS family of proteins.[see comment][comment]. Science 284:1664-1666.

Wegner F, Hartig W, Bringmann A, Grosche J, Wohlfarth K, Zuschratter W, Bruckner G (2003) Diffuse perineuronal nets and modified pyramidal cells immunoreactive for glutamate and the GABA(A) receptor alpha1 subunit form a unique entity in rat cerebral cortex. Exp Neurol 184:705-714.

Westling J, Gottschall PE, Thompson VP, Cockburn A, Perides G, Zimmermann DR, Sandy JD (2004) ADAMTS4 (aggrecanase-1) cleaves human brain versican V2 at Glu405-Gln406 to generate glial hyaluronate binding protein. Biochemical Journal 377:787-795.

Westling J, Fosang AJ, Last K, Thompson VP, Tomkinson KN, Hebert T, McDonagh T, Collins-Racie LA, LaVallie ER, Morris EA, Sandy JD (2002) ADAMTS4 cleaves at the aggrecanase site (Glu373-Ala374) and secondarily at the matrix metalloproteinase site (Asn341-Phe342) in the aggrecan interglobular domain. J Biol Chem 277:16059-16066.

Yamada H, Watanabe K, Shimonaka M, Yamaguchi Y (1994) Molecular cloning of brevican, a novel brain proteoglycan of the aggrecan/versican family. Journal of Biological Chemistry 269:10119-10126.

Yamada H, Fredette B, Shitara K, Hagihara K, Miura R, Ranscht B, Stallcup WB, Yamaguchi Y (1997) The brain chondroitin sulfate proteoglycan brevican associates with astrocytes ensheathing cerebellar glomeruli and inhibits neurite outgrowth from granule neurons. J Neurosci 17:7784-7795.

Yamaguchi Y (1996) Brevican: a major proteoglycan in adult brain. Perspect Dev Neurobiol 3:307-317.

Yamaguchi Y (2000) Lecticans: organizers of brain extracellular matrix. Cell Mol Life Sci 57:276-289.

Young NM, Williams RE (1985) Assignment of lectins specific for D-galactose or N-acetyl-D-galactosamine to two groups, based on their circular dichroism. Can J Biochem Cell Biol 63:268-271.

Yuan W, Matthews RT, Sandy JD, Gottschall PE (2002) Association between protease-specific proteolytic cleavage of brevican and synaptic loss in the dentate gyrus of kainate-treated rats. Neuroscience 114:1091-1101.

CHAPTER 2

EVIDENCE FOR PROTEOLYTIC CLEAVAGE OF BREVICAN BY THE ADAMTSs IN THE DENTATE GYRUS AFTER EXCITOTOXIC LESION IN THE MOUSE ENTORHINAL CORTEX

Joanne Mayer, Michelle G. Hamel, Paul E. Gottschall

Department of Molecular Pharmacology & Physiology, University of South Florida, Tampa, Florida, 33612

This work was published in *BMC Neuroscience,* 2005 Aug 25; 6:52

Acknowledgments: The authors would like to acknowledge that this work was supported in part by Alzheimer's Association Grant IIRG-02-3758 and a grant from the Shriner's Hospitals (research grant #8850). Dr. John Sandy (Shriner's Hospital, Tampa, FL) was instrumental in the conceptual development of the neoepitope antibody.

ABSTRACT

Background: Brevican is a member of the lectican family of aggregating extracellular matrix (ECM) proteoglycans that bear chondroitin sulfate (CS) chains. It is highly expressed in the central nervous system (CNS) and is thought to stabilize synapses and inhibit neural plasticity and as such, neuritic or synaptic remodeling would be less likely to occur in regions with intact and abundant, lectican-containing, ECM complexes. Neural plasticity may occur more readily when these ECM complexes are broken down by endogenous proteases, the ADAMTSs (a disintegrin and metalloproteinase with thrombospondin motifs), that selectively cleave the lecticans. The purpose of these experiments was to determine whether the production of brevican or the ADAMTS-cleaved fragments of brevican were altered after deafferentation and reinnervation of the dentate gyrus via entorhinal cortex lesion (ECL). *Results:* In the C57Bl6J mouse, synaptic density in the molecular layer of the dentate gyrus, as measured by synaptophysin levels in ELISA, was significantly attenuated 2 days (nearly 50% of contralateral) and 7 days after lesion and returned to levels not different from the contralateral region at 30 days. Immunoreactive brevican in immunoblot was elevated 2 days after lesion, whereas there was a significant increase in the proteolytic product at 7, but not 30 days post-lesion. ADAMTS activity, estimated using the ratio of the specific ADAMTS-derived brevican fragment and intact brevican levels was increased at 7 days, but was not different from the contralateral side at 2 or 30 days after deafferentation. *Conclusion:* These findings indicate that ADAMTS activity in the dentate outer molecular layer (OML)

is elevated during the initial synaptic reinnervation period (7 days after lesion). Therefore, proteolytic processing of brevican appears to be a significant extracellular event in the remodeling of the dentate after EC lesion, and may modulate the process of sprouting and/or synaptogenesis.

Key words : extracellular matrix, synaptic plasticity, proteoglycan, ADAMTS, perineuronal nets

INTRODUCTION

Neurons of the entorhinal cortex (EC) send unidirectional, afferent projections to the hippocampus, where terminals synapse on granule cell dendrites in the outer molecular layer (OML) of the dentate gyrus (van Groen et al., 2003). Interruption of entorhinal input to the dentate gyrus, by chemical lesion or severing the afferent fibers, causes anterograde degeneration of the axon terminals and stimulates sprouting of viable fibers from this and other neuronal circuits (Steward, 1994; Frotscher et al., 1996; Deller et al., 2001; Del Turco et al., 2003). The entorhinal cortex lesion (ECL) has been used as a model of neural plasticity for more than three decades (Lynch et al., 1972). To identify and innervate a target after injury or during development, growing neuron terminals must traverse through a complex extracellular milieu that consists of soluble factors, cell surface adhesive ligands and an extracellular matrix (ECM) along the way toward its target. The growing terminal samples this milieu, and appropriate protein-protein binding and activation regulates the direction and

extent of growth, terminal sprouting, and likely synaptogenesis. For example, certain ECM molecules such as laminin are permissive toward neurite outgrowth, whereas others, such as the highly negatively charged, proteoglycans (PGs) substituted with chondroitin sulfate (CS) (ie. versican, neurocan, aggrecan and brevican, in general, lecticans), inhibit neurite outgrowth on permissive substrates (Snow et al., 1990; Bandtlow and Zimmermann, 2000; Rauch, 2004). Interestingly, the expression of several lecticans, including brevican is markedly up-regulated during the neural plasticity response that occurs following ECL (Thon et al., 2000).

The lectican PGs are the most abundant ECM molecules in the adult, uninjured central nervous system (CNS) and of these brevican is the most highly expressed (Yamaguchi, 1996; Bruckner et al., 2003). Brevican and other lecticans are found in perineuronal nets and throughout the neuropil and are components of ECM aggregate complexes that are thought to stabilize synapses in neural networks and inhibit neurite outgrowth (Hockfield et al., 1990; Yamaguchi, 2000). Most evidence suggests that the CS component in these complexes provides the inhibitory signal toward neurite outgrowth, although the protein core plays a role as well (Snow and Letourneau, 1992; Bandtlow and Zimmermann, 2000). However, proteolytic cleavage of the brevican core protein may "loosen" the aggregated complexes and change the extracellular environment to one that is more permissive for neural plasticity to occur (Yamaguchi, 2000; Yuan et al., 2002; Gottschall et al., 2005). A significant proportion of brevican in the adult CNS exists as a fragment formed by

proteolytic cleavage of the protein core, suggesting that this mechanism may play a role in experience-dependent and other forms of neural plasticity in the uninjured, adult. In addition, in disorders such as Alzheimer's disease, alterations in the ECM may be related to diminished synaptic plasticity and therefore play a role in cognitive dysfunction.

The metalloproteinases responsible for cleavage of lectican core proteins and the generation of fragments of aggrecan, brevican, and versican have been cloned and belong to a family of proteins, termed the ADAMTSs (a disintegrin and metalloproteinase with thrombospondin motifs), that include glutamyl endopeptidases. ADAMTS1 and ADAMTS4 are prominently expressed in rat brain (Yuan et al., 2002) and cleave the 145 kD intact core protein of brevican into a 55 kD N-terminal, and an 80 kD C-terminal fragment (Matthews et al., 2000; Nakamura et al., 2000) (see Fig. 2). The ADAMTS-derived 55 kD fragment may be distinguished from total cleaved fragment (cleaved by other proteinases) using a neoepitope antibody raised against the distinctive C-terminal sequence (EAMESE, murine sequence) of the N-terminal, 55 kD fragment (see Fig. 2, "C") that is generated by glutamyl endopeptidase cleavage. Using this antibody, *in vivo* ADAMTS activity may be estimated by expressing the amount of ADAMTS-derived brevican fragment as a proportion of total intact brevican.

Others have demonstrated changes in the levels and activity of matrix metalloproteinases (MMPs) in the deafferented neuropil after various lesions, however in these experiments, the substrate proteolytically processed by the

MMPs was not identified (Phillips and Reeves, 2001; Szklarczyk et al., 2002). Nonetheless, changes in structure and function that were associated with lesion-induced sprouting were reversed by MMP inhibitors (Reeves et al., 2003). Lesions produced by systemic injection of kainic acid produce wide-spread neuronal degeneration in the CNS, including the EC and stimulate expression of the MMPs and the ADAMTSs (Zhang et al., 1997; Yuan et al., 2002). In response to this lesion, the abundance of the neoepitope fragment generated by ADAMTS-cleavage of brevican was markedly elevated in the OML of the dentate gyrus. This increase was preceded by elevated ADAMTS1 and ADAMTS4 mRNA expression in dentate granule neurons (Yuan et al., 2002). Although these results suggest that proteolytic processing of brevican appears to be a significant extracellular event in the remodeling of the dentate after ECL, because of the widespread neuronal death, it was difficult to associate these two particular endpoints as individual, yet associated events involved in neural plasticity. Thus, we decided to employ the classical ECL model in the C57Bl6 mouse, thereby discretely disrupting synaptic innervation of the molecular layer of the dentate gyrus. Our intention was to observe any altered expression of brevican and the ADAMTSs that may be associated with reinnervation of the injured area 2, 7 and 30 days after lesion.

MATERIALS & METHODS

Animals

All animal procedures described here were approved by the Institutional

Animal Care and Use Committee at the University of South Florida. Sixty-two adult male C57Bl6 mice (23 g - 27 g; Harlan, Indianapolis, IN), 12 weeks of age were housed under a 12 h light cycle with regulated temperature and humidity. Mice were housed 3 to 4 per cage and had free access to food and water. Following ECL surgery, the animals were housed individually. Brains from control mice (n=4) and lesioned mice surviving for 2 days (n=6), 7 days (n=5) and 30 days (n=5) after the lesion were perfusion fixed and collected for immunohistochemistry. Tissue extracts of dentate gyrus and EC lesioned animals collected 2 days (n=6), 7 days (n=5) and 30 days (n=6) after surgery were used in Western blot and biochemical immunoassays. For those animals that received a unilateral ECL, the contralateral, non-lesioned hemisphere was considered the control for immunohistochemistry and biochemical analysis.

Surgical procedures - the entorhinal cortex lesion (ECL)

Surgeries were performed using isofluorane /oxygen mixed gas anesthesia. Once deeply anesthetized, animals were placed into the stereotaxic apparatus. A hole was drilled in the skull of the right hemisphere to allow for needle penetration. The right, lateral EC of mice was unilaterally lesioned by lowering a needle attached to a Hamilton syringe (#701N) filled with ibotenic acid through the hole in the skull to the coordinates AP = 4.72 mm, L = 3.75 mm and DV = 4.70 mm using bregma as a reference and oriented 17^{o} rostral-caudal (White et al., 2001). One µl of the neurotoxin, ibotenic acid ((±) α-Amino-3-hydroxy-5-isoxazoleacetic acid, 10 µg/µl) was injected into the lateral EC at a

rate of 0.1 µl every 30 seconds, with the needle remaining in place for an additional minute at the end of the 5 min injection period to allow for complete diffusion of the drug into the lateral EC. Neurons of the lateral EC project preferentially to the septal dentate gyrus. The needle was removed, bone wax used to cover the skull hole, and the animal was allowed to recover on a heating pad after which the animal was returned to a new cage and housed individually. At 2, 7 and 30 days after lesion, mice were injected with an overdose of Nembutal (pentobarbital) for deep anesthesia, perfused transcardially with cold phosphate-buffered saline (pH 7.4) followed by cold 4% paraformaldehyde fixative diluted in 0.1 M phosphate buffer (pH 7.4). The brain was dissected from the skull, post-fixed in 4% paraformaldehyde overnight at 4^{o}C, cryoprotected with consecutive solutions of 15 and 30% sucrose until completely infused, and the cryoprotected brain was sectioned on a cryostat at 30 µm. The extent and magnitude of the lesion in the EC was verified by cresyl violet and brevican staining. Synaptophysin and GFAP immunohistochemistry, using horseradish peroxidase amplification and diaminobenzidine as a chromogen, verified the loss of terminals in the molecular layer of the dentate gyrus.

Region isolation method

A method was developed to isolate dentate gyrus and EC tissue in mouse brain. This method eliminates the collection of much of the surrounding tissue that was unaffected by ECL. The dentate gyrus was subjected to synaptophysin ELISA as a measure of synaptic loss in the molecular layer. The EC underwent

Western blot for PSD-95 (post-synaptic density-95) to quantitate the magnitude of the lesion. In addition, brevican and EAMESE Western blot was conducted on dentate gyrus tissue. Animals were completely anesthetized with a lethal dose of Nembutal (pentobarbital, Abbott Laboratories, North Chicago, IL), the brain was quickly removed and placed on a glass microscope slide, and a millimeter ruler was placed adjacent to the brain to assist in measuring the thickness of slices. Whole brain was dissected and frozen on a flat slab of dry ice for about 5 minutes (a point at which the brain surface is no longer shiny), being careful not to over-freeze the tissue, but to reach a temperature at which the tissue can be easily and efficiently cut into 2 mm coronal slabs. Two 2 mm coronal slabs are cut by referencing the most caudal of cerebral cortex as a land mark, making a coronal cut, moving rostrally 2 mm and making another cut to obtain the first slab for the EC isolation. A third cut was made 2 mm rostral from the previous slice and this slab contained the septal hippocampus and was used to isolate the dentate gyrus. The 2 mm hippocampal slab (outlined in Fig. 10 C) was placed on a glass slide, and the dentate gyrus was localized using a stereomicroscope. The dentate was punctured with a blunt-ended 22 gauge needle (Fig. 10 A) using the medial point of the wings as a landmark. A blunt-ended 18 gauge needle was used in the same manner to puncture and collect the EC from a 2 mm slab caudal to the slab used to collect the dentate gyrus (Fig. 10 B). The frozen tissues were immediately expelled from the needle by attaching an air-loaded syringe to the needle and forcing the tissue into the bottom of a microfuge tube. The dentate gyrus and EC tissues were then homogenized in extraction buffer

(20nM Tris-HCL pH=7.4, 5mM EDTA, 1% Triton-X-100, & 1:100 protease inhibitor; 20 µl for dentate gyrus and 40 µl for EC) using three cycles of 2 min of 4^{o}C incubation and 30 sec of vortex. The solubilized extract was centrifuged at 8000 rpm in a refrigerated microfuge for 3 min, the supernatant collected and frozen for later use in Western blotting and ELISA analysis.

Immunohistochemistry

Mice were anesthetized with an overdose of Nembutal (pentobarbital, Abbott Laboratories, North Chicago, IL) and their brains were fixed via standard cardiac perfusion methods. Briefly, the animal was cleared with phosphate buffered saline (PBS; pH 7.4) and fixed with 4% paraformaldehyde in 0.1M phosphate buffer (PB; pH 7.4). The brains were post-fixed overnight in the same fixative; cryoprotected with 15% sucrose (in 0.1M PB) followed by a 30% sucrose solution for 24 h each. Whole brain was frozen with mounting medium and cut into 30 µm coronal sections using a cryostat. Free-floating sections were washed with PBS, placed in a blocking / permeabilization solution (10% normal goat serum; 3% 1 M Lysine, 3% Triton-X) for 1 h, washed with PBS and incubated with primary antibody overnight at 4^{o}C. For detection of the antigen, sections were washed and incubated in secondary antibody solution (anti-rabbit or anti-mouse IgG conjugated to Alexa-Fluor 488 or 594, Molecular Probes, Eugene, OR) for 1 h. The sections were washed for 15 minutes, wet mounted onto Fisher SuperFrost Plus glass sides and coverslipped with VectaShield mounting medium (Vector Labs, Burlingame, CA). The primary antibodies or

probes used in these experiments were: mouse anti-brevican, raised against the G1 domain of brevican (BD Transduction Labs, San Jose, CA); rabbit anti-EAMESE, the ADAMTS-derived neoepitope of brevican developed in our lab; rabbit anti-glial fibrillary acidic protein (GFAP, DAKO, Carpinteria, CA); and rabbit anti-synaptophysin (DAKO).

Western blotting

Dentate gryus or EC extracts were loaded (equal amounts of protein and 2x sample buffer) on to 4-20% polyacrylamide gels (Invitrogen, Carlsbad, CA) and subjected to SDS-PAGE. Protein was transferred to a polyvinylidine difluoride membrane (PVDF, Immobilon, Millipore, Billerica, MA) and the membrane was blocked with 5% milk in PBS. Membranes were probed with primary antibodies against brevican (1:1000), EAM (1:500), and secondary anti-rabbit or anti-mouse IgG conjugated to horse radish peroxidase (Chemicon, Temecula, CA). Antigens were visualized using a chemiluminescence developing system (SuperSignal, Pierce, Rockford, IL).

Antibody generation

A rabbit antibody raised against the brevican neoepitope on the 55 kD N-terminal fragment derived from glutamyl endopeptidase activity of the ADAMTSs was generated by Sigma-Genosys (St. Louis, MO) and purified in our laboratory. The novel C-terminal sequence "QEAMESE" from the mouse was the neoepitope and the peptide used for antibody generation contained a glycine

spacer "GGGQEAMESE". This peptide was synthesized by Sigma-Genosys, conjugated to keyhole limpet hemocyanin at the N-terminus, and rabbits were subjected to standard immunization protocols. Serum collected after the 5th booster was titered against the peptide using a solid-phase system and specific antibody was purified using peptide affinity chromatography. Interestingly, antibody raised against the rat epitope "QEAVESE" did not recognize the mouse, ADAMTS-derived, "QEAMESE" epitope. On Western blot, the antibody against the mouse fragment recognized a single band at 55 kD in extracts from mouse brain and did not cross react with the intact brevican core protein.

RESULTS

Expression of ADAMTS-derived, brevican fragment

Brevican is an abundantly expressed PG in the CNS that is secreted from astrocytes and neurons as a 145 kD core protein that bears up to three, covalently-linked, CS chains (Fig. 11A). It is also is secreted as a 145 kD core protein without CS chains (Fig. 11B). When cleaved by extracellular glutamyl endopeptidases, the ADAMTSs, a 55 kD N-terminal fragment is formed that contains the unique C-terminal epitope EAMESE (Fig. 11C). Each of these isoforms of brevican was expressed in numerous regions of the CNS. Figure 12A shows a brevican immunoblot of several brain regions from an untreated C57Bl6 mouse. The >145 kD (brevican core plus CS) intact isoform, the 145 kD (brevican core) intact core protein and the generalized 55 kD N-terminal fragment were easily differentiated from one another on Western blot (Fig. 12A) using an

antibody that recognizes an epitope in the N-terminal globular domain (Fig. 11). In the mouse, all isoforms of brevican appeared to be more abundant in brain stem and cerebellum compared to other regions that were measured. Panel B shows a blot with the same extracts and probed using the anti-neoepitope EAMESE antibody. This antibody recognized the ADAMTS-derived, C-terminally truncated, 55 kD fragment with the novel C-terminal epitope EAMESE and did not recognize any of the intact, core brevican proteins (Fig. 12B). Thus, given the ability to quantitate the ADAMTS-derived brevican fragment and its intact substrates using immunoblot, regional *in vivo* ADAMTS activity may be estimated.

Deafferentation and neural plasticity in the dentate gyrus

To validate a complete deafferentation of synapses of the perforant path from the EC to the molecular layer of the dentate gyrus, animals were injected with ibotenic acid into the lateral EC, perfused with fixative, the brain sectioned, and immunostained for brevican. Brevican is a marker expressed by reactive glia in response to brain injury (Jaworski et al., 1999). Thus, after lesion, increased deposition of brevican would be expected in the ipsilateral EC. Brevican immunoreactivity was elevated at the lesion site (Figure 13B) compared to the contralateral, non-lesioned EC (Figure 13A).

Since an endpoint in this experiment is the reinnervation and sprouting of neurites and the formation of new synapses in the OML of the dentate gyrus, synaptophysin immunoreactivity, a vesicular pre-synaptic marker, was examined

two, seven, and thirty days post-lesion. On the contralateral side and in unlesioned mice, a tri-laminar synaptophysin staining pattern was observed that outlines the inner, middle and OMLs (Fig. 14B) of the dentate gyrus. Two days after ECL, there was a marked decline in synaptophysin immunoreactivity in the OML on the ipsilateral side of the dentate (Fig. 14A), that was reflected by a loss of the typical tri-laminar pattern of synaptophysin staining (Fig. 14B) with only the inner molecular layer clearly distinguishable. Seven days after ECL, synaptophysin immunoreactivity in the OML remained markedly reduced, although the pattern was similar to the contralateral side at 30 days (data not shown).

In response to injury and the deafferentation of synapses, there is an activation of astrocytes in the OML (Eng and Ghirnikar, 1994). Tissue immunostained with the astrocytic marker GFAP (glial fibrillary astrocytic protein), showed increased staining selectively in the OML of the dentate seven days after ECL (Fig. 14C) compared to the contralateral side (Fig. 14D). Although these markers may be sufficient to identify some level of diminished innervation to the OML, a synaptophysin ELISA and a specific method to isolate the tissue of the dentate gyrus (Fig. 10) was developed to better quantitate this loss.

Two days after lesion, synaptophysin levels as detected by ELISA, declined by 46% in the ipsilateral dentate compared to the contralateral side ($p=0.039$) (Fig. 14E). This trend was sustained at seven days post-lesion when synaptophysin levels were 41% of the contralateral value ($p=0.033$) (Fig. 14E). However, when tissue was examined thirty days post-lesion, synaptophysin

concentrations were not different from the control side. This observation shows there is a reinnervation of the OML after ECL (Fig. 14E).

The decline in the level of synaptophysin concentrations in the tissue from the "dentate punch" on the ipsilateral side compared to the contralateral side indicates that there was denervation of cortical input to the dentate molecular layer. The question of interest was, however, were there associated changes in the abundance and proteolysis of brevican in this region of neural plasticity?

Abundance and proteolysis of brevican after ECL

Brevican and its various isoforms were identified in immunoblots from isolated dentate gyrus tissue obtained from mice two, seven and thirty days after ECL. At two days post-lesion (Figure 15A), there was a 3-fold increase in the glycosaminoglycan (GAG)-containing form of brevican ($p=0.047$) in the dentate on the denervated side, and a trend for an increase in all the isoforms of brevican on this side. At seven days after insult, a time thought to be the initial synaptic reorganization period after ECL (Steward and Loesche, 1977), intact brevican had returned to contralateral levels, but there was a significant, almost 2-fold elevation in the ADAMTS-derived fragment of brevican in the dentate ($p=0.030$). In addition, there was a trend for an increase in the generalized 55 kD fragment of brevican (Fig. 15B) at this time point. Thirty days after undergoing surgery, all of the forms of brevican had returned to levels not different from the contralateral side; however, a slight increase in the GAG-containing, intact isoform was seen at this time point (Fig. 15C).

To estimate apparent ADAMTS activity *in vivo*, the density of the EAMESE (55 kD) immunoreactive fragment in Western blot was divided by the densitometric level of intact full-length and core protein brevican isoforms (>145 kD + 145 kD) (Fig. 16). Two days post-ECL there was a decrease in apparent ADAMTS activity in the ipsilateral dentate gyrus, however, at the seven day critical reinnervation period, ADAMTS activity was increased almost 50%. This observation is supported by the significant increase in the ADAMTS-derived, 55 kD fragment at this time point. By thirty days post-lesion, the activity was not different from the contralateral side. Thus, this data suggests that the ADAMTSs and the catabolism of brevican may play a prominent role in neural plasticity in the dentate gyrus after lesion of the EC in mice.

DISCUSSION

The purpose of this study was to determine whether the catabolism of brevican is involved in mechanisms of neural plasticity in the hippocampus, and to accomplish this, synaptic input to the OML of the dentate gyrus was denervated by excitotoxic lesion in the lateral EC. Two days after lesion, synaptic input into the OML was significantly reduced and this was accompanied by an increase in the production of full length, intact brevican. At seven days, while brevican levels returned to baseline, a significant increase in the ADAMTS-derived, C-terminally truncated, brevican fragment was observed during this initial, sprouting and reinnervation period. This implies that there was an increase in ADAMTS activity in the OML during the highly plastic, regenerative

phase. However at thirty days post-lesion, there was complete reinnervation of the OML on the ipsilateral side, as synaptic density, brevican and ADAMTS activity were not different from the contralateral side at this time point. These results indicate that the ADAMTSs and their substrate, brevican, that is abundant in the CNS, have a regulatory function in neural plasticity and support earlier data that had demonstrated important actions for the ADAMTSs in plasticity after seizure-induced hippocampal lesion (Yuan et al., 2002).

Previous studies have examined the role of matrix-altering proteases in synaptic plasticity after CNS lesion. The expression of the matrix metalloproteinases (MMPs), MMP-9 and MMP-2, have been shown to be increased in various regions of the hippocampus after seizure-induced lesion (Zhang et al., 1997; Zhang et al., 2000; Szklarczyk et al., 2002; Jourquin et al., 2003). MMP-3 concentrations were elevated in the molecular layer of the dentate after traumatic brain injury (Kim et al., 2005). More specifically after ECL, administration of a non-selective MMP inhibitor was able to diminish sprouting and synaptogenesis in the dentate OML (Reeves et al., 2003), suggesting a direct proteolytic role for the MMPs in this process. In adults, most MMP expression and activity is low and maintained throughout adulthood. After injury and during the recovery and regenerative phase, however, there is increased activity of MMPs derived from glia and neurons that is thought to facilitate axonal reinnervation, sprouting and/or synaptogenesis. Nonetheless, the mechanism(s) of action of the MMPs and the potential substrates on which they act to promote neural plasticity have yet to be determined in these models.

More recently, the activity and expression of the PG-degrading, ADAMTSs have been shown to be elevated in the OML after kainate-induced lesion. In contrast to the absence of a defined substrate for the MMPs, a selective ADAMTS-derived, brevican fragment was localized to the OML after seizure-induced lesion in the rat (Yuan et al., 2002). In the present study, a similar ADAMTS-derived brevican fragment was localized to the OML of the mouse after discrete denervation of the perforant path, suggesting a critical role in neural plasticity for the proteolytic turnover of brevican. Thus, the ability to localize and quantitate the ADAMTS specific, proteolytic product of brevican provides a means to indirectly estimate ADAMTS activity during times of neural plasticity and synaptogenesis.

The expression of brevican was shown previously to be up-regulated in the OML, the area of denervation after ECL in the rat (Thon et al., 2000), however, in contrast to the transient production observed here in the mouse, expression of immunoreactive brevican remained elevated compared to the non-lesioned side for almost 6 months after injury. Neurocan is a lectican that is expressed at high levels during early development but it was found to be up-regulated and synthesized by astrocytes in the OML after ECL. It was suggested that neurocan and possibly brevican may act to maintain the boundary of the denervated dentate after ECL (Haas et al., 1999), yet these complex molecules may be multifunctional during periods of neural plasticity. Each of the lecticans, exhibit a characteristic pattern of expression during development, with neurocan and versican V1 highly expressed in the brain of the fetus and neonate, whereas

aggrecan, versican V2 and brevican increase expression during the period of synaptic stabilization in the adult and expression remains high throughout adulthood (Hockfield et al., 1990; Milev et al., 1998). Each of the lecticans is thought to bind to tenascin R and hyaluronic acid (with varying affinities) forming a multi-molecular lattice of ECM (Yamaguchi, 2000). It may be that proteolytic cleavage of the lectican loosens the lattice to promote neurite growth and synaptogenesis. Classically, the highly negatively charged CS chains on the lecticans inhibits neurite outgrowth, but proteolytic cleavage of the core protein may allow more movement of these chains and actually promote plasticity of neurons. This is a testable notion and preliminary data indicates that the ADAMTSs promote neurite outgrowth and other measures of neural plasticity *in vitro* (our unpublished observations).

The projection from the EC to the hippocampus is called the perforant path (Hjorth-Simonsen and Jeune, 1972), and is thought to be involved in long-term potentiation and learning and memory (Ruthrich et al., 1987; Sutula and Steward, 1987; Liu and Bilkey, 1996). The ECL model to study neural and synaptic plasticity denervates up to 80% of the input to the outer two-thirds of the molecular layer of the dentate gyrus (Scheff and Dekosky, 1989), and due to sprouting of surviving fiber systems will reinnervate nearly fully. This model was developed more than thirty years ago in the rat (Steward et al., 1973), yet it has been only relatively recently that the technique was employed in mice to take advantage of transgenic models (Destrade et al., 1985; Shi and Stanfield, 1996). Surprisingly, there are some differences in the projections from the EC to the

hippocampal formation between rats and mice (van Groen et al., 2002). For example, input to the dentate molecular layer from the contralateral EC is absent in the mouse, yet these contralateral fibers are responsible for much of the sprouting after ECL in the rat. In addition, the width of the inner molecular layer, that contains associational-commissural fibers, is thinner in the mouse than in the rat, causing an increase in the relative width occupied by the middle and OMLs, layers innervated mainly by EC fibers. In the mouse, the middle and OML occupy closer to four-fifths of the total, rather than two-thirds as seen in the rat. Moreover, three layers can be clearly differentiated in an untreated mouse, but not in a rat, using synaptophysin immunohistochemistry (van Groen et al., 2002), and following ECL this laminar feature is lost (Fig. 14B). Synaptophysin immunochemistry has been one of the more common techniques, among many, to quantitate the loss and reinnervation of input into the ipsilateral molecular layer of the dentate gyrus after unilateral ECL (Deller and Frotscher, 1997). Optical density of the synaptophysin signal in the contralateral OML is measured using the sum (or average) of the gray levels of the pixels in this region, and this value is used as a “normal” value to the ipsilateral side. However, with this technique, the ipsilateral dentate usually shows only a 10-30% reduction in signal compared to the contralateral side at seven days after lesion, a time when sprouting has begun (Wilson, 1981). Clearly this absolute value does not reflect the extent to which fibers are actually lost in the OML after ECL. Thus, we decided to develop a fresh tissue, needle punch dissection technique that could be limited to the dentate gyrus in the mouse. This way, biochemical assays could be conducted

on the tissue to measure overall synaptophysin immunoreactivity by ELISA. Using this method, at two and seven days after lesion, there was greater than a 40% reduction in synaptophysin levels in the OML, a value which at least may closer reflect the absolute loss of fibers after ECL. The major disadvantage of this method is that the dissected tissue also includes the granule layer and the hilus of the dentate, regions where input is not lost after ECL. At the same time using this technique, tissue containing the lesion itself may be collected and assayed biochemically or processed for histochemistry to monitor the extent of the lesion in the EC.

The present results suggest that the lecticans and the proteases that cleave the lecticans play a regulatory role in neural plasticity after ECL. There are several potential mechanisms by which this substrate--protease pair may modulate neural plasticity, one of which was described above. Significant changes were observed in the abundance of the different isoforms of brevican including the expression of the C-terminally-truncated ADAMTS-derived brevican fragment during plastic events in the hippocampus. A genetic approach to study the individual lecticans and ADAMTSs could reveal the individual contributions for each of the molecules involved in neural plasticity after ECL, however, there is considerable redundancy among these molecules. For example, there appears to be a compensatory increase in the expression of neurocan in the brain of the brevican null mouse (Brakebusch et al., 2002). In addition, several of the ADAMTSs exhibit proteoglycanase activity, and of these, at least ADAMTS1, 4 and 9 appear to be expressed in the nervous system (unpublished

observations). Whether there are compensatory changes in the expression of any of these molecules in the brain in ADAMTS null mice remains to be determined. Nonetheless, significant protective effects toward arthritic changes were demonstrated just recently in a single mutant, the ADAMTS5 null mouse (Stanton et al., 2005). Should it turn out that these proteases play a significant role in plasticity related mechanisms in the nervous system, it will be interesting to examine how removing this regulatory action will impact development, sprouting after lesion, learning and memory and other plasticity related mechanisms in the adult.

Figure 10. Schematic representation of the micro-dissection of dentate gyrus and entorhinal cortex: This procedure was developed to isolate dentate gyrus and entorhinal cortex tissue from different rostral-caudal slabs in fresh-frozen mouse brain. A: Coronal section of mouse brain showing bore holes left from blunt-ended, 22 gauge needle punch (green) in the ipsilateral and contralateral dentate gyrus. B: Coronal section of mouse brain (2 mm caudal from section in "A") showing bore holes left from blunt-ended, 18 gauge needle punch (green) in the ipsilateral and contralateral entorhinal cortex. C: Sagittal view of 2 mm slices used for the collection of dentate gyrus (A) and entorhinal cortex (B). Diagrams adapted from 'The Mouse Brain' (Paxinos & Franklin, 2001).

Chapter 2, Figure 10

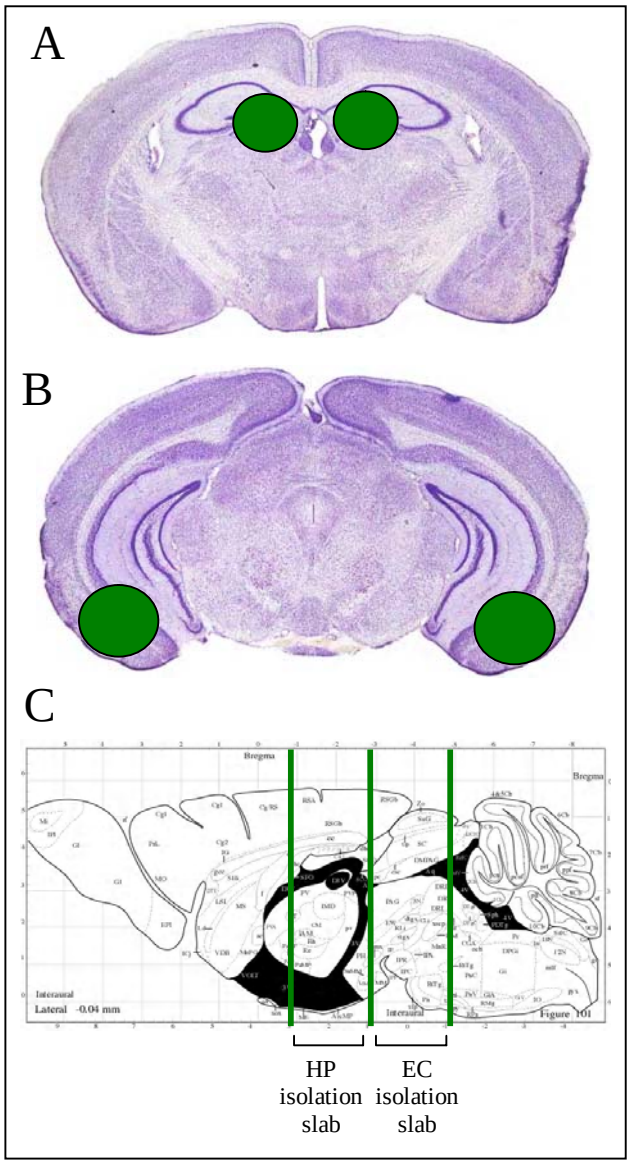

Figure 11. Schematic representation of brevican cleavage by the glutamyl-endopeptidases, the ADAMTSs: A: Secreted brevican core protein that bears chondroitin sulfate chains (MW > 145 kD). B: Secreted brevican core protein without chondroitin sulfate side chains (MW = 145 kD). C: When cleaved by extracellular glutamyl endopeptidases, the ADAMTSs, an N-terminal fragment of brevican (MW = 55 kD) is formed that contains the unique C-terminal epitope EAMESE. The anti-brevican antibody recognizes all three isoforms of brevican, whereas anti-EAMESE antibody selectively recognizes the ADAMTS-derived proteolytic fragment of brevican and not the parent protein or other isoforms.

Chapter 2, Figure 11

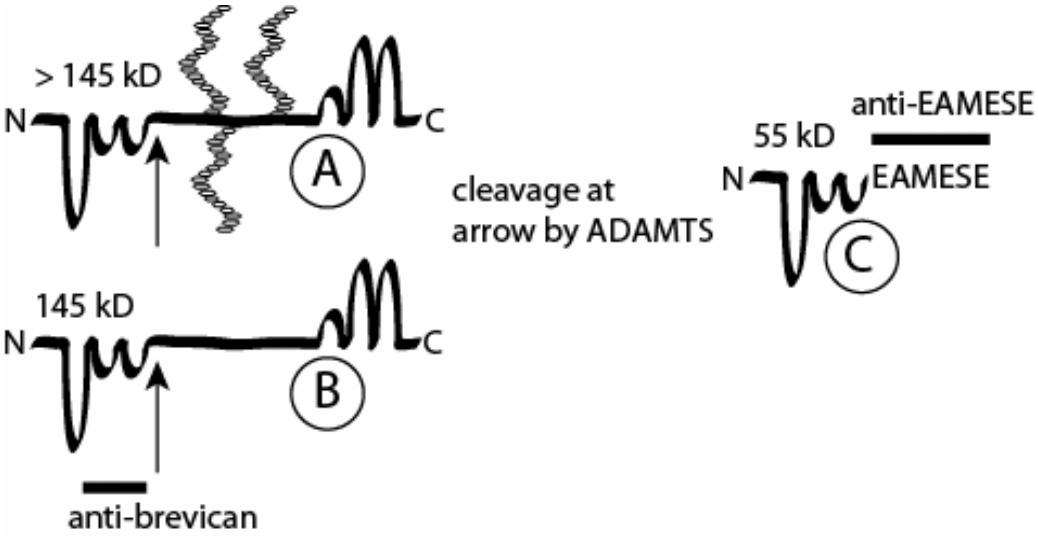

Figure 12. Brevican and EAMESE Western blotting in regions of mouse brain: Panel A shows an immunoblot containing extracts from various regions of mouse brain and probed with anti-brevican antibody. Immunoreactive bands are present at >145 kD (high molecular weight smear), 145 kD core protein, and the generalized 55 kD fragment. Panel B contains a membrane with the same samples probed with anti-EAMESE. This antibody recognized the specific ADAMTS-derived 55 kD fragment of brevican. CB = cerebellum, BS = brain stem, DE = diencephalon, HC = hippocampus, FC = frontal cortex, TL = temporal lobe, and OT = olfactory tubercle.

Chapter 2, Figure 12

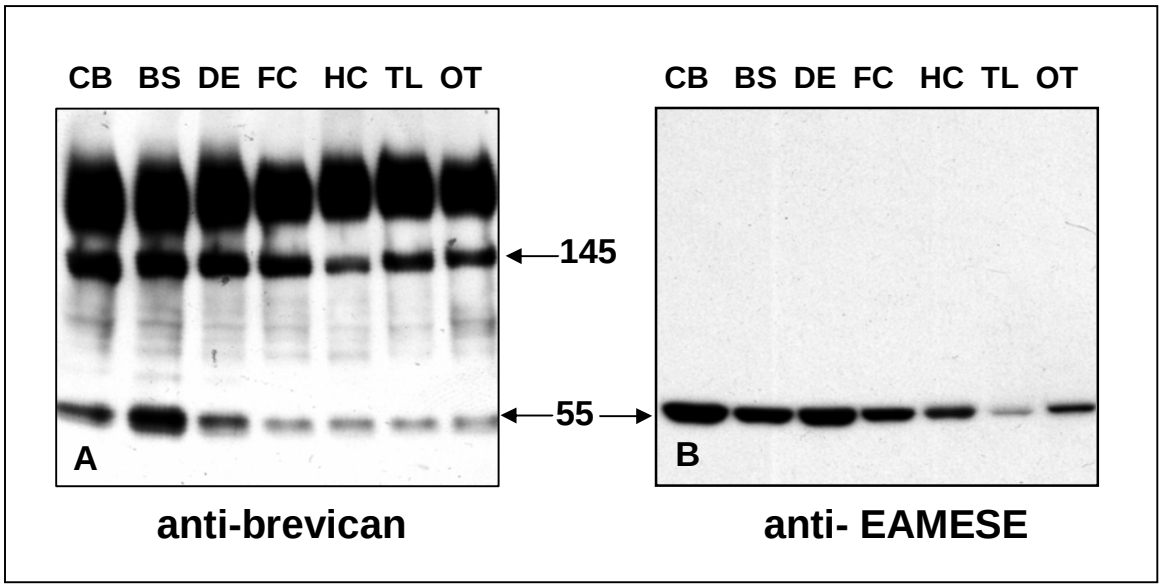

Figure 13. Alterations in brevican levels in lesioned entorhinal cortex: Horizontal sections of entorhinal cortex immunostained with anti-brevican antibody collected two days after entorhinal cortex lesion. A: Contralateral entorhinal cortex showed little immunoreactive signal. B: Ipsilateral entorhinal cortex showed abundant anti-brevican staining in the lateral region.

Chapter 2, Figure 13

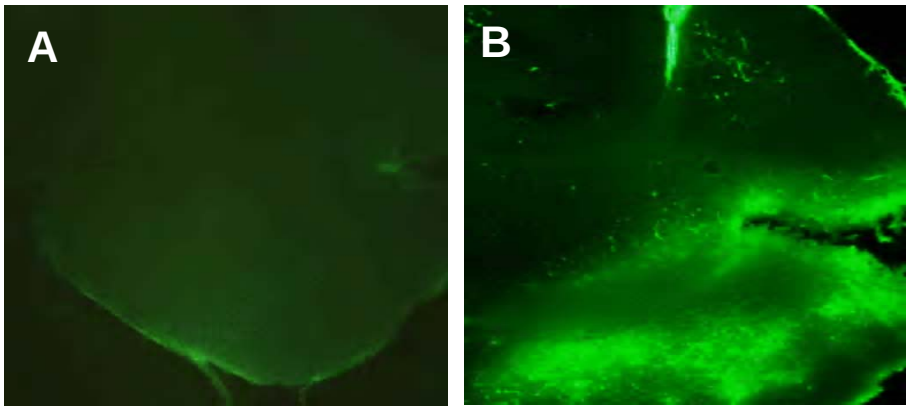

Figure 14. Denervation of the outer molecular layer of the dentate gyrus after entorhinal cortex lesion: A and B: Synaptophysin immunoreactivity in the molecular layer of the dentate gyrus two days after ECL. A: ipsilateral dentate, B: contralateral dentate. Note diminished immunostaining and loss of tri-laminar pattern in the OML after ECL. C and D: GFAP immunoreactivity in the molecular layer of the dentate gyrus seven days after ECL. Note increased astroglial expression of GFAP observed after deafferentation of the ipsilateral (C), but not contralateral (D), OML. E: Synaptophysin levels in extracts from fresh micro-dissected (needle punch, see Fig. 1) dentate gyrus tissue as measured by ELISA. Synaptophysin immunoreactivity was reduced two and seven days post-lesion. The ipsilateral side was not different from contralateral dentate thirty days after lesion. oml = outer molecular layer, mml = middle molecular layer, iml = inner molecular layer, and gcl = granule cell layer.

Chapter 2, Figure 14

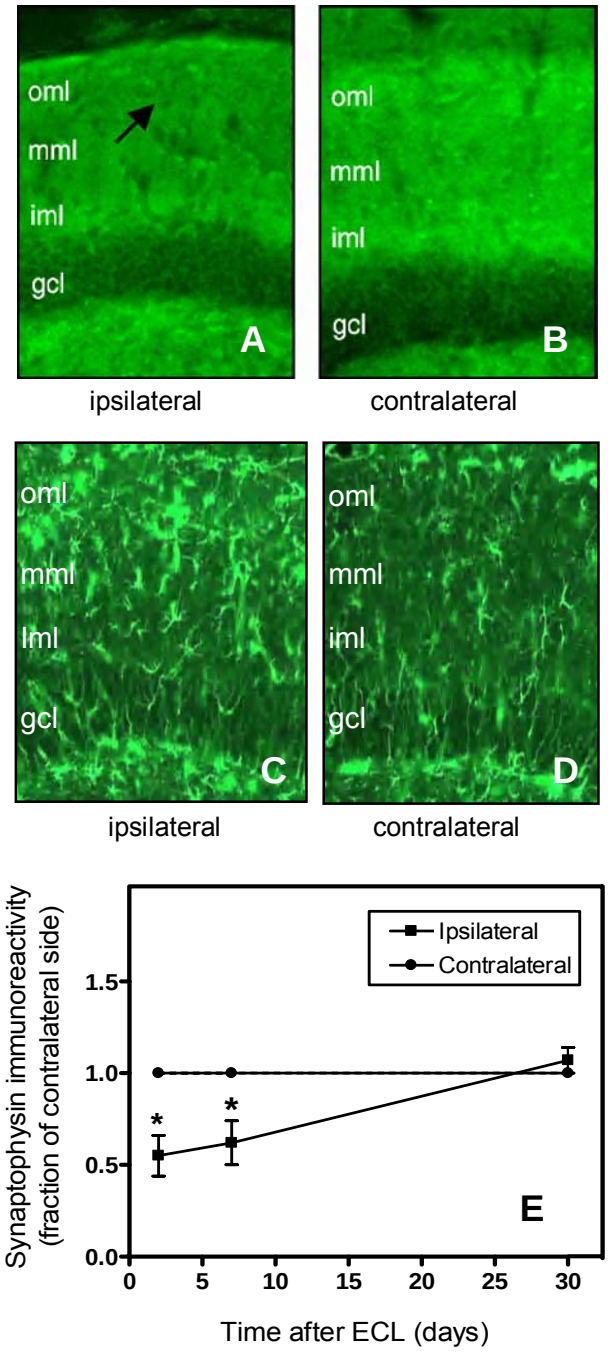

Figure 15. Brevican immunoreactivity in the dentate gyrus after entorhinal cortex lesion: Brevican immunoreactivity in the contralateral (CL) and ipsilateral (IL) dentate gyrus of mice that had undergone ECL two, seven, and thirty days earlier. Optical density was measured on the Western blots and data from the ipsilateral side was expressed as a fraction of the contralateral dentate. A: At two days, the CS-containing, >145 kD brevican was significantly elevated on the lesion side compared to the contralateral side although all fragments showed a trend for increase. B: At seven days, there was a significant elevation of the ADAMTS-derived EAMESE fragment of brevican and a trend for an increase in 55 kD fragment. C: At thirty days, brevican isoforms were not different from the control side, except that the >145 kD core protein was slightly elevated.

Chapter 2, Figure 15

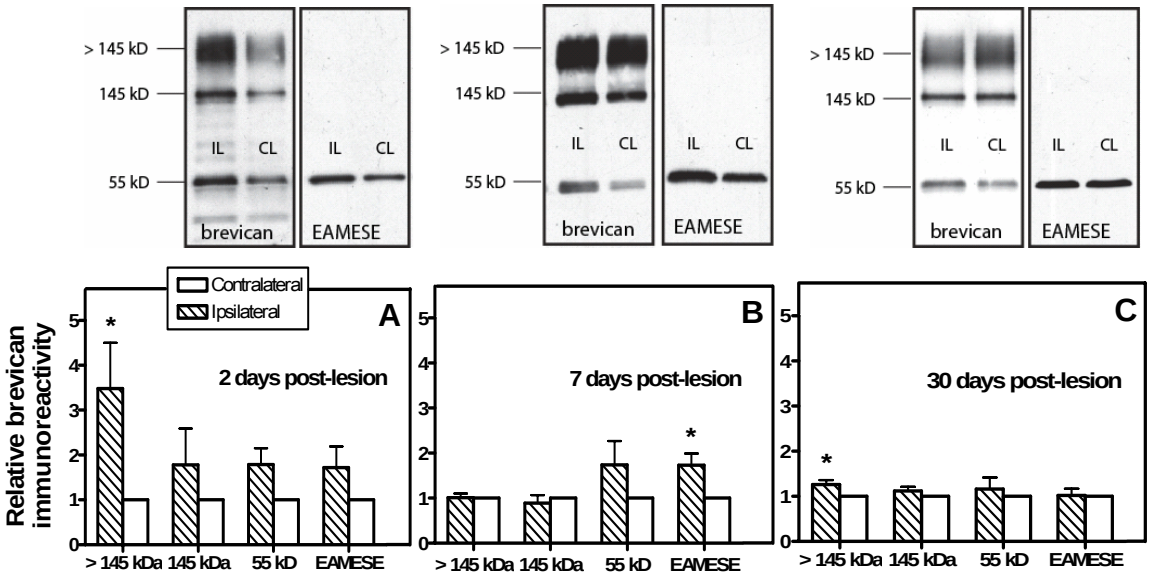

Figure 16. Apparent ADAMTS activity: Apparent activity in the dentate gyrus of mice after entorhinal cortex lesion as measured by the ratio of the optical density of the ADAMTS-derived EAMESE fragment and the sum of the densities of the brevican core protein isoforms (>145 kD + 145 kD). Mean level of apparent activity was calculated at two, seven and thirty days after lesion. At two days after lesion, ADAMTS activity declined, whereas at seven days a significant 47% increase in ADAMTS activity was observed compared to the contralateral ADAMTS activity. Levels on the lesioned side were not different from the non-lesioned dentate in tissue collected thirty days after lesion.

Chapter 2, Figure 16

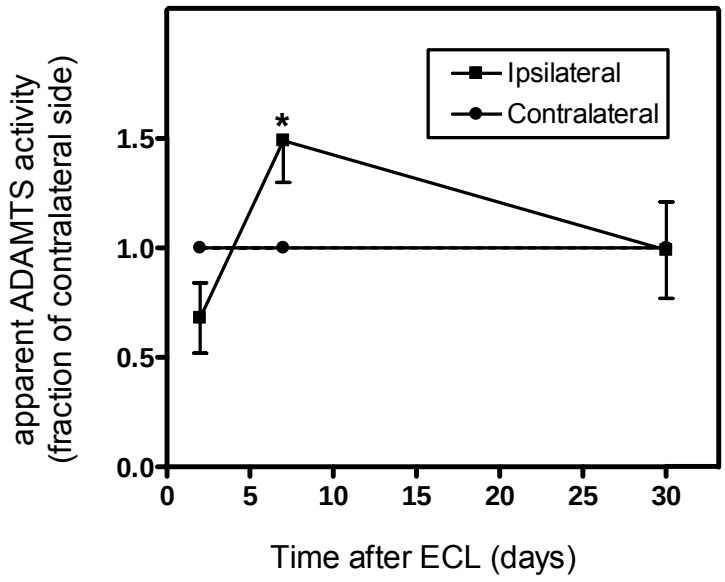

REFERENCES CITED

Bandtlow CE, Zimmermann DR (2000) Proteoglycans in the developing brain: new conceptual insights for old proteins. Physiol Rev 80:1267-1290.

Brakebusch C, Seidenbecher CI, Asztely F, Rauch U, Matthies H, Meyer H, Krug M, Bockers TM, Zhou X, Kreutz MR, Montag D, Gundelfinger ED, Fassler R (2002) Brevican-deficient mice display impaired hippocampal CA1 long-term potentiation but show no obvious deficits in learning and memory. Mol Cell Biol 22:7417-7427.

Bruckner G, Grosche J, Hartlage-Rubsamen M, Schmidt S, Schachner M (2003) Region and lamina-specific distribution of extracellular matrix proteoglycans, hyaluronan and tenascin-R in the mouse hippocampal formation. J Chem Neuroanat 26:37-50.

Del Turco D, Woods AG, Gebhardt C, Phinney AL, Jucker M, Frotscher M, Deller T (2003) Comparison of commissural sprouting in the mouse and rat fascia dentata after entorhinal cortex lesion. Hippocampus 13:685-699.

Deller T, Frotscher M (1997) Lesion-induced plasticity of central neurons: sprouting of single fibres in the rat hippocampus after unilateral entorhinal cortex lesion. Prog Neurobiol 53:687-727.

Deller T, Haas CA, Frotscher M (2001) Sprouting in the hippocampus after entorhinal cortex lesion is layer- specific but not translaminar: which molecules may be involved? Restor Neurol Neurosci 19:159-167.

Destrade C, Gauthier M, Cazala P, Caudarella M (1985) Lesion of the temporo-ammonic perforant path facilitates self-stimulation of the lateral entorhinal cortex in mice. Brain Res 344:377-381.

Eng LF, Ghirnikar RS (1994) GFAP and astrogliosis. Brain Pathol 4:229-237.

Frotscher M, Deller T, Heimrich B, Forster E, Haas C, Naumann T (1996) Survival, regeneration and sprouting of central neurons: the rat septohippocampal projection as a model. Anat Anz 178:311-315.

Gottschall PE, Sandy JD, Zimmermann DR (2005) Matrix metalloproteinases in the Central Nervous System. Singapore: World Scientific Publishing Co.

Haas CA, Rauch U, Thon N, Merten T, Deller T (1999) Entorhinal cortex lesion in adult rats induces the expression of the neuronal chondroitin sulfate proteoglycan neurocan in reactive astrocytes. J Neurosci 19:9953-9963.

Hjorth-Simonsen A, Jeune B (1972) Origin and termination of the hippocampal perforant path in the rat studied by silver impregnation. J Comp Neurol 144:215-232.

Hockfield S, Kalb RG, Zaremba S, Fryer H (1990) Expression of neural proteoglycans correlates with the acquisition of mature neuronal properties in the mammalian brain. Cold Spring Harb Symp Quant Biol 55:505-514.

Jaworski DM, Kelly GM, Hockfield S (1999) Intracranial injury acutely induces the expression of the secreted isoform of the CNS-specific hyaluronan-binding protein BEHAB/brevican. Exp Neurol 157:327-337.

Jourquin J, Tremblay E, Decanis N, Charton G, Hanessian S, Chollet AM, Le Diguardher T, Khrestchatisky M, Rivera S (2003) Neuronal activity-dependent increase of net matrix metalloproteinase activity is associated with MMP-9 neurotoxicity after kainate. Eur J Neurosci 18:1507-1517.

Kim HJ, Fillmore HL, Reeves TM, Phillips LL (2005) Elevation of hippocampal MMP-3 expression and activity during trauma-induced synaptogenesis. Exp Neurol 192:60-72.

Liu P, Bilkey DK (1996) Direct connection between perirhinal cortex and hippocampus is a major constituent of the lateral perforant path. Hippocampus 6:125-135.

Lynch G, Matthews DA, Mosko S, Parks T, Cotman C (1972) Induced acetylcholinesterase-rich layer in rat dentate gyrus following entorhinal lesions. Brain Res 42:311-318.

Matthews RT, Gary SC, Zerillo C, Pratta M, Solomon K, Arner EC, Hockfield S (2000) Brain-enriched hyaluronan binding (BEHAB)/brevican cleavage in a glioma cell line is mediated by a disintegrin and metalloproteinase with thrombospondin motifs (ADAMTS) family member. J Biol Chem 275:22695-22703.

Milev P, Maurel P, Chiba A, Mevissen M, Popp S, Yamaguchi Y, Margolis RK, Margolis RU (1998) Differential regulation of expression of hyaluronan-binding proteoglycans in developing brain: aggrecan, versican, neurocan, and brevican. Biochem Biophys Res Commun 247:207-212.

Nakamura H, Fujii Y, Inoki I, Sugimoto K, Tanzawa K, Matsuki H, Miura R, Yamaguchi Y, Okada Y (2000) Brevican is degraded by matrix metalloproteinases and aggrecanase-1 (ADAMTS4) at different sites. J Biol Chem 275:38885-38890.

Paxinos, Franklin (2001) The Mouse Brain: in stereotaxic coordinates. San Diego: Academic Press.

Phillips LL, Reeves TM (2001) Interactive pathology following traumatic brain injury modifies hippocampal plasticity. Restor Neurol Neurosci 19:213-235.

Rauch U (2004) Extracellular matrix components associated with remodeling processes in brain. Cell Mol Life Sci 61:2031-2045.

Reeves TM, Prins ML, Zhu J, Povlishock JT, Phillips LL (2003) Matrix metalloproteinase inhibition alters functional and structural correlates of deafferentation-induced sprouting in the dentate gyrus. J Neurosci 23:10182-10189.

Ruthrich H, Dorochow W, Pohle W, Ruthrich HL, Matthies H (1987) Colchicine-induced lesion of rat hippocampal granular cells prevents conditioned active avoidance with perforant path stimulation as conditioned stimulus, but not conditioned emotion. Physiol Behav 40:147-154.

Scheff SW, Dekosky ST (1989) Glucocorticoid suppression of lesion-induced synaptogenesis: effect of temporal manipulation of steroid treatment. Exp Neurol 105:260-264.

Shi B, Stanfield BB (1996) Differential sprouting responses in axonal fiber systems in the dentate gyrus following lesions of the perforant path in WLDs mutant mice. Brain Res 740:89-101.

Snow DM, Letourneau PC (1992) Neurite outgrowth on a step gradient of chondroitin sulfate proteoglycan (CS-PG). J Neurobiol 23:322-336.

Snow DM, Lemmon V, Carrino DA, Caplan AI, Silver J (1990) Sulfated proteoglycans in astroglial barriers inhibit neurite outgrowth in vitro. Exp Neurol 109:111-130.

Stanton H, Rogerson FM, East CJ, Golub SB, Lawlor KE, Meeker CT, Little CB, Last K, Farmer PJ, Campbell IK, Fourie AM, Fosang AJ (2005) ADAMTS5 is the major aggrecanase in mouse cartilage in vivo and in vitro. Nature 434:648-652.

Steward O (1994) Cholinergic sprouting is blocked by repeated induction of electroconvulsive seizures, a manipulation that induces a persistent reactive state in astrocytes. Exp Neurol 129:103-111.

Steward O, Loesche J (1977) Quantitative autoradiographic analysis of the time course of proliferation of contralateral entorhinal efferents in the dentate gyrus denervated by ipsilateral entorhinal lesions. Brain Res 125:11-21.

Steward O, Cotman CW, Lynch GS (1973) Re-establishment of electrophysiologically functional entorhinal cortical input to the dentate gyrus deafferented by ipsilateral entorhinal lesions: innervation by the contralateral entorhinal cortex. Exp Brain Res 18:396-414.

Sutula T, Steward O (1987) Facilitation of kindling by prior induction of long-term potentiation in the perforant path. Brain Res 420:109-117.

Szklarczyk A, Lapinska J, Rylski M, McKay RD, Kaczmarek L (2002) Matrix metalloproteinase-9 undergoes expression and activation during dendritic remodeling in adult hippocampus. J Neurosci 22:920-930.

Thon N, Haas CA, Rauch U, Merten T, Fassler R, Frotscher M, Deller T (2000) The chondroitin sulphate proteoglycan brevican is upregulated by astrocytes after entorhinal cortex lesions in adult rats. Eur J Neurosci 12:2547-2558.

van Groen T, Kadish I, Wyss JM (2002) Species differences in the projections from the entorhinal cortex to the hippocampus. Brain Res Bull 57:553-556.

van Groen T, Miettinen P, Kadish I (2003) The entorhinal cortex of the mouse: organization of the projection to the hippocampal formation. Hippocampus 13:133-149.

White F, Nicoll JA, Horsburgh K (2001) Alterations in ApoE and ApoJ in relation to degeneration and regeneration in a mouse model of entorhinal cortex lesion. Exp Neurol 169:307-318.

Wilson RC (1981) Changes in translation of synaptic excitation to dentate granule cell discharge accompanying long-term potentiation. I. Differences between normal and reinnervated dentate gyrus. J Neurophysiol 46:324-338.

Yamaguchi Y (1996) Brevican: a major proteoglycan in adult brain. Perspect Dev Neurobiol 3:307-317.

Yamaguchi Y (2000) Lecticans: organizers of the brain extracellular matrix. Cell Mol Life Sci 57:276-289.

Yuan W, Matthews RT, Sandy JD, Gottschall PE (2002) Association between protease-specific proteolytic cleavage of brevican and synaptic loss in the dentate gyrus of kainate-treated rats. Neuroscience 114:1091-1101.

Zhang JW, Deb S, Gottschall PE (2000) Regional and age-related expression of gelatinases in the brains of young and old rats after treatment with kainic acid. Neurosci Lett 295:9-12.

Zhang X, Gelowitz DL, Lai CT, Boulton AA, Yu PH (1997) Gradation of kainic acid-induced rat limbic seizures and expression of hippocampal heat shock protein-70. Eur J Neurosci 9:760-769.

CHAPTER 3

BREVICAN PROCESSING AND ASSOCIATED LEVELS OF SYNAPTIC MARKERS IN APPsw MICE

Joanne Mayer[1], Keith R. Pennypacker[1], Dave Morgan[1,2], Paul E. Gottschall[1*]

University of South Florida College of Medicine, Department of Molecular Pharmacology and Physiology[1], Alzheimer Research Laboratory[2], 12901 Bruce B. Downs Blvd, Tampa, Florida 33612-4799, USA

[*]To whom correspondence should be addressed:
Paul E. Gottschall
University of South Florida College of Medicine
Department of Pharmacology and Therapeutics
12901 Bruce B Downs Blvd
PHONE: 813-974-9910
FAX: 813-974-2565
E-mail: pgottsch@health.usf.edu jmayer1@health.usf.edu
kpennypa@health.usf.edu scientist.dave@gmail.com

Acknowledgements

This work is supported in part by the National Institutes of Health (R01-AG022101) and Alzheimer's Association (grant # IIRG-02-3758). The authors would like to thank Dr. Yu Yamaguchi for the brevican antibody, RB18 and Autumn K. Eakin in our laboratory for her assistance in data aquisition.

ABSTRACT

Deposition of Aβ into the extracellular matrix (ECM) may be involved in the disruption of matrix processing and alter extracellular molecular events that modulate synaptic plasticity. To test the hypothesis that disruption of ECM processing by the accumulation of Aβ can alter synaptic plasticity via modification of ECM, we examined whether the expression and processing of brevican, an abundant extracellular chondroitin sulfate-bearing proteoglycan, was altered in the brains of Aβ-depositing APPsw mice. The abundance of a major catabolic, proteolytic fragment of brevican was consistently decreased in several telencephalic regions in the brains of plaque-bearing mice, an effect that appeared to be due to diminished matrix metalloproteinase (MMP) activity. In association with the region selective decline in MMP activity, we observed a marked increase in the expression of the synaptic SNARE protein, SNAP-25 in APPsw mice compared to littermate controls. These results suggest that over-expression of Aβ may exert inhibitory effects on the activity of the proteases responsible for the processing of brevican, other proteoglycans and various other substrates. Intact proteoglycan may stabilize synaptic structures, thereby inhibiting synaptic plasticity.

Keywords: amyloid β protein, amyloid precursor protein, extracellular matrix, brevican, proteoglycan, Alzheimer's disease, synaptophysin, SNAP-25, PSD-95, synapse

INTRODUCTION

One hallmark of Alzheimer's disease (AD) is the deposition of insoluble Aβ peptides into amyloid plaques in the extracellular space in the brain (Glenner and Wong, 1984; Selkoe, 1991). Various aggregate forms of Aβ induce oxidative stress and a glial-mediated inflammatory response (McGeer et al., 1989; Hardy and Higgins, 1992; Giulian et al., 1995; Sastre et al., 2006) including the expression of matrix-degrading proteases (Satoh et al., 2000; Deb et al., 2003). Exactly how these pathological responses affect the progression of AD is not clear, however, they likely influence molecular mechanisms involved in neural and synaptic plasticity. Transgenic mouse models that over express the human APP gene bearing the Swedish mutation (APPsw) mimic several characteristics of AD, such as the deposition of amyloid and diminished cognitive function, but certainly not all aspects (Hsiao et al., 1996; Terai et al., 2001) because they lack neuronal loss. Little is known about synaptic changes that occur in these mice.

Brevican is a chondroitin sulfate (CS)-containing, aggregating, extracellular matrix (ECM) proteoglycan that is abundantly expressed in the central nervous system. It inhibits neurite outgrowth and is thought to stabilize synapses (Hockfield et al., 1990; Bandtlow and Zimmermann, 2000; Yamaguchi, 2000). Recent data from seizure-induced and perforant-pathway lesion models indicate that the turnover of brevican contributes to injury-related reinnervation of the dentate gyrus in these models. (Yuan et al., 2002; Mayer et al., 2005). Neurons, astrocytes and microglia express particular members of the MMP (matrix metalloproteinase) and ADAMTS (a disintegrin and metalloproteinase

with thrombospondin motifs) subgroups of metalloproteinases that potently cleave proteoglycans of the ECM, including brevican. Emerging evidence suggests that AD may be a disease of dysregulated plasticity (Mesulam, 1999; Selkoe, 2002), and aggregating PGs play a key repair and regenerative role in neural plasticity, suggesting a potential link between, deposited Aβ and PGs. Levels of a 55 kD, ADAMTS-derived, brevican cleavage fragment were reduced by 64% in AD hippocampus, compared to age-matched control subjects, suggesting that the proteolytic activity of the ADAMTSs was diminished in AD, an effect that was positively correlated with decreased levels of the pre-synaptic, vesicular marker, synaptophysin (Gottschall, 2001). To further investigate this relationship, and to identify additional synaptic pathology that correlates with alterations in PG processing (i.e., Aβ depositing), APPsw mice were examined for changes in proteolytic-derived brevican isoforms. With the development of ADAMTS-specific and MMP-specific neoepitope antibodies that correspond to the respective cleaved fragments of brevican, the amount of brevican degraded by each of these protease families may be quantitated, and related to the activity of the protease itself. In this study, the activity of each protease, as defined by its involvement in brevican turnover, was related to the potential disturbances in synaptic plasticity, as indicated by levels of the synaptic vesicular protein, synaptophysin, the SNARE protein SNAP-25, and the post-synaptic scaffolding protein PSD-95.

MATERIALS & METHODS

Animals

15 month old adult APPsw (Tg2576) mice (23 g - 27 g) from the colony maintained at USF were housed under a 12 hour light cycle with regulated temperature and humidity. Mice were housed 3 to 4 per cage and had free access to food and water. Brain tissue was collected from animals between 15 and 16 mos of age: biochemical analysis n=6, APP (+) tg and n=4, APP (-) non-tg; immunohistochemistry n=6, APP (+) tg and n=6 APP (-) non-tg. Genotyping as described previously by Hsiao et al., (Hsiao et al., 1995; Hsiao et al., 1996).

Western Blotting

For collection of tissue for blotting with antibodies, animals were euthanatized with an exposure to excess CO_2 until death and immediately decapitated. Various brain regions were rapidly dissected and extracted with a teflon-glass homogenizer in about 5 volumes of Triton-X-100-containing buffer (20 mM Tris-HCl at pH 7.4, 10 mM EDTA, 1% Triton-X-100, and 1:100 protease inhibitor cocktail [Calbiochem type III, LaJolla, CA]). The homogenate was centrifuged in a microcentrifuge at 6800 x g for 5 minutes, and the isolated supernatant collected and stored at –80^{o}C.

Tissue extracts were loaded with equal amounts of protein and 2x reducing sample buffer onto pre-cast 4-20% gradient SDS-PAGE gels (Novex gels, Invitrogen, Carlsbad, CA). Protein was electrophoretically transferred to a polyvinylidine difluoride membrane (PVDF, Immobilon, Millipore, Billerica, MA).

For anti-brevican, anti-EAMESE, and anti-SAHPSA immunoblotting, the membranes were washed with Buffer B (10 mM phosphate buffered saline, pH 7.4 containing 0.05% Tween 20) for 5 minutes, blocked in 5% milk diluted in Buffer B for 1 hour and probed for 2 hours using primary antibodies against mouse anti-brevican (1:1000, BD Transduction Labs, San Jose, CA), rabbit anti-EAMESE (1:1000) (Mayer et al., 2005), or rabbit anti-SAHPSA (1:500). Primary antibodies were detected with corresponding secondary antibodies of anti-mouse and anti-rabbit conjugated to horse radish peroxidase (Chemicon, Temecula, CA). Antigens were visualized using a chemiluminescence developing system (SuperSignal, Pierce, Rockford, IL). This is the first use of the neoepitope specific antibody anti-SAHPSA. The antibody was affinity purified on a solid phase column linked to SAHPSA peptide, prior to use (see methods below). It should be noted that ADAMTS-derived and MMP-derived fragment antibodies were raised against the species-specific neoepitopes for mouse.

Immunohistochemistry

Mice were euthanatized with excess Nembutal, and the brains cleared using phosphate buffered saline (PBS; pH 7.4), via cardiac perfusion as described (Aya-ay et al., 2005). The brain was removed and dissected into two hemispheres. One hemisphere was extracted as above and used for biochemical analysis and the other hemisphere was post-fixed with fresh 4% paraformaldehyde in 0.1M phosphate buffer (PB; pH 7.4) overnight and cryoprotected with 15% and 30% sucrose (in PBS) for 24 hours each. The

individual brains were mounted on a cryostat chuck at –20°C and sectioned at 30 µm. Sections were stored freely floating in antifreeze solution at –20°C.

Selected sections to be used for immunohistochemistry were washed in PBS for 15 minutes, blocked and permeabilized in 10% normal goat serum, 3% 1 M lysine and 3% Triton-X for 1h and incubated overnight in primary antibodies against brevican (1:1000, N-terminal (G1); Transduction Labs, San Jose, CA and 1:500, C-terminal (G3) RB18 (Yu Yamaguchi, Burnham Institute, La Jolla, CA), EAMESE (1:1000), SAHPSA (1:500), 4G8 (1:250, AbD Serotec, Raleigh, NC), and Aβ-95-2-2 ("Total Aβ" raised against Aβ1-40 and recognizes both Aβ1-42 and Aβ 1-40; for charaterization see (Morgan et al., 2000; Wilcock et al., 2001) at 4°C. Doubly probed sections were washed and incubated in anti-rabbit IgG conjugated to Alexa-Fluor 488 (Molecular Probes, Eugene, OR) and streptavidin conjugated to Alexa-Fluor 594 (Molecular Probes, Eugene, OR) for 1 hr at room temperature. The sections were washed for 15 minutes, wet mounted on glass slides, and coverslipped with VectaShield mounting medium (Vector Labs, Burlingame, CA).

ELISA

Enzyme-Linked Immunoabsorbant assays were performed to measure immunoreactivity of GFAP, synaptophysin, SNAP-25 and PSD-95. Coating antibodies were diluted in 0.01 M PB and let to dry overnight in a EIA/RIA high-binding 96-well plate (Costar - Sigma; St. Louis, MO) using mouse x anti-synaptophysin; Chemicon, Temecula, CA 1:250; mouse x anti-SNAP-25,

Chemicon, 1:200; mouse x PSD95, Chemicon, 1:100 and mouse x GFAP, Chemicon, 1:250). The wells were washed with sample/wash buffer (PBS with 0.05% Tween-20) one time and blocking buffer (PBS with 0.05% Tween-20 and 5% dry milk) was added to the wells and incubated at room temperature for 1 hr with agitation. The wells were washed and prepared sample was added for a 2 hr incubation on a shaker. After samples were washed from the well, primary antibody diluted in sample/wash buffer was added and allowed to incubate for 2 hrs with agitation (rabbit anti-synaptophysin DAKO, Carpenteria, CA 1:2000; rabbit anti-SNAP-25 Sigma, St. Louis, MO, 1:1000; sheep anti-PSD95 ZYMED, San Francisco, CA, 1:100; and rabbit anti-GFAP DAKO, 1:1000). The wells were washed three times before adding secondary antibodies, allowed to incubate for 45 minutes on a shaker (goat anti-rabbit IgG-HRP, Chemicon, 1:5000; anti-sheep/goat, Chemicon, 1:1000). Next, TMB (tetramethyl benzidine, Sigma, St. Louis, MO) solution was applied and the color allowed to develop. The colormetric reaction was stopped with 1M H_2SO_4. Absorbance levels were measured with a Wallac Victor2 1420 multilabel counter (Perkin Elmer, Wellesley, MA) and Workout software (version 1.5, Perkin Elmer), and the readings were normalized for concentration of protein in the sample added to the well. The means from the experiment groups were compared using ANOVA and pair-wise comparisons were made with Bonferroni post-hoc test (GraphPad, San Diego, CA). A p-value < 0.05 was considered significant.

Antibody generation

A rabbit antibody raised against the brevican neoepitope on the 55 kD N-terminal fragment derived from proteoglycanase activity of the MMPs was generated by Sigma-Genosys (St. Louis, MO) and purified in our laboratory. The novel C-terminal sequence "SAHPSA" from the mouse was the neoepitope and the peptide used for antibody generation contained a glycine spacer "GGGQSAHPSA". Synthesized by Sigma-Genosys, this peptide was conjugated to keyhole limpet hemocyanin at the N-terminus and rabbits were subjected to standard immunization protocols. Serum collected after the fifth booster was titered against the peptide using a solid-phase system and specific antibody was purified using peptide affinity chromatography. On Western blot, the antibody against the mouse fragment recognized a single band at ~53 kD in extracts from mouse brain and did not cross react with the intact brevican core protein.

Microscopy and image acquisition

Single and multi-labeled, epifluorescent photomicrographs were acquired using a Zeiss Axioskop microscope, interfaced with an Axiocam and images acquired with Openlab software. Controls for each immunomarker included secondary antibody in the absence of a primary antibody, in which the staining in control sections was minimal to absent. Exposure times and aperture opening were constant for each magnification and antibody used. All pictures were minimally and equally modified using Abobe photoshop.

RESULTS

Brevican is secreted as a glycosylated protein or as the holoprotein alone that appears on Western blot as a smear at >145 kD and a distinct band at 145 kD, respectively (Fig. 17A-C). There is an abundance of the 55 kD proteolytic fragment of brevican that is prevalent in brain and can be detected on Western blot with an N-terminal (G1-domain) antibody that detects all three isoforms (Fig. 17C). Brevican and other lecticans are selectively cleaved by endogenous proteases such as the ADAMTSs and MMPs at site-specific regions revealing novel sequences of amino acids at their termini (Fig. 17D & E). In the mouse brevican sequence, the ADAMTS cleavage site (residues 395-396) is 35 amino acids downstream from the MMP site (residues 360-361), resulting in an N-terminal, ADAMTS-derived fragment that should theoretically be about 4 kD larger than the MMP fragment (Nakamura et al., 2000). Antibodies raised against the newly exposed C-termini amino acid sequences distinguish between the protease-specific (ADAMTS- vs. MMP-derived) N-terminal fragments of brevican. Since the proteolytic degradation of brevican may play an important role in synaptic plasticity, the ability to detect the protease specific cleavage fragments of brevican is important. The characterization of the ADAMTS-derived fragment, EAMESE, has been reported previously (Mayer et al., 2005) and here we introduce the antibody raised against the neoepitope derived from the cleavage of brevican by members of the MMP family, which results in the C-terminal amino acid sequence, SAHPSA. When probed on a Western blot, the

SAHPSA antibody detects a single immunoreactive band at ~53 kD (see Fig. 18A).

AD exhibits dysregulated plasticity, and because brevican may play a role in synaptic plasticity, we examined brevican immunoreactivity in the brains of APPsw mice. Hippocampal tissue samples of APPsw mice and non-transgenic littermates were probed with anti-brevican antibody that detects an N-terminal region epitope. Three immunoreactive isoforms of brevican were identified; the >145 kD brevican that bears CS chains, the 145 kD core protein, which does not contain CS chains, and an undistinguished, general ~55 kD N-terminal fragment (Fig. 18A). After densitometric analysis, in hippocampus, there was no significant change in the amount of CS-containing brevican at >145 kD, however, there was a clear shift in the molecular weights (lower) of the molecules that compose this isoform in APPsw mice. There was a significant increase the abundance of the core protein that did not bear CS chains (145 kD band) and this was associated with a marked decrease in the abundance of the 55 kD, generalized N-terminal fragment. To delineate the family of proteases which may be responsible for the decrease in the ~55 kD generalized fragment, these samples were probed with the ADAMTS- and MMP-specific neoepitope antibodies. No changes were seen in the amount of ADAMTS-derived fragment (EAMESE), but interestingly a significant decrease in the abundance of the MMP-derived fragment (SAHPSA) was observed in the hippocampus of APPsw mice compared to non-transgenic littermates. Several brain regions of APPsw and non-transgenic littermates were probed for the brevican isoforms using

generalized and protease-specific antibodies. The results are shown in Table 3. Similar to hippocampus, the shift in the molecular weight of the >145 kD isoform, along with the increase in the amount of the 145 kD core protein and a decrease in the abundance of the 55 kD fragment were also found in frontal cortex and temporal lobe. These brain regions are burdened with Aβ plaques. However, this pattern was consistent even in a brain region that does not bear Aβ-containing plaques, the cerebellum, where there was also an increase in core protein and a decline in the MMP-derived brevican fragment. Brain stem and hypothalamus, both relatively lacking in plaques, revealed no changes in the generalized fragment of brevican even though an increase in the core protein was apparent in these regions.

To localize these molecules in the APPsw mouse brain, immuno-histochemistry revealed unique patterns of brevican-related immunoreactivity around the Aβ plaques. Brevican immunoreactivity and Aβ substantially co-localized within the plaque (Fig. 19A-C). However, when staining for the neoepitope antibodies, a different pattern was apparent. There was an increase of anti-EAMESE and anti-SAHPSA immunoreactivity (Fig. 19D-L) on the periphery of the plaque, forming a ring; that was especially evident with anti-EAMESE immunoreactivity (Fig. 19D-F). The same pattern was observed for anti-SAHPSA (Fig. 19J-L), however, the "ring" appeared to have a wider distribution and the diameter of the ring itself was wider than just outside the plaque. Little to no immunoreactivity for the brevican fragments was found within

the center of the plaque, even though this region was abundant with immunoreactivity for brevican.

Activated astrocytes, which secrete brevican and various ECM-degrading proteases, are associated with senile plaques in AD brain (Itagaki et al., 1989; Mrak et al., 1996) and AD pathology results from the ongoing glial-mediated response to the deposition of Aβ. Brain tissue samples of APPsw and non-transgenics were measured for glial fibrillary acidic protein (GFAP) as a measure of the inflammatory response generated by the presence of activated astrocytes. The regions heavily laden with Aβ plaques, such as the frontal cortex ($p=0.0443$), hippocampus ($p=0.0163$) and temporal lobe ($p=0.0490$) showed a marked increase in GFAP compared to those regions that do not bear Aβ plaques, such as cerebellum, hypothalamus and the brain stem (Fig. 20A).

Since brevican may play a role in synaptic plasticity and here we have reported alterations in brevican isoforms within the ECM of the plaque and surrounding tissue, and AD presents dysregulated plasticity, we were interested in whether these changes in the matrix were associated with levels of synaptic markers. The synaptic markers represent a measure of the density of synapses. The markers measured were, the vesicular pre-synaptic protein, synaptophysin, the pre-synaptic, membrane bound SNARE protein, SNAP25, and the post-synaptic scaffolding protein, PSD-95 were measured via ELISA. Synaptophysin (Fig. 20B) or PSD-95 (Fig. 20C) immunoreactivity were not different in any brain region of 15 month old APPsw animals compared to littermate non-transgenics. However, SNAP-25 levels were significantly increased in samples from frontal

cortex, hippocampus, and temporal lobe of the APPsw animals (Fig. 20D). Interestingly, APPsw cerebellum also showed small, but significant increases in SNAP-25 immunoreactivity.

DISCUSSION

Aβ peptides and the processing of the APP protein appear critical in the pathogenesis of AD, yet, their functional relationship to neuronal physiology and synaptic modulation remain remarkably unclear (Palop et al., 2006; Schott et al., 2006). As Aβ plaques form within the extracellular space, there is a disruption of molecular complexes surrounding neurons that may contribute to the AD-associated, dysfunctional neural plasticity. Several ECM components, such as laminin-1, agrin, glypican-1, thrombospondin and integrins, bind Aβ and modulate Aβ aggregation and neurotoxicity (Kowalska and Badellino, 1994; Drouet et al., 1999; Cotman et al., 2000; Watanabe et al., 2004) suggesting that ECM molecules produce a molecular response important in AD pathogenesis. Here, a change in the abundance of all three isoforms of the ECM proteoglycan brevican was observed in brain samples from APPsw mice. There was clearly a decline in the amount of an MMP-derived proteolytic fragment of brevican in several brain regions of APPsw mice that may be associated with an environment less permissive to neural plasticity and these alterations were accompanied by changes in the expression of the pre-synaptic, SNARE protein SNAP-25.

In brain extracts of APPsw mice, the brevican immunoreactive smear that was >145 kD was markedly more condensed and appeared at a lower molecular

weight compared to a "longer" smear found in non-transgenic animals. The higher molecular weight smear represents CS-containing isoforms of brevican, and it may be that extracts from APPsw mice bear fewer numbers of CS chains bound to the core protein, i.e. one or two in APPsw mice instead of two or three, shifting the smear in APPsw mice to a lower molecular weight. In addition, the abundance of the brevican isoform containing no CS chains was markedly increased in APPsw mice. Evidence indicates that ADAMTSs have a higher activity and binding affinity for lecticans bearing CS chains (Tortorella et al., 2000; Flannery et al., 2002), compared to the holoprotein. Thus, diminished cleavage of the holoprotein with no CS chains may account for the greater abundance of this isoform. A reduced level of G1 proteolytic fragment is consistent with this notion. In the control animals, the higher number of CS chains linked to the core protein makes proteolytic cleavage more efficient. The cause for the lack of CS chains bound to brevican in APPsw mice brain is unclear and shear speculation, but may involve decreased glycosyltransferase activity or changes in the catabolism of these forms after interaction with Aß.

The abundance of the N-terminal, G1 generalized fragment of brevican is attenuated in APPsw mice brain, but *in vitro*, data suggest that Aβ can bind to ADAMTSs and inhibit their proteolytic action (Gottschall et al., 2003). However, when brain extracts were probed with an ADAMTS-specific neoepitope antibody (anti-EAMESE), no difference in fragment abundance was found between the APPsw mice compared to non-transgenic. However, the amount of the MMP-derived fragment (anti-SAHPSA) was reduced in the hippocampus, suggesting

that the decline in the generalized fragment in this region was due to a decline in MMP activity in APPsw mice. Similar results were found with extracts of cerebellum where plaques are predominantly of the diffuse type and fibrillar senile plaques are rarely observed (van Horssen et al., 2002).

Although relatively low in normal brain, MMP-9 activity in AD brain is increased (Backstrom et al., 1996; Asahina et al., 2001) and is capable of degrading Aβ and ECM (Backstrom et al., 1996; Lorenzl et al., 2003; Lee et al., 2005; Yan et al., 2006). In three month old APPsw mice, before the accumulation of plaques, MMP immunoreactivity was reported to be absent (Lee et al., 2003) but elevated in astrocytes surrounding plaques in plaque-bearing mice (Lee et al., 2005; Yan et al., 2006). In normal mouse brain, MMPs may cleave CS-containing substrate, but this activity appears to be reduced in plaque bearing mice. The production of MMPs has been shown to be induced by Aβ in cultured rat astrocytes (Deb et al., 2003) and recent data indicates that MMP-9 can degrade fibrillary A□, and may aid to the ongoing clearance of plaques from amyloid laden brains (Yin et al., 2006). The current results suggest that in the presence of A□ plaques in APPsw mice, the ability of MMPs to cleave brevican was diminished. Thus, our data indicate that MMPs contribute to the deposition of Aβ rather than its clearance. In this model, the diminished capacity for MMP to cleave brevican may be due to (1) the inability of MMPs to bind proteoglycan substrates that bear fewer number of CS chains on the core protein, (2) Aβ may bind to the protease in turn directly inhibiting its activity or (3) Aβ can potentially block protease activity by binding directly to brevican. Further experiments are

required to determine the contribution of each to diminished proteolytic degradation of proteoglycans.

By immunohistochemistry, brevican immunoreactivity co-localized within the Aβ plaque; however, a unique staining pattern was observed around the periphery of the Aβ plaque that represented the ADAMTS- and MMP-derived fragments of brevican. The increase of immunoreactivity adjacent to and surrounding the plaque suggests a local increase of protease activity in the region of abnormal neurite growth, but diminished activity within the plaque as denoted by the absence of protease-specific staining. MMP-9 immunoreactivity has been reported in the proximity of extracellular plaques (Backstrom et al., 1996). This further supports the notion that Aβ may exert inhibitory effects on the protease responsible for the catabolism of brevican. MMPs and ADAMTSs may also play a role in dysfunctional neural plasticity by their possible involvement in the formation of dystrophic neurites surrounding the plaque. These proteases may promote neurite outgrowth and synaptogenesis after injury (Malemud, 2006; Pizzi and Crowe, 2006) by creating a more permissive ECM. Change in the activity of the protease, due to interaction with Aβ, disrupts this recovery mechanism and may ultimately affect neural plasticity.

It is possible that the catabolism of brevican is important in the modulation of neural plasticity, and it appears that Aβ affects the abundance of brevican isoforms by altering activity of the proteases, we examined the expression of synaptic markers as a measure of synaptic abundance and neural plasticity in APPsw mice. Here, synaptophysin, SNAP-25 and PSD-95 were measured by

ELISA in extracts from several brain regions taken from APPsw and non-transgenic animals. The vesicular pre-synaptic protein synaptophysin has been to shown to decrease in AD brain terminals (Honer et al., 1992; Masliah et al., 1994; Dickson et al., 1995; Sze et al., 1997) or remain unchanged in mouse models of AD (Irizarry et al., 1997; King and Arendash, 2002). The post-synaptic density marker PSD-95 has been reported to decrease in the presence of Aβ in both AD (Love et al., 2006) and mouse models of AD (Almeida et al., 2005). No changes in synaptophysin or PSD-95 were observed with ELISA, yet there were significant increases in the membrane bound pre-synaptic marker SNAP25 levels in hippocampus, frontal cortex, temporal lobe, and cerebellum compared to SNAP-25 concentrations in brain from non-transgenic animals. APP is expressed at high levels in the pre-synaptic active zone likely in proximity to the SNARE protein SNAP-25, which has been implicated in neurite outgrowth and synaptic remodeling *in vitro* (Oyler et al., 1989; Catsicas et al., 1991; Lakin et al., 1995). This marker has been shown to decline in the presence of Aβ (Chauhan and Siegel, 2002). Since APP is over-expressed in each of the four regions showing increased SNAP-25, high levels of APP at appropriate regionally-selective developmental times, rather than deposition of Aβ alone, may be important to account for over expression of this synaptic marker. In AD, there is no apparent increase in APP protein expression, but altered processing may be responsible for increased levels of Aβ and its deposition (Holtzman, 2004). Thus, this phenomenon may be simply due to over expression of APP in the transgenic mouse, with little relationship to AD. There is a significant literature describing

the expression of synaptic markers in AD, and in APP over-expressing transgenic mice, almost all with histochemical techniques and present conflicting data.

Overall, the deposition of Aβ into the ECM may be involved in the disruption of matrix processing and alter molecular extracellular events that modulate neural plasticity. The biomarker of strongest correlation with dementia of AD is a loss of synapses. In correlation to the region specific-decline in MMP activity, we observed an increase in the expression of the membrane-bound synaptic SNARE protein, SNAP-25. These results suggest that Aβ may exert inhibitory effects on the activity of the proteases responsible for matrix regulation and processing of brevican and other proteoglycans, as well as vesicle recruitment and synaptogenesis, effects potentially related to diminished neural plasticity in AD. Of course, how these changes more broadly relate to the total time course of the pathology in AD, or more proximally to the pathology of the APPsw mouse, remain to be examined.

Figure 17. Detection of brevican isoforms and proteolytic degradation by endogenous proteases at specific cleavage sites. Brevican is secreted as a >145 kD protein bearing 1-3 CS chains (A). Brevican can also be secreted as the holoprotein at 145 kD (B). When probed on Western blot with the N-terminal antibody (transduction labs) three immunoreactive bands appear: a >145 smear (glycosylated brevican), the 145 kD core protein, and a ~55 kD proteolytic fragment (C). The fragment of brevican is generated by endogenous proteases such as the MMPs (D) and ADAMTSs (E). Each has a different, specific cleavage site on the brevican protein. Shown here are the specific cleavage sites of the MMPs and ADAMTSs on the brevican protein in the mouse, rat and human sequences. The MMP cleavage-site is just 35 amino acid residues upstream from the ADAMTS-specific site.

Chapter 3, Figure 17

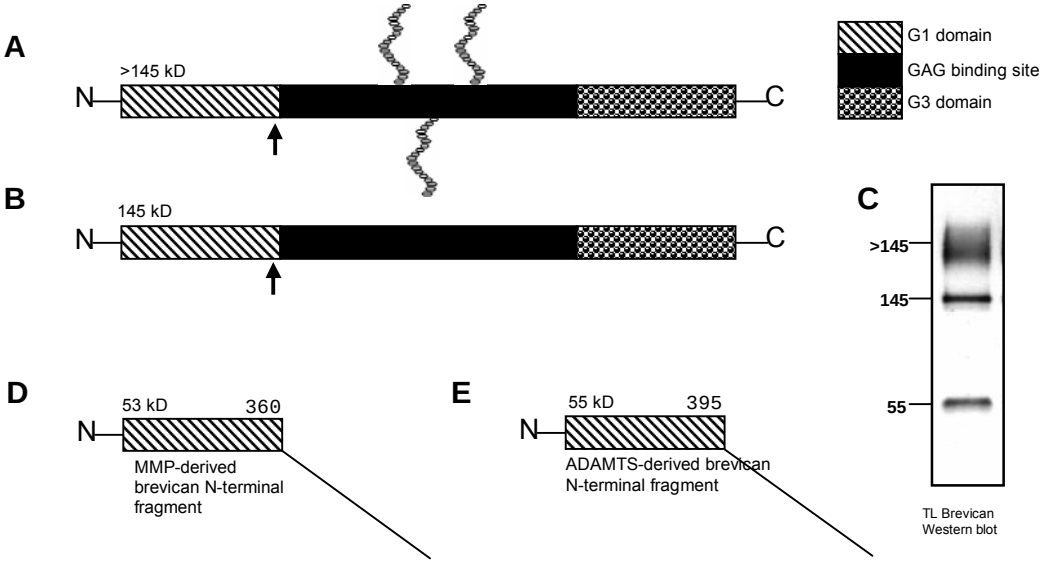

		360	361	395	396
rat brevican	351	CFRDSAHPSA	FSEASSPASDGLEAIVTVTEKLEELQLPQEAVESE	SRGAIYSI	403
		360	361	395	396
mouse brevican	351	CFRD**SAHPSA**	SSEASSPASDGLEAIVTVTEKLEELQLPQ**EAMESE**	SRGAIYSI	403
		361	362	400	401
human brevican	352	CFRDSAQPSA	IPEASNPASDGLEAIVTVTETLEELGLPQEATESE	SRGAIYSI	408

Figure 18. Relative immunoreactivity of brevican isoforms in the hippocampus of APPsw transgenic mice compared to littermate non-transgenic mice. (A) Brain extracts were probed for anti-brevican, anti-EAMESE and anti-SAHPSA in 15-month-old APPsw plaque-bearing mice (+) and 15-month-old non-transgenic (-) littermates (IC = internal control, C57Bl/6 hippocampal tissue, used for interblot variation and protein migration): There was no change in abundance of >145 kD protein in hippocampus, although a shift or change in glycosylation (lower molecular weight) was apparent. There was a significant increase in the abundance of the core 145 kD brevican accompanied by a decrease in the generalized fragment of brevican in the APPsw plaque-bearing tissue. No apparent change was observed in the ADAMTS-derived fragment, visualized by anti-EAMESE immunoreactivity. However, there was a marked decrease in the fragment of brevican generated by MMP-mediated proteolytic cleavage, denoted by anti-SAHPSA immunoreactivity, in hippocampal samples of APPsw mice. (B) Densitometric analysis of hippocampus tissue on Western blot.

Chapter 3, Figure 18

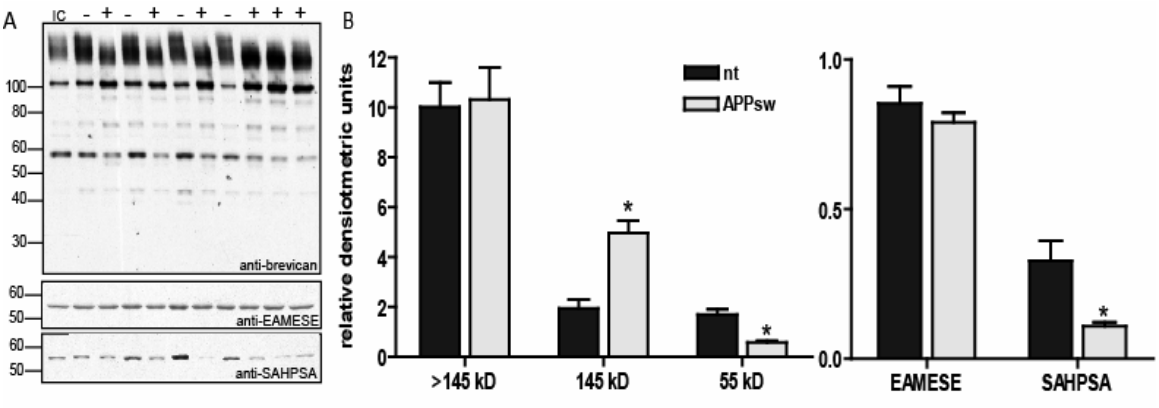

Table 3. Relative immunoreactivity of brevican isoforms in several brain regions of APPsw transgenic (+) mouse brain compared to littermate wild-type (-) control.

		G1 brevican Isoforms			ADAMTS-derived fragment	MMP-derived fragment
brain region	tg	>145 kD	145 kD	55kD	EAMESE	SAHPSA
Frontal cortex	-	28.3 ± 3.20	5.93 ± 0.43	1.87 ± 0.55	0.85 ± 0.16	0.18 ± 0.13
	+	17.4 ± 2.21*	7.85 ± 0.86*	1.62 ± 0.62	1.06 ± 0.14	0.08 ± 0.05
Temporal lobe	-	25.1 ± 2.13	2.50 ± 0.03	1.35 ± 0.26	0.93 ± 0.28	0.59 ± 0.15
	+	17.2 ± 2.40*	6.31 ± 0.44*	3.18 ± 0.96*	1.02 ± 0.20	0.47 ± 0.11
Cerebellum	-	11.3 ± 1.08	2.98 ± 0.23	4.53 ± 0.44	1.22 ± 0.03	0.93 ± 0.05
	+	8.54 ± 0.72*	6.85 ± 0.28*	2.37 ± 0.23*	1.41 ± 0.20	0.43 ± 0.12*
Hypothalamus	-	11.9 ± 1.19	2.37 ± 0.56	0.75 ± 0.11	3.67 ± 0.31	0.68 ± 0.21
	+	7.99 ± 1.36*	4.98 ± 0.74*	1.35 ± 0.39*	3.18 ± 0.23	0.83 ± 0.30
Brain Stem	-	9.64 ± 2.25	1.90 ± 0.51	5.72 ± 0.81	2.31 ± 0.31	0.79 ± 0.26
	+	7.31 ± 1.60	4.73 ± 0.83*	5.28 ± 0.72	2.29 ± 0.24	0.73 ± 0.26

*significantly different from non-transgenic; tg = transgene; APPsw = (+), n=6; and non-transgenic = (-), n=4.

Figure 19. Immunohistochemical localization of brevican, the proteolytically cleaved fragment of brevican, and Aβ plaques in APPsw transgenic mice. Epifluorescent micrographs of brevican immunoreactivity (A, H, K), anti-EAMESE immunoreactivity (D, G), anti-SAHPSA immunoreactivity (J) and Aβ (B, E) in fixed brain sections. Merged composites (C, F, I & L). Brevican was co-localized with Aβ. The immunoreactivity for brevican fragments revealed a ring around the plaque that suggests increased activity adjacent to the amyloid deposition. All images captured at 40x magnification. Marker represents 50 μm.

Chapter 3, Figure 19

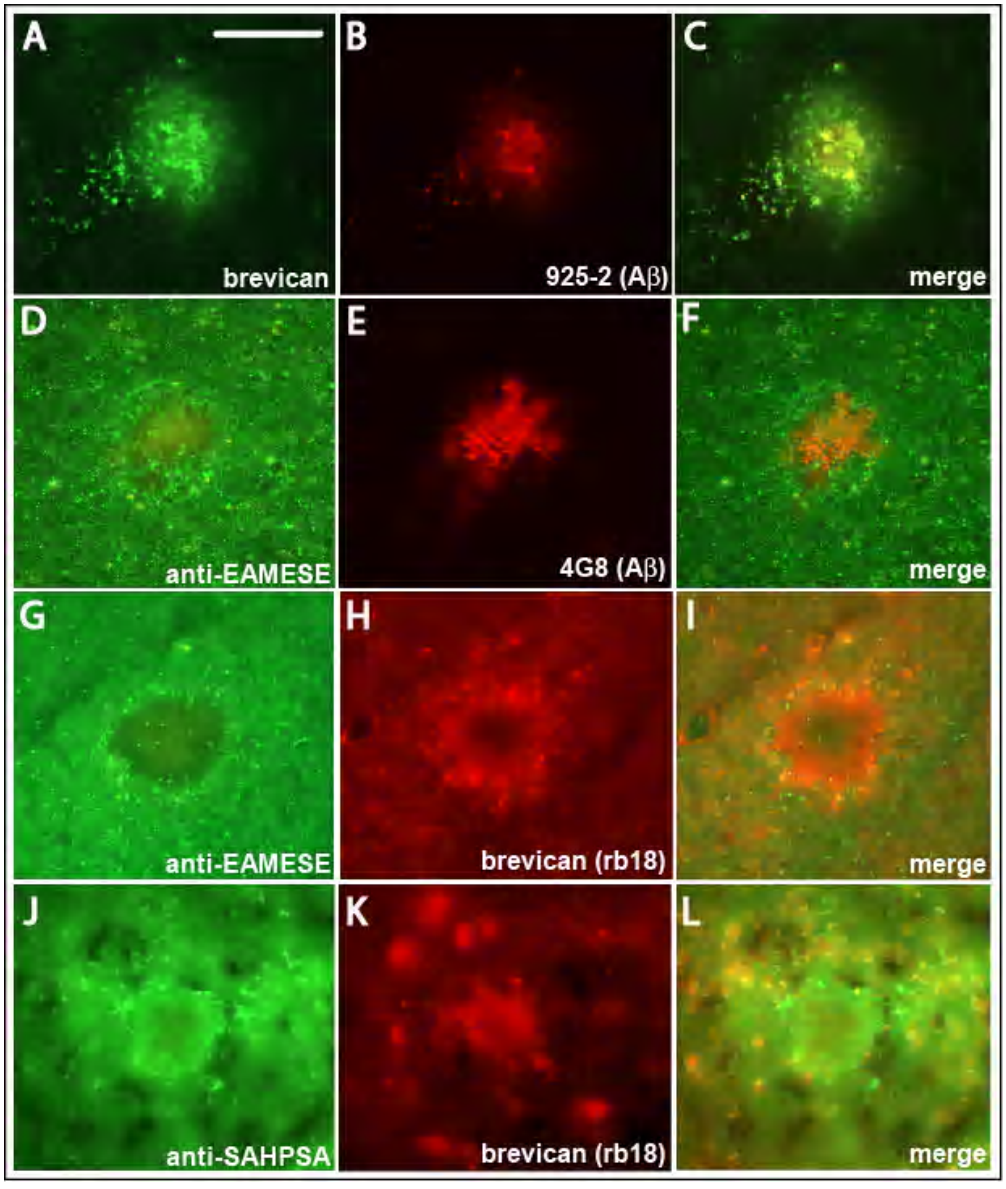

Figure 20. Synaptic markers as measured by ELISA in brain regions of APPsw and non-transgenic control animals. Relative GFAP (A), synaptophysin (B), PSD-95 (C) and SNAP-25 (D) immunoreactivity in samples of cerebellum (CB), hippocampus (HC), brain stem (BS), temporal lobe (TL) and hypothalamus (HT) from non-transgenic and APPsw mice. GFAP levels were elevated in the FC ($p=0.0443$), HC ($p=0.0163$) and TL ($p=0.0490$) of APPsw mice compared to non-transgenic. No changes detected in synaptophysin and PSD-95 synaptic markers. In APPsw mice, SNAP-25 immunoreactivity was elevated in the FC ($p=0.0315$), HC ($p=0.0482$), TL ($p=0.0351$) and CB ($p=0.0112$) compared to samples from non-transgenic littermates.

Chapter 3, Figure 20

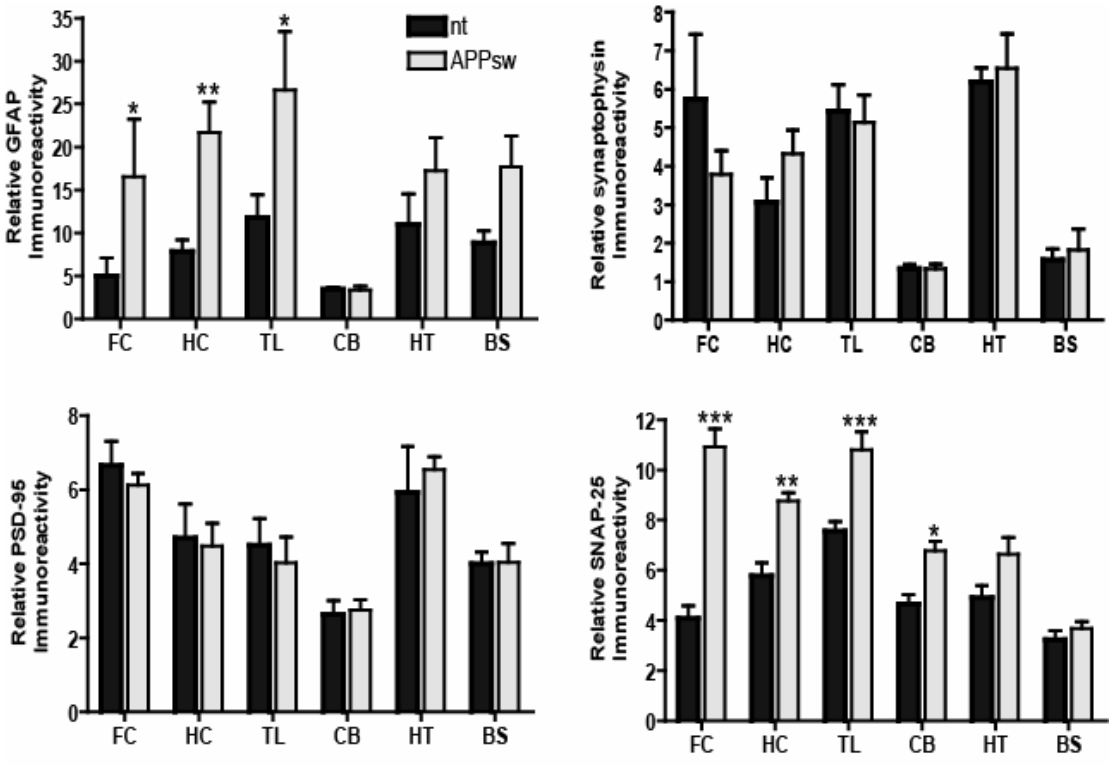

REFERENCES CITED

Almeida CG, Tampellini D, Takahashi RH, Greengard P, Lin MT, Snyder EM, Gouras GK (2005) Beta-amyloid accumulation in APP mutant neurons reduces PSD-95 and GluR1 in synapses. Neurobiol Dis 20:187-198.

Asahina M, Yoshiyama Y, Hattori T (2001) Expression of matrix metalloproteinase-9 and urinary-type plasminogen activator in Alzheimer's disease brain. Clin Neuropathol 20:60-63.

Aya-ay J, Mayer J, Eakin AK, Muffly BG, Anello M, Sandy JD, Gottschall PE (2005) The effect of hypoxic-ischemic brain injury in perinatal rats on the abundance and proteolysis of brevican and NG2. Exp Neurol 193:149-162.

Backstrom JR, Lim GP, Cullen MJ, Tokes ZA (1996) Matrix metalloproteinase-9 (MMP-9) is synthesized in neurons of the human hippocampus and is capable of degrading the amyloid-beta peptide (1-40). J Neurosci 16:7910-7919.

Bandtlow CE, Zimmermann DR (2000) Proteoglycans in the developing brain: new conceptual insights for old proteins. Physiol Rev 80:1267-1290.

Catsicas S, Larhammar D, Blomqvist A, Sanna PP, Milner RJ, Wilson MC (1991) Expression of a conserved cell-type-specific protein in nerve terminals coincides with synaptogenesis. Proc Natl Acad Sci U S A 88:785-789.

Chauhan NB, Siegel GJ (2002) Reversal of amyloid beta toxicity in Alzheimer's disease model Tg2576 by intraventricular antiamyloid beta antibody. J Neurosci Res 69:10-23.

Cotman SL, Halfter W, Cole GJ (2000) Agrin binds to beta-amyloid (Abeta), accelerates abeta fibril formation, and is localized to Abeta deposits in Alzheimer's disease brain. Mol Cell Neurosci 15:183-198.

Deb S, Wenjun Zhang J, Gottschall PE (2003) Beta-amyloid induces the production of active, matrix-degrading proteases in cultured rat astrocytes. Brain Res 970:205-213.

Dickson DW, Crystal HA, Bevona C, Honer W, Vincent I, Davies P (1995) Correlations of synaptic and pathological markers with cognition of the elderly. Neurobiol Aging 16:285-298; discussion 298-304.

Drouet B, Pincon-Raymond M, Chambaz J, Pillot T (1999) Laminin 1 attenuates beta-amyloid peptide Abeta(1-40) neurotoxicity of cultured fetal rat cortical neurons. J Neurochem 73:742-749.

Flannery CR, Zeng W, Corcoran C, Collins-Racie LA, Chockalingam PS, Hebert T, Mackie SA, McDonagh T, Crawford TK, Tomkinson KN, LaVallie ER, Morris EA (2002) Autocatalytic cleavage of ADAMTS-4 (Aggrecanase-1) reveals multiple glycosaminoglycan-binding sites. J Biol Chem 277:42775-42780.

Giulian D, Haverkamp LJ, Li J, Karshin WL, Yu J, Tom D, Li X, Kirkpatrick JB (1995) Senile plaques stimulate microglia to release a neurotoxin found in Alzheimer brain. Neurochem Int 27:119-137.

Glenner GG, Wong CW (1984) Alzheimer's disease: initial report of the purification and characterization of a novel cerebrovascular amyloid protein. Biochem Biophys Res Commun 120:885-890.

Gottschall PE (2001) Abeta blah blah in humans. In: Society for Neuroscience. New Orleans, LA.

Gottschall PE, Yuan W, Muffly BG (2003) Attenuated Proteoglycanase activity in Alzheimer's Disease hippocampus: Associated with diminished synaptic density and inhibition of actvity by abeta-amyloid. In: Society for Neuroscience. New Orleans, Louisiana: Abstarct Viewer / Itinerary Planner.

Hardy JA, Higgins GA (1992) Alzheimer's disease: the amyloid cascade hypothesis. Science 256:184-185.

Hockfield S, Kalb RG, Zaremba S, Fryer H (1990) Expression of neural proteoglycans correlates with the acquisition of mature neuronal properties in the mammalian brain. Cold Spring Harb Symp Quant Biol 55:505-514.

Holtzman DM (2004) In vivo effects of ApoE and clusterin on amyloid-beta metabolism and neuropathology. J Mol Neurosci 23:247-254.

Honer WG, Dickson DW, Gleeson J, Davies P (1992) Regional synaptic pathology in Alzheimer's disease. Neurobiol Aging 13:375-382.

Hsiao K, Chapman P, Nilsen S, Eckman C, Harigaya Y, Younkin S, Yang F, Cole G (1996) Correlative memory deficits, Abeta elevation, and amyloid plaques in transgenic mice. Science 274:99-102.

Hsiao KK, Borchelt DR, Olson K, Johannsdottir R, Kitt C, Yunis W, Xu S, Eckman C, Younkin S, Price D, et al. (1995) Age-related CNS disorder and early death in transgenic FVB/N mice overexpressing Alzheimer amyloid precursor proteins. Neuron 15:1203-1218.

Irizarry MC, McNamara M, Fedorchak K, Hsiao K, Hyman BT (1997) APPSw transgenic mice develop age-related A beta deposits and neuropil abnormalities, but no neuronal loss in CA1. J Neuropathol Exp Neurol 56:965-973.

Itagaki S, McGeer PL, Akiyama H, Zhu S, Selkoe D (1989) Relationship of microglia and astrocytes to amyloid deposits of Alzheimer disease. J Neuroimmunol 24:173-182.

King DL, Arendash GW (2002) Maintained synaptophysin immunoreactivity in Tg2576 transgenic mice during aging: correlations with cognitive impairment. Brain Res 926:58-68.

Kowalska MA, Badellino K (1994) beta-Amyloid protein induces platelet aggregation and supports platelet adhesion. Biochem Biophys Res Commun 205:1829-1835.

Lakin ND, Morris PJ, Theil T, Sato TN, Moroy T, Wilson MC, Latchman DS (1995) Regulation of neurite outgrowth and SNAP-25 gene expression by the Brn-3a transcription factor. J Biol Chem 270:15858-15863.

Lee JM, Yin KJ, Hsin I, Chen S, Fryer JD, Holtzman DM, Hsu CY, Xu J (2003) Matrix metalloproteinase-9 and spontaneous hemorrhage in an animal model of cerebral amyloid angiopathy. Ann Neurol 54:379-382.

Lee JM, Yin K, Hsin I, Chen S, Fryer JD, Holtzman DM, Hsu CY, Xu J (2005) Matrix metalloproteinase-9 in cerebral-amyloid-angiopathy-related hemorrhage. J Neurol Sci 229-230:249-254.

Lorenzl S, Albers DS, Relkin N, Ngyuen T, Hilgenberg SL, Chirichigno J, Cudkowicz ME, Beal MF (2003) Increased plasma levels of matrix metalloproteinase-9 in patients with Alzheimer's disease. Neurochem Int 43:191-196.

Love S, Siew LK, Dawbarn D, Wilcock GK, Ben-Shlomo Y, Allen SJ (2006) Premorbid effects of APOE on synaptic proteins in human temporal neocortex. Neurobiol Aging 27:797-803.

Malemud CJ (2006) Matrix metalloproteinases (MMPs) in health and disease: an overview. Front Biosci 11:1696-1701.

Masliah E, Mallory M, Hansen L, DeTeresa R, Alford M, Terry R (1994) Synaptic and neuritic alterations during the progression of Alzheimer's disease. Neurosci Lett 174:67-72.

Mayer J, Hamel MG, Gottschall PE (2005) Evidence for proteolytic cleavage of brevican by the ADAMTSs in the dentate gyrus after excitotoxic lesion of the mouse entorhinal cortex. BMC Neurosci 6:52.

McGeer PL, Akiyama H, Itagaki S, McGeer EG (1989) Immune system response in Alzheimer's disease. Can J Neurol Sci 16:516-527.

Mesulam MM (1999) Neuroplasticity failure in Alzheimer's disease: bridging the gap between plaques and tangles. Neuron 24:521-529.

Morgan D, Diamond DM, Gottschall PE, Ugen KE, Dickey C, Hardy J, Duff K, Jantzen P, DiCarlo G, Wilcock D, Connor K, Hatcher J, Hope C, Gordon M, Arendash GW (2000) A beta peptide vaccination prevents memory loss in an animal model of Alzheimer's disease. Nature 408:982-985.

Mrak RE, Sheng JG, Griffin WS (1996) Correlation of astrocytic S100 beta expression with dystrophic neurites in amyloid plaques of Alzheimer's disease. J Neuropathol Exp Neurol 55:273-279.

Nakamura H, Fujii Y, Inoki I, Sugimoto K, Tanzawa K, Matsuki H, Miura R, Yamaguchi Y, Okada Y (2000) Brevican is degraded by matrix metalloproteinases and aggrecanase-1 (ADAMTS4) at different sites. J Biol Chem 275:38885-38890.

Oyler GA, Higgins GA, Hart RA, Battenberg E, Billingsley M, Bloom FE, Wilson MC (1989) The identification of a novel synaptosomal-associated protein, SNAP-25, differentially expressed by neuronal subpopulations. J Cell Biol 109:3039-3052.

Palop JJ, Chin J, Mucke L (2006) A network dysfunction perspective on neurodegenerative diseases. Nature 443:768-773.

Pizzi MA, Crowe MJ (2006) Matrix metalloproteinases and proteoglycans in axonal regeneration. Exp Neurol.

Sastre M, Klockgether T, Heneka MT (2006) Contribution of inflammatory processes to Alzheimer's disease: molecular mechanisms. Int J Dev Neurosci 24:167-176.

Satoh K, Suzuki N, Yokota H (2000) ADAMTS-4 (a disintegrin and metalloproteinase with thrombospondin motifs) is transcriptionally induced in beta-amyloid treated rat astrocytes. Neurosci Lett 289:177-180.

Schott JM, Kennedy J, Fox NC (2006) New developments in mild cognitive impairment and Alzheimer's disease. Curr Opin Neurol 19:552-558.

Selkoe DJ (1991) Alzheimer's disease. In the beginning. Nature 354:432-433.

Selkoe DJ (2002) Alzheimer's disease is a synaptic failure. Science 298:789-791.

Sze CI, Troncoso JC, Kawas C, Mouton P, Price DL, Martin LJ (1997) Loss of the presynaptic vesicle protein synaptophysin in hippocampus correlates with cognitive decline in Alzheimer disease. J Neuropathol Exp Neurol 56:933-944.

Terai K, Iwai A, Kawabata S, Tasaki Y, Watanabe T, Miyata K, Yamaguchi T (2001) beta-amyloid deposits in transgenic mice expressing human beta-amyloid precursor protein have the same characteristics as those in Alzheimer's disease. Neuroscience 104:299-310.

Tortorella MD, Pratta M, Liu RQ, Austin J, Ross OH, Abbaszade I, Burn T, Arner E (2000) Sites of aggrecan cleavage by recombinant human aggrecanase-1 (ADAMTS-4). J Biol Chem 275:18566-18573.

van Horssen J, Kleinnijenhuis J, Maass CN, Rensink AA, Otte-Holler I, David G, van den Heuvel LP, Wesseling P, de Waal RM, Verbeek MM (2002) Accumulation of heparan sulfate proteoglycans in cerebellar senile plaques. Neurobiol Aging 23:537-545.

Watanabe N, Araki W, Chui DH, Makifuchi T, Ihara Y, Tabira T (2004) Glypican-1 as an Abeta binding HSPG in the human brain: its localization in DIG domains and possible roles in the pathogenesis of Alzheimer's disease. Faseb J 18:1013-1015.

Wilcock DM, Gordon MN, Ugen KE, Gottschall PE, DiCarlo G, Dickey C, Boyett KW, Jantzen PT, Connor KE, Melachrino J, Hardy J, Morgan D (2001) Number of Abeta inoculations in APP+PS1 transgenic mice influences antibody titers, microglial activation, and congophilic plaque levels. DNA Cell Biol 20:731-736.

Yamaguchi Y (2000) Lecticans: organizers of the brain extracellular matrix. Cell Mol Life Sci 57:276-289.

Yan P, Hu X, Song H, Yin K, Bateman RJ, Cirrito JR, Xiao Q, Hsu FF, Turk JW, Xu J, Hsu CY, Holtzman DM, Lee JM (2006) Matrix metalloproteinase-9 degrades amyloid-beta fibrils in vitro and compact plaques in situ. J Biol Chem 281:24566-24574.

Yin KJ, Cirrito JR, Yan P, Hu X, Xiao Q, Pan X, Bateman R, Song H, Hsu FF, Turk J, Xu J, Hsu CY, Mills JC, Holtzman DM, Lee JM (2006) Matrix metalloproteinases expressed by astrocytes mediate extracellular amyloid-beta peptide catabolism. J Neurosci 26:10939-10948.

Yuan W, Matthews RT, Sandy JD, Gottschall PE (2002) Association between protease-specific proteolytic cleavage of brevican and synaptic loss in the dentate gyrus of kainate-treated rats. Neuroscience 114:1091-1101.

CHAPTER 4

CHARACTERIZATION OF LECTICAN PROCESSING AND SYNAPTIC MARKERS IN THE BRAIN OF A MUTANT MOUSE DEFICIENT FOR THE PROTEOGLYCANSE, ADAMTS1

Joanne Mayer[1], Autumn K. Eakin[1], Christopher C. Leonardo[1],

Paul E. Gottschall[1]*

[1]University of South Florida College of Medicine, Department of Molecular Pharmacology and Physiology, 12901 Bruce B. Downs Blvd, Tampa, Florida 33612-4799, USA

*To whom correspondence should be addressed:
Paul E. Gottschall
University of South Florida College of Medicine
Department of Molecular Pharmacology and Physiology
12901 Bruce B Downs Blvd
PHONE: 813-974-9910
FAX: 813-974-2565
e-mail: pgottsch@hsc.usf.edu jmayer1@health.usf.edu
aeakin@hsc.usf.edu cleonard@hsc.usf.edu

ABSTRACT

Lecticans, a sub-family of chondroitin sulfate (CS)-containing proteoglycans, are expressed in aggregates in the extracellular matrix (ECM) of the central nervous system (CNS) where they likely stabilize synapses and inhibit neural plasticity. Proteolytic cleavage of the proteoglycans by endogenous glutamyl endopeptidases of the ADAMTS (a disintegrin and metalloproteinase with thrombospondin motifs) family appears to release this inhibition and promote neural plasticity. ADAMTS1 is expressed in neurons and glia in the CNS, it is induced under inflammatory conditions and may play a role in neuritic repair and regeneration. The purpose of this study was to characterize the effects of deleting the ADAMTS1 gene on the processing of neural-expressed lecticans, and whether this deletion affected the regional expression and abundance of synaptic markers in the CNS. Changes in the expression of brevican isoforms were limited to the temporal lobe with no changes observed in five other brain regions compared to wild-type CNS regions. Marked attenuation in versican processing was observed especially in frontal cortex and hippocampus of ADAMTS1 knockout CNS compared to wild-type regions. Enzyme-linked immunoabsorbant assays (ELISAs) were conducted to measure levels of synaptophysin, SNAP-25 and PSD-95 in brain regions. Marked elevations (~2.5-fold) in synaptophysin and SNAP-25 concentrations were observed in the hippocampus, whereas, in frontal cortex all three markers were elevated in ADAMTS1-deficient mice compared to their littermate controls. The classical entorhinal cortex lesion model of neural plasticity was employed to investigate

the neural plasticity response to lesion in the protease deficient mouse. There was a trend for diminished sprouting and re-innervation of the molecular layer target regions of ADAMTS1 deficient mice when neurons of the medial entorhinal cortex were lesioned. These results suggest that endogenous proteases such as the ADAMTSs may play a role in synaptogenesis during development or in synaptic maintenance in the adult.

Keywords: extracellular matrix, proteoglycan, brevican, versican, SNAP-25, synaptophysin, PSD-95, entorhinal cortex lesion

INTRODUCTION

ADAMTS1 (a disintegrin and metalloproteinase with thrombospondin motifs-1) was first described by Kuno et al, in 1997 and since has proven to be important in normal growth, fertility and the development of several tissue types (Kuno et al., 1997, Shindo et al., 2000). ADAMTS1 belongs to a sub group of the ADAMTS glutamyl endopeptidases that are expressed in the central nervous system (CNS) (Yuan et al., 2002), where they bind and cleave proteoglycans in the extracellular matrix (ECM). In particular, substrates for this subgroup of ADAMTSs are large negatively charged aggregating, chondroitin sulfate (CS)-containing proteoglycans, termed lecticans, which include aggrecan, brevican and versican (Yamaguci, 2000; Kuno et al., 2000; Sandy et al., 2001). Expression of ADAMTS1 is low under basal conditions, yet recent data suggest that it is up-regulated after injury (Sasaki et al., 2001; Yuan et al., 2002), during

tumor progression (Masui et al, 2001; Kuno et al., 2004), in other disease states (Miguel et al., 2005; Haddock et al., 2006), and accompanying inflammatory responses (Kuno et al., 1997; Cross et al., 2006, Ng et al., 2006). The ADAMTS1 deficient mouse undergoes abnormal growth and development, as well as changes in matrix processing that account for irregularities in ovulation, urogenital function and angiogenesis (Kuno et al 1997, Kuno & Rodriguez), suggesting ADAMTS1 may play an important role in matrix maintenance and regulation.

Lecticans form aggregate complexes in the ECM that inhibit neurite outgrowth (Bandtlow and Zimmermann, 2000) and stabilize synapses (Hockfield et al., 1990). Our working hypothesis and that of others (Yamaguchi, 2000; Yuan et al., 2002; Gottschall et al., 2005a, b; Hamel et al., 2005; Mayer et al., 2005) is that lectican cleavage by the ADAMTSs loosens these aggregates and promotes neural plasticity mechanisms, i.e. neuritic growth, axonal sprouting, synaptogenesis.

One goal of this study was to examine and characterize lectican processing in the CNS of the ADAMTS1 deficient mouse. Interestingly, the turnover of aggrecan in cartilage was not altered in this mouse model (Little et al., 2005). In addition, a great deal has been assumed about the role of lecticans and lectican turnover in neural plasticity without significant direct evidence to support it. Thus, a second goal was to determine whether a deficiency of ADAMTS1 during development and into adulthood, influences the expression of

synaptic markers, and, secondly, in a classical model of neuritic sprouting, whether it affects neural reinnervation after injury.

MATERIALS & METHODS

Animals

All animal procedures described here were approved by the Institutional Animal Care and Use Committee at the University of South Florida. Forty-six adult ADAMTS1 knockout mice of the 129/Sv x C57BL/6 hybrid (Shindo et al., 2000) (23 g - 27 g; Eli Lily, Indianapolis, IN) 12 weeks of age were housed under a 12 h light cycle with regulated temperature and humidity. Mice were housed 3 to 4 per cage and had free access to food and water. Heterozygote genotypes were mated since female -/- were infertile and these offspring provided both wild-type (+/+) and knockout (-/-) mice for the experiments. Typical of ADAMTS1 deficient mice, litters were small and averaged about 3-4 pups per litter. PCR for genotyping was performed as described by Shindo et al., 2000. Eight wild-type littermates and eight knockout animals were collected for characterization and 15 ADAMTS1 deficient mice and 15 wild-type littermates were used in the entorhinal cortex lesion (ECL) experiments. Following ECL surgery, the animals were housed individually. Tissue extracts of dentate gyrus collected as described (Mayer et al., 2005) from control mice (n=15) and lesioned mice (n=15) collected 7 days (wild-type, n=7; knockout, n=8) and 21 (wild-type, n=7; knockout, n=8) days after surgery were used in biochemical immunoassays.

Surgical procedures - the entorhinal cortex lesion (ECL)

Surgeries were performed using isofluorane/oxygen mixed gas anesthesia. Once deeply anesthetized, animals were placed into the stereotaxic apparatus and a hole was drilled in the skull of the right hemisphere to allow for needle penetration. The right, lateral EC of mice was unilaterally lesioned by lowering a needle attached to a Hamilton syringe (#701N) through the hole in the skull to the coordinates AP = 4.72 mm, L = 3.75 mm and DV = 4.70 mm using bregma as a reference and oriented 17^{o} rostral-caudal (White et al., 2001; Mayer et al., 2005). One µl of the neurotoxin, ibotenic acid ((±) α-Amino-3-hydroxy-5-isoxazoleacetic acid, 10 µg/µl) was injected into the lateral EC at a rate of 0.1 µl every 30 seconds, with the needle remaining in place for an additional minute at the end of the 5-minute injection period to allow for complete diffusion of the drug into the lateral EC. Neurons of the lateral EC project preferentially to the septal (dorsal) dentate gyrus. The needle was removed, bone wax applied to cover the hole, and the animal recovered on a heating pad and was returned to a new cage and housed individually. At 7 and 21 days after lesion, mice were injected with an overdose of Nembutal (pentobarbital) for deep anesthesia, the brain was removed and 2 mm sections collected. The anterior hippocampal section was collected with the 'regional isolation method' (Mayer et al., 2005) for biochemistry and the posterior entorhinal cortex containing 2 mm section was fixed by immersion with cold 4% paraformaldehyde fixative diluted in 0.1 M phosphate buffer (pH 7.4). The sections was post-fixed overnight at 4^{o}C, cryoprotected with consecutive solutions of 15 and 30% sucrose until completely infused, and the

frozen cryoprotected entorhinal cortex 'slab' was sectioned on a cryostat at 30 µm. The extent and magnitude of the lesion in the EC was verified by cresyl violet staining.

Tissue preparation

Various brain regions (hippocampus, frontal cortex, temporal lobe, hypothalamus, cerebellum and brain stem) were rapidly dissected and extracted with a teflon-glass homogenizer in 5 volumes of detergent-containing RIPA buffer (50mM Tris base, 150mM NaCl, 1mM EDTA, 1mM EGTA, 1% Triton-X-100, 1% sodium deoxycholate, 1% SDS, pH = 7.4 & 1:100 protease inhibitor cocktail; 5% wet-weight for whole tissue for characterization experiments). The isolated dentate gyrus ECL tissue was homogenized in 0.6 ml microcentrifuge tubes with 20 µl RIPA buffer using three cycles of 2 minutes of 4^{o}C incubation and 30 sec of vortex, centrifuged 6,800 x g for 1 minutes and stored at –80^{o}C. For the whole tissue regions, the homogenate was centrifuged in a microcentrifuge at 6800 x g for 5 minutes, and the isolated supernatant collected and stored at –80^{o}C.

Western blotting

Whole tissue extracts and dentate gyrus extracts (collected as described in 'regional isolation method', Mayer et al., 2005) were loaded (equal amounts of protein and 2x sample buffer) onto 4-20% polyacrylamide gels (Invitrogen, Carlsbad, CA) and subjected to SDS-PAGE. Protein was transferred to a polyvinylidine difluoride membrane (PVDF, Immobilon, Millipore, Billerica, MA)

and the membrane was blocked with 5% milk in PBS. Membranes were probed with primary antibodies against brevican (1:1000), EAMESE (1:500), SAHPSA (1:300), 12C5 (1:500; Developmental Studies Hybridoma Bank, Iowa City, IA), NIVNSE (1:500) and secondary anti-rabbit or anti-mouse IgG conjugated to horseradish peroxidase (Chemicon, Temecula, CA). Antigens were visualized using a chemiluminescence developing system (SuperSignal, Pierce, Rockford, IL) and CL-XPosure Film (Pierce). In some experiments, brain tissue extract was treated with chondroitinase ABC prior to Western blot to detect full-length versican with anti-12C5. Thus, 25 µl of sodium acetate buffer (50 mM sodium acetate, 1 M Tris, 10 mM EDTA) containing 10 mU of chondroitinase ABC (Sigma-Aldrich, St. Louis, MO) was added to 25 µl of brain tissue extract and incubated for 1.5 h at 37^{o}C. Brevican samples were reduced (mercaptoethanol-containing, SDS-PAGE sample buffer) and versican samples probed for 12C5 were placed in non-reducing buffer (SDS-PAGE sample buffer without mercaptoethanol), denatured for 4 minutes at 95^{o}C, and subjected to SDS-PAGE.

ELISA

Enzyme-linked immunoabsorbant assays (ELISAs) were performed to measure immunoreactivity of synaptophysin, SNAP-25 and PSD-95. Coating antibodies were diluted in 0.01 M PB and let to dry overnight in a EIA/RIA high-binding 96-well plate (Costar - Sigma; St. Louis, MO) using mouse anti-synaptophysin; Chemicon, Temecula, CA 1:250; mouse anti-SNAP-25,

Chemicon, 1:200; and mouse anti-PSD-95, Chemicon, 1:100). The wells were washed with sample/wash buffer (PBS with 0.05% Tween-20) one time and blocking buffer (PBS with 0.05% Tween-20 and 5% dry milk) was added to the wells and incubated at room temperature for 1 hr with agitation. The wells were washed, standard and samples were added for a 2 hr incubation on a shaker (highest standard = rat brain homogenate at 10ug/ul with serial dilutions). After samples were washed from the well, primary antibody diluted in sample/wash buffer was added and allowed to incubate for 2 hrs with agitation (rabbit anti-synaptophysin DAKO, Carpenteria, CA 1:2000; rabbit anti-SNAP-25 Sigma, St. Louis, MO, 1:1000; and sheep anti-PSD95 ZYMED, San Francisco, CA, 1:100). The wells were washed three times before adding secondary antibodies, allowed to incubate for 45 minutes on a shaker (goat anti-rabbit IgG-HRP, Chemicon, 1:5000; anti-sheep, Chemicon, 1:1000). Next, TMB (tetramethyl benzidine, Sigma, St. Louis, MO) solution was applied and the color allowed to develop. The colometrtic reaction was stopped with 1M H_2SO_4. Absorbance levels were measured with a Wallac Victor2 1420 multilabel counter (Perkin Elmer, Wellesley, MA) and Workout software (version 1.5, Perkin Elmer), and the readings were normalized with concentration of protein in the sample added to the well. Samples were extrapolated from the rat brain standard curve within the same assay. The means from the experiments groups were compared using ANOVA and pair-wise comparisons were made with Bonferroni post-hoc test (GraphPad, San Diego, CA). A p-value < 0.05 was considered significant.

RESULTS

To determine if the gene-deletion had any effect on lectican processing in the CNS, hippocampal tissue from ADAMTS1 knockout (-) and littermate wild-type (+) hippocampus was probed with anti-brevican antibody, that detects an internal epitope in the G1 globular domain of brevican (Fig. 21A) and analyzed with densitomety (Fig. 21B). No changes were observed in the molecular size of the isoforms, or in the abundance of the full-length brevican isoform containing CS chains (>145 kD), the full-length core protein without CS chains (145 kD) or the generalized proteolytic fragment (55 kD). When probed with the ADAMTS-specific (anti-EAMESE) and MMP-specific antibodies (anti-SAHPSA) (Fig. 21C), no changes in abundance of either fragment was observed (Fig. 21D). The relative immunoreactivity of brevican isoforms in the hippocampus, frontal cortex, cerebellum, hypothalamus and brain stem did not show any isoform differences between the ADAMTS1 knockout and the control. However, temporal lobe alone revealed an increase in overall 55 kD fragment generated (Table 4). Probing with antibodies raised against the specific neoepitope sequences exposed after cleavage by proteases, an increase in the fragment generated by ADAMTSs in general and a decline in the MMP-derived fragment was observed.

Hippocampal tissue was probed for full-length versican (using the G1 versican antibody 12C5) and the ADAMTS-derived fragment of versican (anti-NIVNSE) (Fig. 22A). An increase in the abundance of the full-length versican (245 kD) was observed in the ADAMTS1 knockout tissue, while a decrease was apparent in the ADAMTS-specific fragment (~66kD). Densitometric analysis

suggested altered processing of versican in the ADAMTS1 knockout tissue (-/-) compared to wild-type (+/+) (Fig. 22B). Relative versican immunoreactivity for hippocampus, frontal cortex, temporal lobe, cerebellum, hypothalamus and brain stem was examined (table 5). With the exception of brain stem, a significant increase of full-length versican was observed in the ADAMTS1 knockout. Concurrent with this finding, a simultaneous decline in the proteolytic fragment occurred in all brain regions.

Since altered matrix may be necessary for neural plasticity to occur, the vesicular, pre-synaptic marker synaptophysin, the membrane bound pre-synaptic SNARE protein, SNAP-25 and the post-synaptic density marker PSD-95 were measured by ELISA in the ADAMTS1 knockout compared to wild-type (table 6). The hippocampus was higher in abundance, or synaptic density, for both pre-synaptic markers (synaptophysin, $p=0.0003$; SNAP-25, $p=>0.0001$) with a trend for an increase in PSD-95. Moreover, all three markers were up regulated in the frontal cortex (synaptophysin, $p=0.0376$; SNAP-25, $p=0.0449$; PSD-95, $p=0.0278$). No difference in synaptic markers was observed in the temporal lobe, hypothalamus, cerebellum or brain stem.

An abundance of brevican isoforms in the dentate gyrus was observed at 7 and 21 days after ECL. In the wild-type animal, there were no significant changes in any of the brevican isoforms compared to the contralateral side at 7 days post-ECL (Fig. 23A) or 21 days post ECL (Fig. 23B). However, at 7 days post-lesion in the ADAMTS1 knockout, there was a significant increase in the >145 kD core protein and the generalized 55 kD (Fig. 23C). It appears that the

knockout animals are producing more core brevican in the dentate gyrus on the injured side and catabolized by endogenous proteases compared to contralateral. At 21 days post-lesion, the brevican isoforms in the knockout animal are not different from the non-lesion side (Fig. 23D).

To estimate apparent ADAMTS activity *in vivo*, the density of the EAMESE (55 kD) immunoreactive fragment in Western blot was divided by the densitometric level of intact full-length and core protein brevican isoforms (>145 kD + 145 kD) (Fig. 24). Seven days post-ECL there was a 40% increase in apparent ADAMTS activity in the ipsilateral dentate gyrus of the wild-type tissue, however, at the seven-day critical reinnervation period, ADAMTS activity was decreased by almost 25% in the ADAMTS1 knockout. This observation is supported by the increase in the >145 kD and the 145 kD isoforms in the knockout at this time point. By 21 days post-lesion, the activity was not different from the contralateral side for either wild-type or knockout. ANOVA analysis revealed that the effect of genotype was significant ($p=0.0298$).

Seven days after lesion, synaptophysin levels as detected by ELISA (Fig. 25A), declined by 30% in the knockout dentate compared to the contralateral side and 25% in the wild-type. However, when isolated dentate gyrus tissue was examined 21 days post-lesion, synaptophysin concentrations were not different from the control side in the wild-type. This observation shows there is a reinnervation of the OML after ECL. In the knockout, it appeared to remain at a 20% decline in synaptophysin immunoreactivity compared to the contralateral side at 21 days after ECL. This suggests that a delay may occur in the

reinnervation of the dentate gyrus after ECL in the knockout due the absence of the protease. For SNAP-25 immunoreactivity, the wild-type and knockout showed similar patterns at 7 and 21 days post-lesion (Fig. 25B). A similar relative pattern was observed in PSD-95 levels, yet the knockout animals appeared to have lower levels of immunoreactivity and a trend for a slower increase compared to wild-type at 7 and 21 days post lesion.

DISCUSSION

The purpose this study was to examine lectican processing and associated synaptic markers levels in the CNS of the ADAMTS1 knockout mouse. The ADAMTSs cleave lecticans and this process is thought to facilitate ECM organization and neural plasticity. Currently, there is no literature available that examines the brain tissue of the ADAMTS1 deficient mouse. Here, there were no changes in the abundance of brevican isoforms in any region except for temporal lobe, which is involved with neural plasticity associated with memory and language. We observed that the temporal lobe showed an increase in the generalized brevican fragment in the knockout. This increase appears to be attributed to the ADAMTSs since there is a concurrent increase in the fragment generated by the ADAMTSs and a decrease in the fragment generated by MMPs. Even though this animal does not express ADAMTS1, there may be some compensation or a synergistic effect from other ADAMTS family members, such as ADAMTS4 or ADAMTS5.

Prominent lectican processing was found when tissue was probed for

versican isoforms, where in the ADAMTS1 knockout five out of six regions revealed an increase in full-length versican compared to wild-type. The ADAMTS-derived fragment of versican was diminished and this effect may be directly caused by the deletion of the ADAMTS1 gene and an apparent decline in proteolytic activity. This suggests that ADAMTS1 may have a preference in cleaving versican over brevican. In this study, full-length aggrecan and the ADAMTS-derived fragment of aggrecan were not different from wild-type in brain tissue (our unpublished observations) and it has been shown that the ADAMTS1 knockout mouse does not show abnormalities in aggrecan catabolism of cartilage *in vitro* or *in vivo* (Little et al., 2005). This suggests that ADAMTS1 may be the prominent protease responsible for versican processing.

Versican has been shown to be a cue for pre-synaptic maturation (Yamagata and Sanes, 2005) and if altered may disrupt matrix. Matrix abnormalites are thought to play a hand in altered neural plasticity, therefore, synaptic marker levels were examined in the ADAMTS1 knockout mouse. The hippocampus had higher levels of both pre-synaptic markers, synaptophysin and SNAP-25 in the knockout compared to wild-type. There were significant increases in synaptophysin, SNAP-25 and PSD-95 in the frontal cortex, a region (Burke and Barnes, 2006) associated with aspects of cognitive function and plays an important role in retaining long-term memories which are not task-based (for review, see Faw, 2003). Up regulation of these synaptic markers may derive from an “abnormal” matrix in the ADAMTS1 knockout, therefore relying on an over abundance of specific markers to make “correct and precise” synaptic

connections during events that require neural plasticity.

ADAMTS1 is induced after hypoglossal nerve injury (Sasaki et al., 2001), the inflammatory response associated with experimental autoimmune encephalomyelitis (EAE), an animal model of inflammatory demyelination (Cross et al., 2006b) and transient middle cerebral artery occlusion (Cross et al., 2006a). ADAMTSs are thought to be responsible for matrix turnover after injury and have been shown to be up regulated almost 50% seven days after ECL in the mouse (Mayer et al., 2005). Here the processing of brevican was examined after undergoing ECL and tissue collected at seven and twenty-one days post lesion. At seven days after lesion there is a slight increase in 55 kD fragment and a trend for an increase at twenty-one days post-lesion in the wild-type. However, in the knockout tissue, there was a significant increase in the 145 kD core protein and the generalized fragment, and trend for the increase in abundance of >145 core with CS chains. It appears that the knockout animal may contain some compensatory changes in the expression of other essential proteases, in particular the MMPs since no change in the ADAMTS-derived fragment was observed at seven days. When these optical densities were used to estimate 'apparent ADAMTS activity', due to the decline in EAMESE in the wild-type, there remained nearly a 50% increase in ADAMTS activity compared to contralateral, as seen in basal experiments at the seven day time-point. The apparent ADAMTS activity in the knockout was diminished almost 25%. This may be due to the increase in full-length isoforms with no significant change in ADAMTS-derived fragment compared to the control side. The difference between the wild-

type ADAMTS activity at seven days post lesion and the knockout activity was significant (p=0.0298) and the effect of the genotype was considered significant after ANOVA analysis. Both wild-type and knockout reach levels not different from control after twenty-one days. Given a lower activity, it appears that in the knockout, there is a delay in ADAMTS activity to facilitate synaptic reinnervation. The ADAMTS activity may peak at a later time point or never reach exceed baseline. After ECL, it appears that ADAMTS1 deficiency may affect brevican processing and ultimately the reinnervation that is required to occur after injury. It would be interesting in the future to examine versican processing in the ADAMTS1 knockout mouse after ECL.

Since it may be that the decline in ADAMTS activity might effect the reinnervation of synapses, it was noted that associated changes in synaptophysin. The knockout was diminished by 25% and the knockout showed a decline of 30% at seven days after ECL. The knockout was no different from control (equal to 1) at twenty-one days after ECL while the knockout appeared to have a trend for lower levels of ECL, or potentially a lower reinnervation over time, again lagging behind the wild-type. There were no changes in SNAP-25 levels and PSD-95 revealed a trend for lower levels of PSD-95 in the knockout animal compared to wild-type.

Overall, it appears that in this model, ADAMTS1 may prefer to degrade versican over brevican, even though temporal lobe revealed brevican processing in the ADAMTS1 knockout. The deletion of ADAMTS1 protease may formulate an environment that is not capable of ‘keeping up’ with matrix turnover due to the

increase in versican full-length and the decline in the fragment. With this, a tremendous increase in synaptic marker levels was observed in certain regions, suggesting some alteration of synaptic density at the synapse. This phenotype displays a diminished capacity for apparent ADAMTS activity and associated synaptophysin levels after ECL.

Figure 21. Brevican processing in the ADAMTS1 knockout compared to littermate control: No changes in the abundance of brevican isforms (>145 kD w/ CS-chains; 145 kD core protein without CS-chains and 55 kD generalized proteolytic fragment) as detected by Western blot (A), or the ADAMTS-derived fragment on brevican (C, top panel), and the MMP-derived fragment of brevican (C, bottom panel) was observed in the hippocampus of wild-type (+/+) and knockout (-/-) animals. Denitometric analysis of brevican Western blot in the hippocampus (B).

Chapter 4, Figure 21

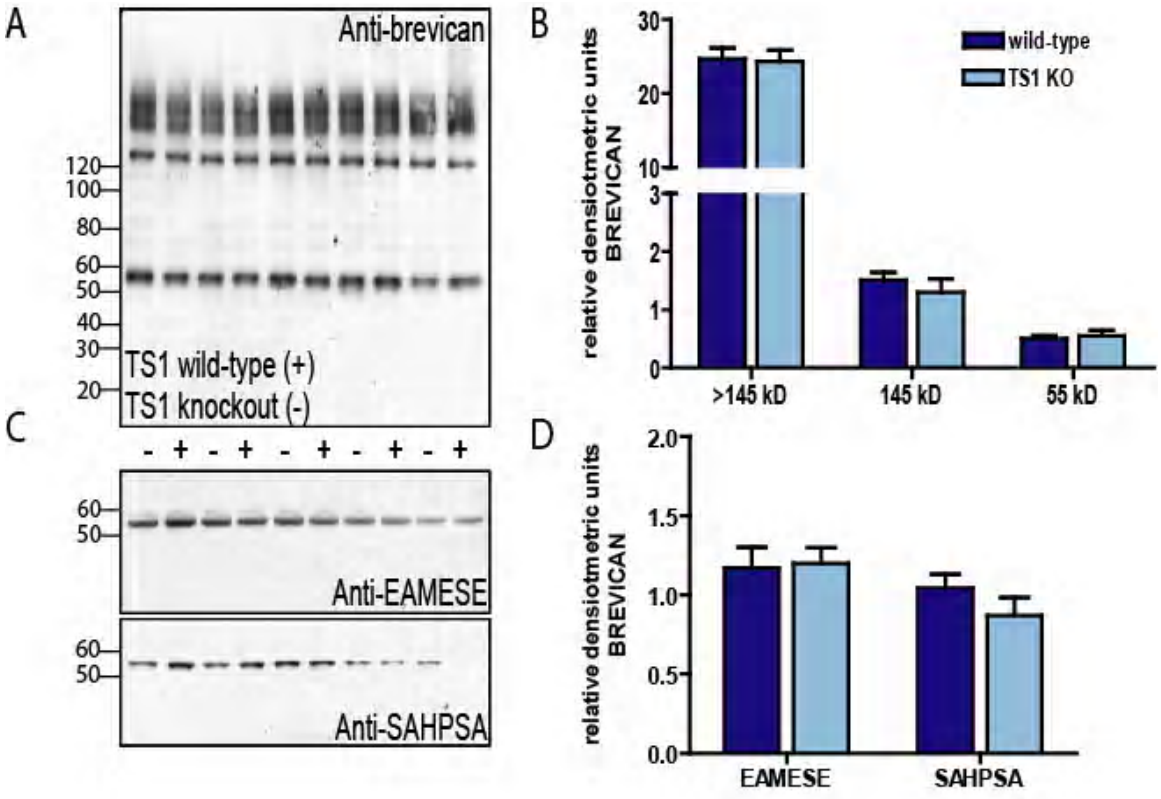

Table 4. Relative immunoreactivity of brevican isoforms in brain regions of ADAMTS1 knockout (-/-) mouse brain compared to wild-type (+/+).

		G1 brevican Isoforms			ADAMTS-derived fragment	MMP-derived fragment
Brain region	tg	>145 kD	145 kD	55kD	EAMESE	SAHPSA
Hippocampus	+/+	27.9 ± 2.87	1.59 ± 0.41	0.51 ± 0.11	1.38 ± 0.25	0.99 ± 0.19
	-/-	27.7 ± 3.45	1.26 ± 0.34	0.46 ± 0.07	1.22 ± 0.14	1.09 ± 0.22
Frontal cortex	+/+	35.5 ± 6.37	2.81 ± 0.53	2.34 ± 0.33	2.77 ± 0.34	1.29 ± 0.08
	-/-	38.3 ± 6.67	2.53 ± 0.70	1.48 ± 0.47	4.07 ± 1.12	1.38 ± 0.11
Temporal lobe	+/+	13.9 ± 2.17	1.37 ± 0.17	0.31 ± 0.08	1.46 ± 0.29	2.34 ± 0.46
	-/-	16.3 ± 2.99	1.92 ± 0.44	0.70 ± 0.06*	3.78 ± 0.29*	0.85 ± 0.34*
Cerebellum	+/+	6.95 ± 1.21	1.55 ± 0.31	1.98 ± 0.15	1.36 ± 0.28	1.48 ± 0.27
	-/-	7.83 ± 1.66	1.87 ± 0.34	2.25 ± 0.19	1.92 ± 0.40	1.79 ± 0.24
Hypothalamus	+/+	0.93 ± 0.18	1.27 ± 0.34	4.06 ± 0.65	2.13 ± 0.51	0.53 ± 0.18
	-/-	1.10 ± 0.44	1.69 ± 0.28	4.24 ± 0.75	1.81 ± 0.24	0.47 ± 0.13
Brain Stem	+/+	6.95 ± 1.21	1.55 ± 0.31	1.98 ± 0.15	1.36 ± 0.28	1.48 ± 0.27
	-/-	7.83 ± 1.66	1.87 ± 0.34	2.25 ± 0.19	1.92 ± 0.40	1.79 ± 0.24

*significantly different from wild-type, p = >0.05, wt (+/+) n=8; knockout (-/-) n=8

Figure 22. Versican processing in the ADAMTS1 knockout compared to littermate control: In the hippocampal brain tissue, full-length versican (anti-12C5, ~245 kD) was increased in the knockout compared to control (A, top panel), while the ADAMTS-derived fragment (anti-NIVNSE, 66 kD) was significantly diminished (A, bottom panel). Denitometric analysis of versican Western blots in the hippocampus (B). Full-length versican was significantly increased (p=0.0016) in the knockout compared to wild-type as the ADAMTS-derived fragment was signifcantly decreased (p=>0.0001).

Chapter 4, Figure 22

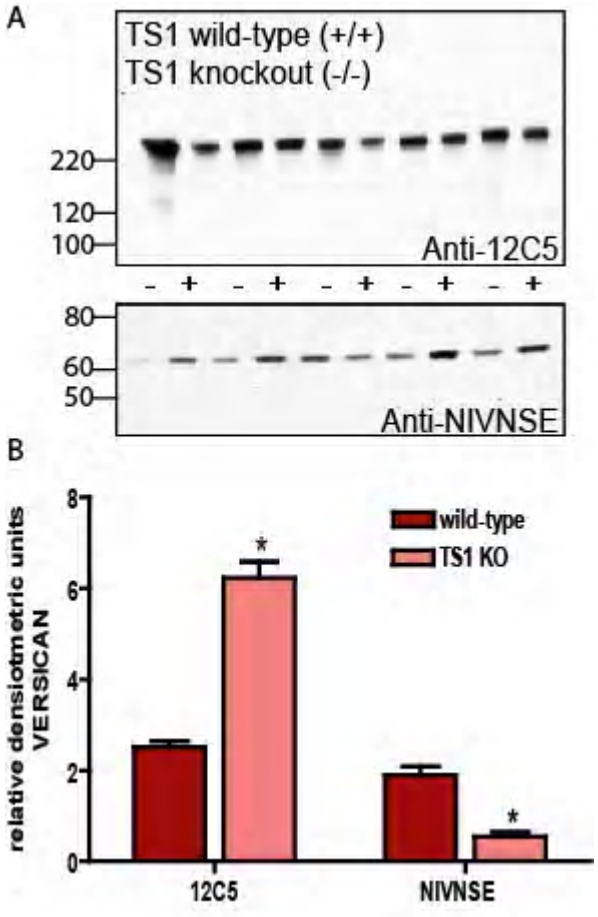

Table 5. Relative immunoreactivity of versican isoforms in brain regions of ADAMTS1 knockout (-/-) mouse brain compared to wild-type (+/+).

		G1 versican	ADAMTS-derived fragment
Brain region	tg	12C5	NIVNSE
Hippocampus	+/+	2.40 ± 0.74	1.82 ± 0.12
	-/-	6.20 ± 1.48*	0.43 ± 0.09*
Frontal cortex	+/+	1.07 ± 0.21	0.86 ± 0.22
	-/-	4.70 ± 1.05*	0.44 ± 0.14*
Temporal lobe	+/+	7.91 ± 0.70	2.99 ± 0.14
	-/-	11.1 ± 1.29*	1.09 ± 0.12*
Cerebellum	+/+	0.84 ± 0.25	2.40 ± 0.14
	-/-	3.49 ± 1.07*	1.03 ± 0.36*
Hypothalamus	+/+	2.12 ± 0.41	3.24 ± 0.50
	-/-	5.24 ± 0.80*	1.69 ± 0.26*
Brain Stem	+/+	3.16 ± 0.40	4.61 ± 0.46
	-/-	3.33 ± 1.13	2.59 ± 0.44*

*significantly different from wild-type, p = >0.05,
wt (+/+) n=8; knockout (-/-) n=8

Table 6. Relative synaptophysin, SNAP-25 and PSD-95 levels as measured by ELISA in several regions of mouse brain in ADAMTS1 knockout mice compared to littermate control.

		hippocampus	frontal cortex	temporal lobe	diencephalon	cerebellum	brain stem
Synaptophysin							
	Wild-type	0.87 ± 0.03	8.43 ± 3.29	5.24 ± 1.18	2.23 ± 0.28	1.56 ± 0.09	0.91 ± 0.12
	ADAMTS1 ko	1.46 ± 0.12*	22.2 ± 4.99*	5.98 ± 1.76	2.43 ± 0.30	1.75 ± 0.25	0.89 ± 0.06
SNAP-25							
	Wild-type	3.82 ± 0.14	16.7 ± 4.30	13.3 ± 3.07	7.21 ± 0.94	7.54 ± 0.24	6.37 ± 0.31
	ADAMTS1 ko	4.99 ± 0.17*	54.3 ± 18.4*	12.3 ± 4.71	7.09 ± 0.67	7.97 ± 0.51	7.00 ± 0.36
PSD-95							
	Wild-type	17.25 ± 0.89	33.6 ± 6.54	37.4 ± 6.97	9.41 ± 2.55	9.39 ± 0.29	9.82 ± 0.42
	ADAMTS1 ko	15.55 ± 0.48	90.8 ± 23.6*	36.9 ± 9.83	11.6 ± 2.40	10.1 ± 0.62	9.82 ± 0.51

*significant compared to control

Figure 23. Brevican immunoreactivity in the dentate gyrus of ADAMTS1 knockout and control animals after entorhinal cortex lesion: Brevican immunoreactivity in the contralateral and ipsilateral dentate gyrus of ADAMTS1 knockout mice and wild-type littermates that had undergone ECL seven and twenty-one days earlier. Optical density was measured on Western blot and data from the ipsilateral side was expressed as a fraction of the contralateral dentate. At seven and twenty-one days, no alterations in brevican isoforms were observed in the wild-type animals (A and B). Seven days post-ECL in the knockout, there was a significant elevation of the 145 kD core protein and generalized proteolytic fragment of brevican and a trend for an increase in the >145 kD isoform (C). At thirty days, brevican isoforms were not different from the control side in the knockout (D).

Chapter 3, Figure 23

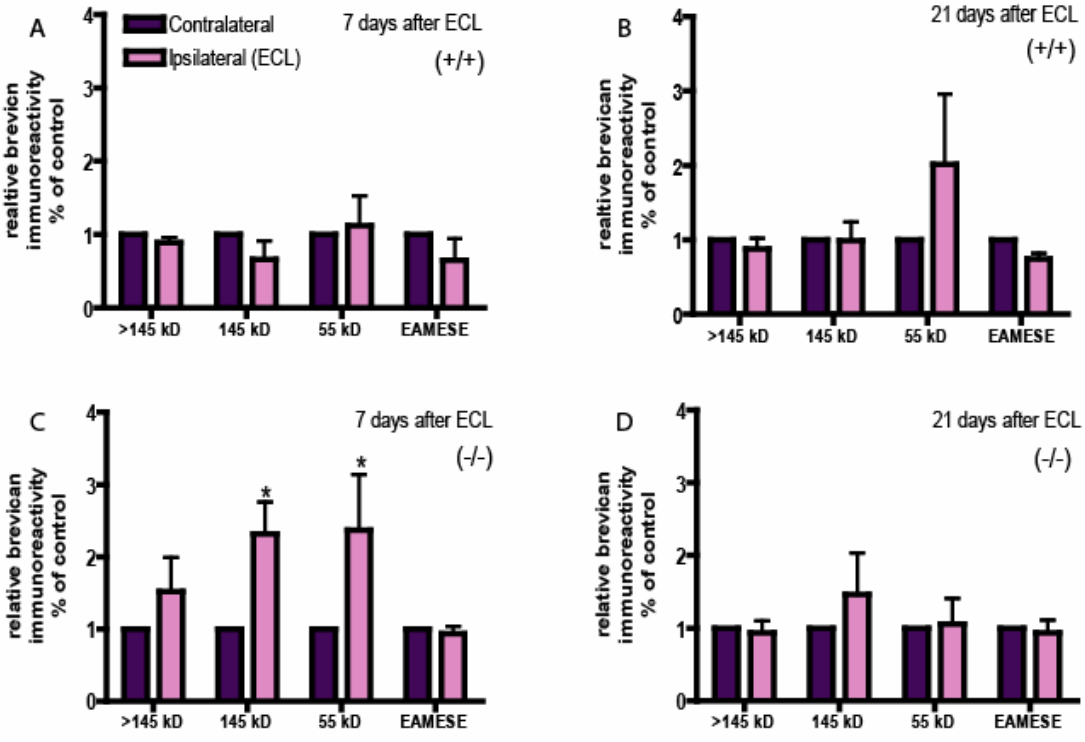

Figure 24. Apparent ADAMTS activity seven and twenty-one days after ECL: Apparent activity in the dentate gyrus of mice after entorhinal cortex lesion as measured by the ratio of the optical density of the ADAMTS-derived EAMESE fragment and the sum of the densities of the brevican core protein isoforms (>145 kD + 145 kD). Mean level of apparent activity was calculated at seven and twenty-one days after lesion. At seven days after lesion in the wild-type tissue, ADAMTS activity was increased about 40%, whereas at seven days in the knockout tissue, ADAMTS activity was lower compared to the contralateral side and declined about 25%. Apparent ADAMTS activity on the lesioned side was not different from the non-lesioned dentate in tissue collected twenty-one days after lesion in both groups.

Chapter 4, Figure 24

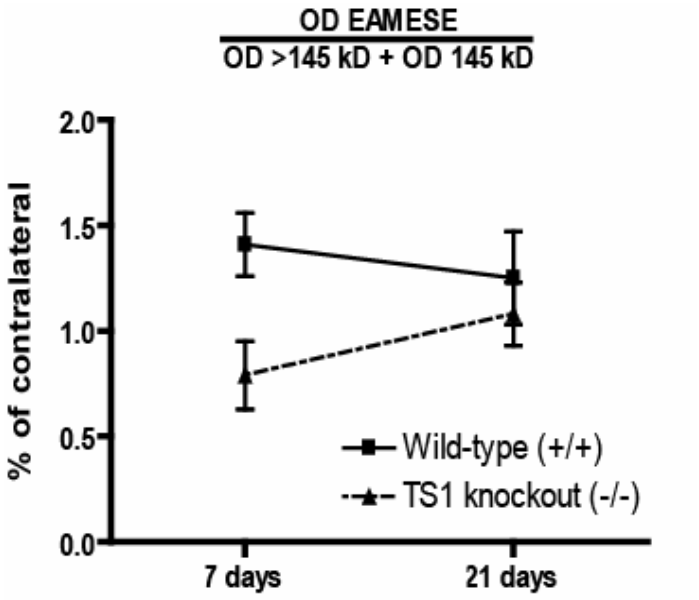

Figure 25. Synaptic marker levels as measured by ELISA seven and twenty-one days after ECL: Synaptophysin, SNAP-25 and PSD-95 levels in extracts from fresh micro-dissected dentate gyrus tissue of knockout and control mouse brain, seven and twenty-one days post ECL, as measured by ELISA. Synaptophysin immunoreactivity was reduced by 25% in the wild-type at seven days post-lesion, while a 30% reduction in immunoreactivity was observed in the knockout (A). The ipsilateral side was not different from contralateral dentate twenty-one days after lesion in the wild-type; however, synaptophysin immunoreactivity in the knockout was still below contralateral side. SNAP-25 immunoreactivity was not different in the knockout compared to littermate controls (B). PSD-95 levels appeared lower at seven and twenty-one days post-lesion in the knockout compared to the wild-type (C).

Chapter 4, Figure 25

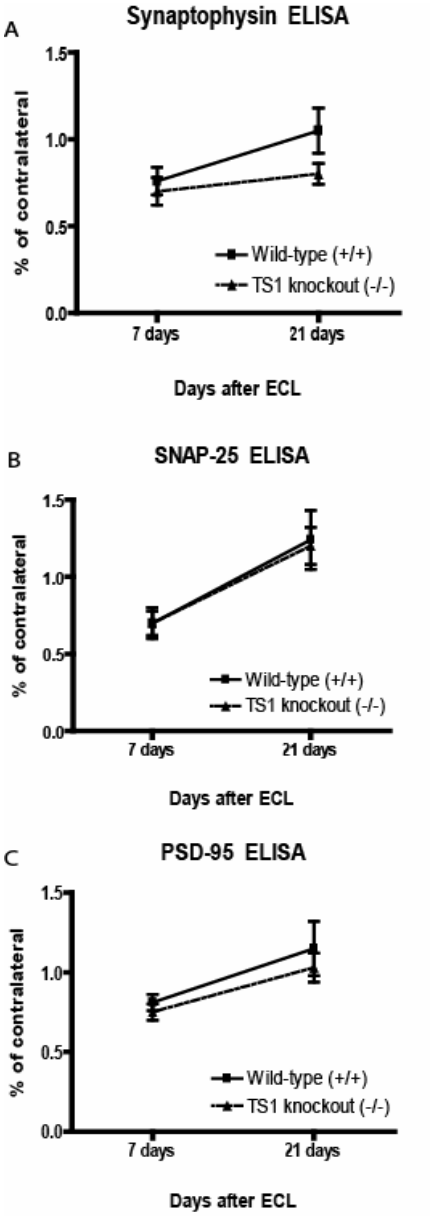

REFERENCES

Bandtlow CE, Zimmermann DR (2000) Proteoglycans in the developing brain: new conceptual insights for old proteins. Physiol Rev 80:1267-1290.

Burke SN, Barnes CA (2006) Neural plasticity in the ageing brain. Nat Rev Neurosci 7:30-40.

Cross AK, Haddock G, Surr J, Plumb J, Bunning RA, Buttle DJ, Woodroofe MN (2006a) Differential expression of ADAMTS-1, -4, -5 and TIMP-3 in rat spinal cord at different stages of acute experimental autoimmune encephalomyelitis. J Autoimmun 26:16-23.

Cross AK, Haddock G, Stock CJ, Allan S, Surr J, Bunning RA, Buttle DJ, Woodroofe MN (2006b) ADAMTS-1 and -4 are up-regulated following transient middle cerebral artery occlusion in the rat and their expression is modulated by TNF in cultured astrocytes. Brain Res 1088:19-30.

Cross NA, Chandrasekharan S, Jokonya N, Fowles A, Hamdy FC, Buttle DJ, Eaton CL (2005) The expression and regulation of ADAMTS-1, -4, -5, -9, and -15, and TIMP-3 by TGFbeta1 in prostate cells: relevance to the accumulation of versican. Prostate 63:269-275.

Faw B (2003) Pre-frontal executive committee for perception, working memory, attention, long-term memory, motor control, and thinking: a tutorial review. Conscious Cogn 12:83-139.

Gottschall PE, Sandy JD, Zimmermann DR (2005a) Chapter 4: Substrates for metalloproteinases in the central nervous system. In: Matrix metalloproteinases in the central nervous system. (Conant K, Gottschall PE, eds), pp 87-118. London: Imperial College Press.

Gottschall PE, Sandy JD, Zimmermann DR (2005b) Matrix metalloproteinases in the Central Nervous System. Singapore: World Scientific Publishing Co.

Haddock G, Cross AK, Plumb J, Surr J, Buttle DJ, Bunning RA, Woodroofe MN (2006) Expression of ADAMTS-1, -4, -5 and TIMP-3 in normal and multiple sclerosis CNS white matter. Mult Scler 12:386-396.

Hamel MG, Mayer J, Gottschall PE (2005) Altered production and proteolytic processing of brevican by transforming growth factor beta in cultured astrocytes. Journal of Neurochemistry 93:1533-1541.

Hockfield S, Kalb RG, Zaremba S, Fryer H (1990) Expression of neural proteoglycans correlates with the acquisition of mature neuronal properties in the mammalian brain. Cold Spring Harb Symp Quant Biol 55:505-514.

Kuno K, Bannai K, Hakozaki M, Matsushima K, Hirose K (2004) The carboxyl-terminal half region of ADAMTS-1 suppresses both tumorigenicity and experimental tumor metastatic potential. Biochem Biophys Res Commun 319:1327-1333.

Kuno K, Kanada N, Nakashima E, Fujiki F, Ichimura F, Matsushima K (1997) Molecular cloning of a gene encoding a new type of metalloproteinase-disintegrin family protein with thrombospondin motifs as an inflammation associated gene. J Biol Chem 272:556-562.

Kuno K, Okada Y, Kawashima H, Nakamura H, Miyasaka M, Ohno H, Matsushima K (2000) ADAMTS-1 cleaves a cartilage proteoglycan, aggrecan. FEBS Lett 478:241-245.

Little CB, Mittaz L, Belluoccio D, Rogerson FM, Campbell IK, Meeker CT, Bateman JF, Pritchard MA, Fosang AJ (2005) ADAMTS-1-knockout mice do not exhibit abnormalities in aggrecan turnover in vitro or in vivo. Arthritis Rheum 52:1461-1472.

Masui T, Hosotani R, Tsuji S, Miyamoto Y, Yasuda S, Ida J, Nakajima S, Kawaguchi M, Kobayashi H, Koizumi M, Toyoda E, Tulachan S, Arii S, Doi R, Imamura M (2001) Expression of METH-1 and METH-2 in pancreatic cancer. Clin Cancer Res 7:3437-3443.

Mayer J, Hamel MG, Gottschall PE (2005) Evidence for proteolytic cleavage of brevican by the ADAMTSs in the dentate gyrus after excitotoxic lesion of the mouse entorhinal cortex. BMC Neurosci 6:52.

Miguel RF, Pollak A, Lubec G (2005) Metalloproteinase ADAMTS-1 but not ADAMTS-5 is manifold overexpressed in neurodegenerative disorders as Down syndrome, Alzheimer's and Pick's disease. Brain Res Mol Brain Res 133:1-5.

Ng YH, Zhu H, Pallen CJ, Leung PC, MacCalman CD (2006) Differential effects of interleukin-1beta and transforming growth factor-beta1 on the expression of the inflammation-associated protein, ADAMTS-1, in human decidual stromal cells in vitro. Hum Reprod 21:1990-1999.

Sandy JD, Westling J, Kenagy RD, Iruela-Arispe ML, Verscharen C, Rodriguez-Mazaneque JC, Zimmermann DR, Lemire JM, Fischer JW, Wight TN, Clowes AW (2001) Versican V1 proteolysis in human aorta in vivo occurs at the Glu441-Ala442 bond, a site that is cleaved by recombinant ADAMTS-1 and ADAMTS-4. J Biol Chem 276:13372-13378.

Sasaki M, Seo-Kiryu S, Kato R, Kita S, Kiyama H (2001) A disintegrin and metalloprotease with thrombospondin type1 motifs (ADAMTS-1) and IL-1 receptor type 1 mRNAs are simultaneously induced in nerve injured motor neurons. Brain Res Mol Brain Res 89:158-163.

Shindo T, Kurihara H, Kuno K, Yokoyama H, Wada T, Kurihara Y, Imai T, Wang Y, Ogata M, Nishimatsu H, Moriyama N, Oh-hashi Y, Morita H, Ishikawa T, Nagai R, Yazaki Y, Matsushima K (2000) ADAMTS-1: a metalloproteinase-disintegrin essential for normal growth, fertility, and organ morphology and function. J Clin Invest 105:1345-1352.

White F, Nicoll JA, Horsburgh K (2001) Alterations in ApoE and ApoJ in relation to degeneration and regeneration in a mouse model of entorhinal cortex lesion. Exp Neurol 169:307-318.

Yamagata M, Sanes JR (2005) Versican in the developing brain: lamina-specific expression in interneuronal subsets and role in presynaptic maturation. J Neurosci 25:8457-8467.

Yamaguchi Y (2000) Lecticans: organizers of the brain extracellular matrix. Cell Mol Life Sci 57:276-289.

Yuan W, Matthews RT, Sandy JD, Gottschall PE (2002) Association between protease-specific proteolytic cleavage of brevican and synaptic loss in the dentate gyrus of kainate-treated rats. Neuroscience 114:1091-1101.

CONCLUSIONS

In some regions of the brain neural plasticity can occur, an event that has the ability to change the organization of stable neuronal circuitry. Neural plasticity can be defined in and is most studied during neuronal development and maturation, neurite outgrowth, synaptogenesis, recovery after injury and events related to memory and learning. In order for neural plasticity to occur, neurons must traverse through the extracellular milieu. The extracellular space makes up approximately 20% of the total volume of the brain and is composed of aggregating molecular complexes that provide a stable environment for neurite processes and synapses that help to maintain the integrity of the circuitry in the adult brain. ECM molecules have been shown to limit neurite remodeling and regeneration in the CNS (Snow et al., 1990; Oakley and Tosney, 1991; Brittis et al., 1992). This is partly due to the nature of the ECM molecules. Many are highly negatively charged molecules, such as chondroitin sulfate-containing PGs, that bear glycosaminoglycan side chains. The catabolism of these molecules, and the resulting breakdown or "loosening" of the matrix can allow neural plasticity to occur (Fig. 26). Endogenous proteases are expressed in the ECM, exist throughout the brain, and are known to cleave CS-containing PGs (Kuno et al., 2000; Yamaguchi, 2000a; Sandy et al., 2001). This is one way in which neural plasticity may be regulated in normal brain, and this regulation appears to

be altered in certain neurodegenerative disorders (Rosenberg, 2002; Levicar et al., 2003; Cross et al., 2005; Cross et al., 2006; Haddock et al., 2006). These studies examine the proteolytic degradation of ECM complexes and how this modification influences neural plasticity. First, the localization of a protease-specific, detectable proteolytic fragment of the ECM molecule brevican was localized throughout the rodent brain and increases in immunoreactivity in areas known to undergo neural plasticity was observed. A second study revealed changes in the abundance of brevican isoforms and increased proteolytic activity after injury, during the synaptic reinnervation period, in a classical injury model of neural plasticity. In the third study, the proteolytic fragment of brevican was diminished in an animal model of Alzheimer's disease, which is thought to have decreased capability to undergo neural plasticity. If there is a decline in the mechanism of proteolysis of the ECM in general, which may correlate with an environment that is less permissive to neural plasticity and therefore diminished learning and memory function. Alterations in brevican isoforms, a decline in proteolytic activity and an associated increase in synaptic marker levels was observed in this animal model of AD. In the final study, characterization of brevican and proteolytic activity was examined in an animal model with a gene-deletion of the protease. It appeared that only one region showed altered brevican processing in this model, but the lectican family member versican showed marked alterations in proteolytic degradation, more specifically, a significant decline in the amount of proteolytic fragment generated. This model also revealed associated changes in synaptic marker levels in the protease-

deficient animal, suggesting that some regulation of neural plasticity may be altered, ultimately at the synapse. Overall, these results provide evidence that endogenous proteases and the degradation of ECM can influence neural plasticity.

An integral part of these experiments was the development of the antibodies raised against cleavage sites of the lecticans that are specific to different families of proteases. Antibodies raised against these neoepitopes formed after cleavage by the ADAMTSs have been developed for aggrecan and versican and previously examined in spinal cord, cartilage, aorta and ovary matrix (Lemons et al., 2001; Sandy et al., 2001; Russell et al., 2003). In our laboratory, the proteolytic fragment of brevican generated by the ADAMTSs is denoted by antibodies raised against the neoepitope 'EAMESE' for mouse, (Mayer et al., 2005), 'EAVESE' for the rat; (Aya-ay et al., 2005), and for versican, 'NIVNSE' (Yuan et al., 2002). The MMP-specific site for mouse brevican cleaved by MMPs was detected with the neoepitope recently raised against, 'SAHPSA', and the antibody for the MMP-specific site for versican is currently being developed. These antibodies were important in the initial localization experiments (chapter 1, figure 2, 3, 5, 7 & 8 and tables 1 & 2), detecting levels of fragment in APP and ADAMTS1 knockout mice (chapter 3, figure 18 & 19; chapter 4, figure 21 & 22) and the ability to estimate an apparent 'ADAMTS activity' (chapter 2, figure 15 & 16; chapter 4, figure 23 & 24) with the ratio of fragment to the addition of the full-length isoforms. The fate of the fragment after

cleavage is yet to be discovered, it may be turned over, sequestered or may even proceed to promote a biochemical cascade or signaling event.

Interestingly there is a significant proportion of brevican fragment immunoreactivity formed by proteolytic cleavage of lectican core protein. At the beginning of these experiments is was important to localize this fragment as well as full-length brevican throughout the rodent brain. Although it appeared that there is more fragment expressed throughout the brain compared to brevican, the antibodies may have different affinities due to the steric hindrance in the complex matrix aggregates for full-length brevican and 'free' fragment in fixed tissue sections compared to SDS-PAGE homogenate. However, the relative abundance and localization of WFA, brevican and the fragment was examined and documented (chapter 1, table 1 (rat), table 2 (mouse)).

Wisteria floribunda agglutinin (WFA) was used as a marker for CS-containing regions, assuming that areas of the brevican fragment would co-localize with the CS-containing core protein and regions with more WFA would mark areas of high CS deposition and suggest a more stable, rigid matrix potentially resistant to neural plasticity. Areas with more fragment, would signify regions more permissive to neural plasticity. WFA has been widely used and accepted as a marker for CSPG deposition (Brauer et al., 1993; Bruckner et al., 1996; Bruckner et al., 1998) and we expected that the distribution of the signal from both reagents would be similar, since fragments of brevican are stable after cleavage (Yamaguchi, 2000a, b), and much of the C-terminal fragments bear CS chains. The purpose of this study was to describe the distribution and

characteristic immunoreactivity for the ADAMTS-cleaved fragment of brevican, and compare this with WFA binding in the rodent CNS. Even though WFA is supposed to label CSPGs, the results show a marked discordance between the two, with the extent of distribution of the ADAMTS-derived brevican fragment much greater than that of WFA reactivity. This is the first report comparing brevican and WFA, and observed little WFA and most of brevican in the soluble fraction, in which no bands of WFA correspond to those immunoreactive for brevican (chapter 1, figure 3).

These markers showed a distinct discordance in certain areas, more specifically, areas that are thought to presently undergo neural plasticity such as the hippocampus, reticular thalamic nuclei and the cerebellum (chapter 1, figure 7). This discordance led us to question if WFA detects brevican or CS at all. There is debate in the literature about which molecules in the CNS are labeled by WFA, which is often used as a marker for PNNs that contain CS chains, and some believe that WFA binds directly to CS. We determined that brevican, and its CS chains, was not a binding partner for this lectin (chapter 1, figure 4). One explanation for the discordance in reactivity between brevican and WFA is from Murakami et al., whom have significant evidence that supports the concept that WFA-binding proteins are cell surface glycoproteins. They demonstrated that terminal N-acetylgalactosamine residues, which are present on neuronal cell surface glycoproteins, and may be responsible for the PNN reactivity seen with WFA lectin binding (Murakami et al., 1999; Murakami et al., 2001) and suggest that brevican, and other lecticans are bound to these glycoproteins. If WFA

immunoreactivity is extinguished after chondroitinase treatment, it suggests that it is indeed binding to CSPGs; however, it is also possible that WFA recognizes the surface glycoprotein and when chondroitinased the CSPG is removed along with the glycoprotein. Which may explain why WFA PNN staining is absent after treating with chondroitinase. WFA may no be able to recognize brevican's CS-chains due to the conformation or WFA is incapable of binding to only a few chains, as brevican can hold only 1-3 chains.

One disease associated with the inability to breakdown CS-chains within the cell is called mucopolysaccharidosis (the former name for glycosaminoglycans, GAGs) in which people do not produce enough of one of the enzymes required to break down the sugar chains attached to proteoglycans into proteins and simpler molecules, or the enzymes they produce simply do not work properly. There is no treatment for mucopolysaccharidosis and eventually, the cells, blood, and tissues collect an over abundance of glycosaminoglycans, which results in permanent, chronic cellular damage that effects the person's appearance, physical capabilities, organ function, overall system function and mental development. The large CS-containing molecules must be sequestered back into the cell and into lysosomes in order for the CS-chains to be removed. It is possible that the proteolysis of CS-containing proteoglycans by endogenous proteases, such as MMPs and ADAMTSs outside the cell may regulate and assist these molecules get back into the cell. If this process is disrupted, it may ultimately effect the processing and removal of the chains needed to maintain a normal balance of chain removal in the lysosomes.

Previous studies have showed that matrix-altering proteases, such as MMPs, may play a role in neural plasticity after a lesion in the CNS (Zhang et al., 2000; Szklarczyk et al., 2002; Jourquin et al., 2003) and more recently the activity and expression of the ADAMTS became elevated in the outer molecular layer (OML) after kainite-induced lesions (Yuan et al., 2002). A classical model of neural plasticity, the entorhinal cortex lesion, was employed to examine brevican and its fragments at several time points after lesion. In order to localize the injury, and yield better sampling of the injury compared to the entire hippocampus, the development of the 'regional isolation technique' provided a more concentrated sample of the injury in the OML (chapter 2, figure 10) compared to collecting the entire region. In this model, the injury was localized in a region away from the lesion site itself. Full-length brevican isoforms were increased two and seven days post-lesion, whereas the generalized 55 kD fragment and the ADAMTS-derived fragments were increased at the seven day, initial synaptic reinnervation period (chapter 2, figure 15). It is possible that the initial response of the brain is to create a "glial scar" after ECL injury. A glial scar is formed which usually contains CSPGs, the major axon growth inhibitory component of the glial scar tissue that blocks successful regeneration (for reviews see: (Morgenstern et al., 2002; Properzi et al., 2003; Carulli et al., 2005). This may explain the significant increase seen in the glycosylation form (>145 kD) of brevican two days post lesion (chapter 2, figure 15) and may be related to a trend for an increase in the core protein.

To estimate apparent ADAMTS activity, the optical density of the fragment

was divided by the optical density of the addition of full-length brevican isoforms. With this calculation, ADAMTS activity was increased 50% at the seven-day time point after lesion (chapter 2, figure 16). This occurs before a complete reinnervation of synaptophysin levels in the OML, going from a 50% decline to basal levels at the thirty-day time point. These results suggest that lecticans and the proteases that cleave them can play a potential role in neural plasticity after ECL, to prepare a path within the ECM for neurite outgrowth and eventually synaptogenesis. Thus, growth, sprouting and targeting in neural plasticity of an ECL model may involve extracellular cues whose expression and/or secretion is altered following the lesion. One of these cues is the extracellular PG, brevican. It would be of interest to perform this experimental model in the brevican knockout mouse (Brakebusch et al., 2002) and observe ADAMTS activity and the processing of other lecticans. Brevican-deficient mice showed significant deficits in the maintenance of hippocampal long-term potentiation (LTP) although detailed behavioral analysis revealed no statistically significant deficits in learning and memory. The knockout animal showed a compensatory increase in the brain specific lectican family member neurocan; this and other models with deficient lecticans or proteases may help in revealing the individual contribution of each of these molecules to neural plasticity. Here we have demonstrated changes in brevican expression and turnover after ECL injury that is associated with the loss and time-dependent reinnervation of the outer molecular layer of the dentate gyrus, an event related to neural plasticity.

Since we observed increased brevican fragment in areas of known neural plasticity, and after injury during the critical synaptic reinnervation period, we wanted to investigate the processing of brevican in a disease model that is thought to have dysregulated neural plasticity. Alzheimer's disease (AD), the most common type of dementia, is a neurodegenerative disease characterized by progressive cognitive decline. In human brain, the pathologies include neuronal loss and vesicle enlargement in response to an inflammatory response to the deposition of amyloid plaques and neurofibrillary tangles. The absolute cause of AD is still unknown, yet many factors and hypotheses have been studied. One of the most popular is the amyloid cascade hypothesis that suggests that the progressive neuritic and synaptic injuries are caused by the deposition or altered processing and accumulation of Aβ peptide (Hardy, 2002). Memory and learning, and ultimately neural plasticity, is impaired in this disease.

Previous data suggests that the proteolytic cleavage of brevican is significantly decreased in Alzheimer's brain compared to age-match normal and Parkinson's diseased brains and Aβ may have the ability to bind and inhibit the activity of the ADAMTSs (Gottschall et al., 2003); our unpublished observations). In an animal model of AD that over expresses the human APP (Hsiao et al., 1996), and contains learning and memory deficits associated with plaque pathologies (Terai et al., 2001), brevican processing was indeed altered in the transgenic mice (chapter 3, figure. 19). Here, we observed an increase in core protein and a decline in the generalized fragment, suggesting a decline in the proteolytic degradation of brevican overall which may maintain a matrix less

permissive to neural plasticity. However, when probed with the specific neoepitopes for the ADAMTS-derived fragment (EAMESE) and the MMP-derived fragment (SAHPSA), it appeared that the MMP-derived fragment was diminished in the APPsw mice and thus indicating a decline in MMP activity in this model. MMPs have been shown to mediate extracellular Aβ peptide catabolism (Deb et al., 2003; Yin et al., 2006) and may be increased in attempt to regulate the invasion of Aβ plaques and the lectican-rich glial activation (to break down brevican, etc). It is possible, in this animal model, that MMPs are activated to assist with the deposition of Aβ whether it is on behalf of the inflammatory response and the formation of a glial scar or to attempt to break it down. We propose that further experiments are required to determine the contribution of each metalloproteinase family to the diminished proteolytic degradation of proteoglycans.

Given these lecticans and the proteases that degrade them may attribute to neural plasticity, we sought to examine synaptic markers and discovered associated changes in the APPsw mouse model. This animal only bears Aβ plaques within the ECM and surprisingly, exhibits no neuronal loss like the human disease development. In four out of six regions, the pre-synaptic marker SNAP-25 was significantly increased in the APPsw mice (chapter 3, figure 20). SNAP-25 undergoes changes in expression during early fetal development and in aging (Shimohama et al., 1997). SNAP-25 is expressed as two isoforms, both of which can be induced by stimuli producing long-term potentiation (LTP) in the hippocampus (Roberts et al., 1998; Genoud et al., 1999) and are integral to the

process of Ca-sensitive, stimulus-evoked transmitter vesicle exocytosis (Mehta et al., 1996; Wilson et al., 1996; Ferrer et al., 1998; Washbourne et al., 2002). APP is known to be transported down neuronal processes to synapses by fast axonal transport (Koo et al., 1990) and lesioning the perforant path reduced plaques deposited in APPsw mice (Lazarov et al., 2002; Sheng et al., 2003). Therefore, this implies that synaptic input is essential for the development of plaques. Axonal transport of APP may be deficient in APPsw mice and there is axonal swelling due to the over accumulation or altered processing of Aβ, therefore we get an increase in the recruitment of SNAP-25 since vesicle formation is required to insert Aβ into the membrane. Changes in pre-synaptic levels of SNAP-25 may indicate changes in the regulation of synaptic vesicle exocytosis and transmitter release and if this membrane-bound synaptic protein is altered, it may disrupt these processes.

Cerebellar plaques are predominantly of the diffuse type, whereas fibrillar senile plaques are rarely observed (van Horssen et al., 2002) and since APP level are over expressed in each of the four regions showing altered SNAP-25 levels, the presence of high levels of APP, rather than deposition of Aβ may be important in the over expression of this synaptic marker. There is a significant literature describing the expression of synaptic markers in AD (Lassmann et al., 1993; Counts et al., 2006; Ishibashi et al., 2006) and in APP over-expressing transgenic mice (APPsw) (Irizarry et al., 1997; King and Arendash, 2002) almost all with histochemical techniques and present conflicting data. In AD, there is no apparent increase in APP protein expression, but altered processing is

responsible for increase levels of Aβ and its deposition and this event may be due to over expression of APP in the transgenic mouse, with little relationship to AD. These results suggest that in this animal model, A□ may exert inhibitory effects on the activity of the proteases responsible for matrix alteration and processing of brevican and other lecticans, an effect potentially related to diminished neural plasticity in AD.

To further investigate lectican processing and neural plasticity, a mouse deficient in the proteoglycanase ADAMTS1 was examined for brevican and versican processing along with associated levels of synaptic markers.
As of yet, no literature is available that examines the brain tissue of the ADAMTS1 deficient mouse. It was of interest to see that no regions were altered for the abundance of brevican isoforms (chapter 4, figure 21 and table 4), except for the temporal lobe, which is involved in neural plasticity associated with memory and language (for reviews see; Rolls, 1995; Squire and Zola, 1996). The increase in generalized fragment appears to be attributed by the ADAMTSs since there is a concurrent increase in the fragment generated by the ADAMTS and therefore 'ADAMTS activity' upon this region. This suggests that even though this animal does not express ADAMTS1, there may be some compensation or a synergistic effect from other ADAMTS family members, such as ADAMTS4 or ADAMTS5. Brevican isoforms were increased after ECL at seven days in the knockout, in response to the injury, along with an increase in 'apparent ADAMTS activity'. The full-length isoform of brevican, compared to the fragments, was high in the knockout, after ECL injury suggesting a decline in

proteolysis.

It was interesting to see prominent lectican processing found when tissue was probed for versican isoforms, where in the ADAMTS1 knockout five out of six regions revealed an increase in full-length versican (12C5) and a decline in six regions of the ADAMTS-derived fragment (NINVSE) compared to wild-type (chapter 4, figure 22. and table 5). The ADAMTS-derived fragment of versican was diminished and this effect may be directly caused by the deletion of the ADAMTS1 gene and an apparent decline in proteolytic activity exerted upon versican. This suggests that ADAMTS1 may have a preference in cleaving versican over brevican in certain regions of the brain. ADAMTS1 may be the prominent protease responsible for versican processing and provide preliminary evidence that these molecules form 'protease-substrate' pairs. Versican was not examined in the ECL experiments, but future investigation may provide insight into versican processing or expression of versican after inury and during reinnervation of the OML.

In correlation to the lectican processing alterations, concurrent changes in synaptic markers were apparent in the ADAMTS1 deficient mouse. The frontal cortex showed increases in all three markers and in hippocampus both of the pre-synaptic markers were elevated (chapter 4, table 6). Up regulation or increased expression of these synaptic markers may derive from an "abnormal" matrix in the ADAMTS1 knockout, therefore relying on an over abundance of specific markers to make whatever synaptic connection can be made during events that require neural plasticity. After ECL, it appeared that in the knockout

there was delay in ‘apparent ADAMTS activity’ (chapter 4, figure 24) to facilitate synaptic reinnervation and showed similar trends for synaptophysin levels during the reinnervation period (chapter 4, figure 25). These results suggest that altered protease may affect matrix turnover and ultimately synaptic reinnervation and synaptogenesis.

The data presented here in these experiments a) defines the proteolytic fragment of brevican is abundant in regions capable of undergoing neural plasticity; b) increased ADAMTS activity in a classical model of neural plasticity, c) in a model thought to have dysregulated plasticity, such as Alzheimer’s disease, brevican processing is altered and d) by altering one of the proteases responsible for the catabolism of brevican, pronounced changes in the levels of synaptic markers are observed in regions involved in neural plasticity (table 7). We propose that the catabolism of brevican and lecticans in general, by endogenous proteases such as the ADAMTSs and the MMPs in the matrix, promotes neurite outgrowth and synaptogenesis to occur more readily in the brain in response to injury and during recovery.

Figure 26. Summary schematic of the tertiary complex in the brain between a pre-synaptic neuron and a post-synaptic neuron (or a glial cell) as it relates to the inhibition (-) of neural plasticity and the ability (+) to undergo neural plasticity. Proteolytic cleavage of the brevican core protein by endogenous proteases, such as MMPs and ADAMTSs, may "loosen" the aggregated complexes and change the extracellular environment to one that is more permissive for neural plasticity to occur.

Conclusions, Figure 26

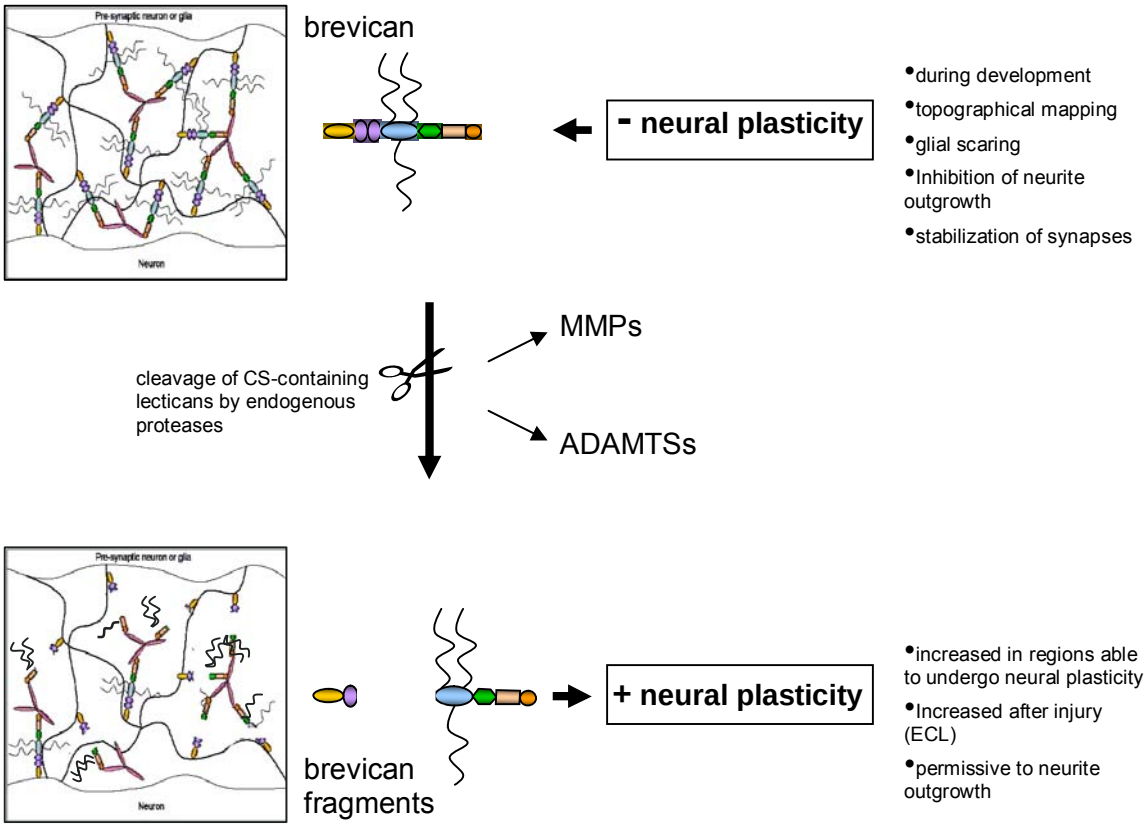

Table 7. Summary of evidence found for models investigated, supporting proteolytic degradation of lecticans in ECM influence neural plasticity.

	Paper 1	Paper 2	Paper 3	Paper 4
Purpose of experiment	Characterization of brevican isoforms in brain extracellular Matrix	Alterations of brevican expression after the entorhinal cortex lesion model of neural plasticity	Alterations of brevican expression in a disease model with dysregulated plasticity	Alterations in neural plasticity as a result of protease gene deletion
Alterations in lectican isoforms		Increased full-length and ADAMTS-derived fragment of brevican	Changes in CS-bearing >145 kD, decline in generalized fragment and MMP-derived fragments of brevican	Brevican changed in temporal lobe alone, but all regions of versican showed increased full-length and decline in ADAMTS-derived fragment
Associated changes in synaptic markers		Complete reinnervation of the OML 30 days after lesion	Increase in SNAP-25 in HC, FC, TL and CB as measured by ELISA	Increase in synaptophysin, SNAP-25 and PSD-95 in FC, synaptophysin and SNAP-25 in HC. After ECL, slower reinnervation of synaptic markers
Results / conclusions	The proteolytic fragment of brevican is abundant in regions capable of undergoing neural plasticity	Increased apparent ADAMTS activity in a classical model of neural plasticity	A decline in brevican fragment may assist in cognitive decline due to diminished matrix turnover and neural plasticity	The protease deletion affected processing of lecticans and increased expression of synaptic markers

REFERENCES CITED

Aya-ay J, Mayer J, Eakin AK, Muffly BG, Anello M, Sandy JD, Gottschall PE (2005) The effect of hypoxic-ischemic brain injury in perinatal rats on the abundance and proteolysis of brevican and NG2. Exp Neurol 193:149-162.

Brakebusch C, Seidenbecher CI, Asztely F, Rauch U, Matthies H, Meyer H, Krug M, Bockers TM, Zhou X, Kreutz MR, Montag D, Gundelfinger ED, Fassler R (2002) Brevican-deficient mice display impaired hippocampal CA1 long-term potentiation but show no obvious deficits in learning and memory. Mol Cell Biol 22:7417-7427.

Buer K, Hartig W, Bigl V, Bruckner G (1993) Distribution of parvalbumin-containing neurons and lectin-binding perineuronal nets in the rat basal forebrain. Brain Res 631:167-170.

Brittis PA, Canning DR, Silver J (1992) Chondroitin sulfate as a regulator of neuronal patterning in the retina. Science 255:733-736.

Bruckner G, Hartig W, Kacza J, Seeger J, Welt K, Brauer K (1996) Extracellular matrix organization in various regions of rat brain gray matter. J Neurocytol 25:333-346.

Bruckner G, Bringmann A, Hartig W, Koppe G, Delpech B, Brauer K (1998) Acute and long-lasting changes in extracellular-matrix chondroitin-sulphate proteoglycans induced by injection of chondroitinase ABC in the adult rat brain. Exp Brain Res 121:300-310.

Carulli D, Laabs T, Geller HM, Fawcett JW (2005) Chondroitin sulfate proteoglycans in neural development and regeneration. Curr Opin Neurobiol 15:116-120.

Counts SE, Nadeem M, Lad SP, Wuu J, Mufson EJ (2006) Differential expression of synaptic proteins in the frontal and temporal cortex of elderly subjects with mild cognitive impairment. J Neuropathol Exp Neurol 65:592-601.

Cross AK, Haddock G, Surr J, Plumb J, Bunning RA, Buttle DJ, Woodroofe MN (2006) Differential expression of ADAMTS-1, -4, -5 and TIMP-3 in rat spinal cord at different stages of acute experimental autoimmune encephalomyelitis. J Autoimmun 26:16-23.

Cross NA, Chandrasekharan S, Jokonya N, Fowles A, Hamdy FC, Buttle DJ, Eaton CL (2005) The expression and regulation of ADAMTS-1, -4, -5, -9, and -15, and TIMP-3 by TGFbeta1 in prostate cells: relevance to the accumulation of versican. Prostate 63:269-275.

Deb S, Wenjun Zhang J, Gottschall PE (2003) Beta-amyloid induces the production of active, matrix-degrading proteases in cultured rat astrocytes. Brain Res 970:205-213.

Ferrer I, Marti E, Tortosa A, Blasi J (1998) Dystrophic neurites of senile plaques are defective in proteins involved in exocytosis and neurotransmission. J Neuropathol Exp Neurol 57:218-225.

Genoud S, Pralong W, Riederer BM, Eder L, Catsicas S, Muller D (1999) Activity-dependent phosphorylation of SNAP-25 in hippocampal organotypic cultures. J Neurochem 72:1699-1706.

Gottschall PE, Yuan W, Muffly BG (2003) Attenuated Proteoglycanase activity in Alzheimer's Disease hippocampus: Associated with diminished synaptic density and inhibition of activity by abeta-amyloid. In: Society for Neuroscience. New Orleans, Louisiana: Abstarct Viewer / Itinerary Planner.

Haddock G, Cross AK, Plumb J, Surr J, Buttle DJ, Bunning RA, Woodroofe MN (2006) Expression of ADAMTS-1, -4, -5 and TIMP-3 in normal and multiple sclerosis CNS white matter. Mult Scler 12:386-396.

Hardy J (2002) Testing times for the "amyloid cascade hypothesis". Neurobiol Aging 23:1073-1074.

Hsiao K, Chapman P, Nilsen S, Eckman C, Harigaya Y, Younkin S, Yang F, Cole G (1996) Correlative memory deficits, Abeta elevation, and amyloid plaques in transgenic mice. Science 274:99-102.

Irizarry MC, McNamara M, Fedorchak K, Hsiao K, Hyman BT (1997) APPSw transgenic mice develop age-related A beta deposits and neuropil abnormalities, but no neuronal loss in CA1. J Neuropathol Exp Neurol 56:965-973.

Ishibashi K, Tomiyama T, Nishitsuji K, Hara M, Mori H (2006) Absence of synaptophysin near cortical neurons containing oligomer Abeta in Alzheimer's disease brain. J Neurosci Res 84:632-636.

Jourquin J, Tremblay E, Decanis N, Charton G, Hanessian S, Chollet AM, Le Diguardher T, Khrestchatisky M, Rivera S (2003) Neuronal activity-dependent increase of net matrix metalloproteinase activity is associated with MMP-9 neurotoxicity after kainate. Eur J Neurosci 18:1507-1517.

King DL, Arendash GW (2002) Maintained synaptophysin immunoreactivity in Tg2576 transgenic mice during aging: correlations with cognitive impairment. Brain Res 926:58-68.

Koo EH, Sisodia SS, Archer DR, Martin LJ, Weidemann A, Beyreuther K, Fischer P, Masters CL, Price DL (1990) Precursor of amyloid protein in Alzheimer disease undergoes fast anterograde axonal transport. Proc Natl Acad Sci U S A 87:1561-1565.

Kuno K, Okada Y, Kawashima H, Nakamura H, Miyasaka M, Ohno H, Matsushima K (2000) ADAMTS-1 cleaves a cartilage proteoglycan, aggrecan. FEBS Lett 478:241-245.

Lassmann H, Fischer P, Jellinger K (1993) Synaptic pathology of Alzheimer's disease. Ann N Y Acad Sci 695:59-64.

Lazarov O, Lee M, Peterson DA, Sisodia SS (2002) Evidence that synaptically released beta-amyloid accumulates as extracellular deposits in the hippocampus of transgenic mice. J Neurosci 22:9785-9793.

Lemons ML, Sandy JD, Anderson DK, Howland DR (2001) Intact aggrecan and fragments generated by both aggrecanse and metalloproteinase-like activities are present in the developing and adult rat spinal cord and their relative abundance is altered by injury. J Neurosci 21:4772-4781.

Levicar N, Nuttall RK, Lah TT (2003) Proteases in brain tumour progression. Acta Neurochir (Wien) 145:825-838.

Mayer J, Hamel MG, Gottschall PE (2005) Evidence for proteolytic cleavage of brevican by the ADAMTSs in the dentate gyrus after excitotoxic lesion of the mouse entorhinal cortex. BMC Neurosci 6:52.

Mehta PP, Battenberg E, Wilson MC (1996) SNAP-25 and synaptotagmin involvement in the final Ca(2+)-dependent triggering of neurotransmitter exocytosis. Proc Natl Acad Sci U S A 93:10471-10476.

Morgenstern DA, Asher RA, Fawcett JW (2002) Chondroitin sulphate proteoglycans in the CNS injury response. Prog Brain Res 137:313-332.

Murakami T, Murakami S, Fuyama Y, Taguchi T, Ohtsuka A (2001) The extracellular matrix in the mature brain: its reactions to endo-alpha-N-acetylgalactosaminidase and collagenase. Ital J Anat Embryol 106:475-480.

Murakami T, Ohtsuka A, Su WD, Taguchi T, Oohashi T, Murakami T, Abe K, Ninomiya Y (1999) The extracellular matrix in the mouse brain: its reactions to endo-alpha-N-acetylgalactosaminidase and certain other enzymes. Arch Histol Cytol 62:273-281.

Oakley RA, Tosney KW (1991) Peanut agglutinin and chondroitin-6-sulfate are molecular markers for tissues that act as barriers to axon advance in the avian embryo. Dev Biol 147:187-206.

Properzi F, Asher RA, Fawcett JW (2003) Chondroitin sulphate proteoglycans in the central nervous system: changes and synthesis after injury. Biochem Soc Trans 31:335-336.

Roberts LA, Morris BJ, O'Shaughnessy CT (1998) Involvement of two isoforms of SNAP-25 in the expression of long-term potentiation in the rat hippocampus. Neuroreport 9:33-36.

Rolls ET (1995) Learning mechanisms in the temporal lobe visual cortex. Behav Brain Res 66:177-185.

Rosenberg GA (2002) Matrix metalloproteinases and neuroinflammation in multiple sclerosis. Neuroscientist 8:586-595.

Russell DL, Doyle KM, Ochsner SA, Sandy JD, Richards JS (2003) Processing and localization of ADAMTS-1 and proteolytic cleavage of versican during cumulus matrix expansion and ovulation. J Biol Chem 278:42330-42339.

Sandy JD, Westling J, Kenagy RD, Iruela-Arispe ML, Verscharen C, Rodriguez-Mazaneque JC, Zimmermann DR, Lemire JM, Fischer JW, Wight TN, Clowes AW (2001) Versican V1 proteolysis in human aorta in vivo occurs at the Glu441-Ala442 bond, a site that is cleaved by recombinant ADAMTS-1 and ADAMTS-4. J Biol Chem 276:13372-13378.

Sheng JG, Price DL, Koliatsos VE (2003) The beta-amyloid-related proteins presenilin 1 and BACE1 are axonally transported to nerve terminals in the brain. Exp Neurol 184:1053-1057.

Shimohama S, Kamiya S, Taniguchi T, Akagawa K, Kimura J (1997) Differential involvement of synaptic vesicle and presynaptic plasma membrane proteins in Alzheimer's disease. Biochem Biophys Res Commun 236:239-242.

Snow DM, Lemmon V, Carrino DA, Caplan AI, Silver J (1990) Sulfated proteoglycans in astroglial barriers inhibit neurite outgrowth in vitro. Exp Neurol 109:111-130.

Squire LR, Zola SM (1996) Memory, memory impairment, and the medial temporal lobe. Cold Spring Harb Symp Quant Biol 61:185-195.

Szklarczyk A, Lapinska J, Rylski M, McKay RD, Kaczmarek L (2002) Matrix metalloproteinase-9 undergoes expression and activation during dendritic remodeling in adult hippocampus. J Neurosci 22:920-930.

Terai K, Iwai A, Kawabata S, Tasaki Y, Watanabe T, Miyata K, Yamaguchi T (2001) beta-amyloid deposits in transgenic mice expressing human beta-amyloid precursor protein have the same characteristics as those in Alzheimer's disease. Neuroscience 104:299-310.

van Horssen J, Kleinnijenhuis J, Maass CN, Rensink AA, Otte-Holler I, David G, van den Heuvel LP, Wesseling P, de Waal RM, Verbeek MM (2002) Accumulation of heparan sulfate proteoglycans in cerebellar senile plaques. Neurobiol Aging 23:537-545.

Washbourne P, Thompson PM, Carta M, Costa ET, Mathews JR, Lopez-Bendito G, Molnar Z, Becher MW, Valenzuela CF, Partridge LD, Wilson MC (2002) Genetic ablation of the t-SNARE SNAP-25 distinguishes mechanisms of neuroexocytosis. Nat Neurosci 5:19-26.

Wilson MC, Mehta PP, Hess EJ (1996) SNAP-25, enSNAREd in neurotransmission and regulation of behaviour. Biochem Soc Trans 24:670-676.

Yamaguchi Y (2000a) Lecticans: organizers of the brain extracellular matrix. Cell Mol Life Sci 57:276-289.

Yamaguchi Y (2000b) Lecticans: organizers of brain extracellular matrix. Cell Mol Life Sci 57:276-289.

Yin KJ, Cirrito JR, Yan P, Hu X, Xiao Q, Pan X, Bateman R, Song H, Hsu FF, Turk J, Xu J, Hsu CY, Mills JC, Holtzman DM, Lee JM (2006) Matrix metalloproteinases expressed by astrocytes mediate extracellular amyloid-beta peptide catabolism. J Neurosci 26:10939-10948.

Yuan W, Matthews RT, Sandy JD, Gottschall PE (2002) Association between protease-specific proteolytic cleavage of brevican and synaptic loss in the dentate gyrus of kainate-treated rats. Neuroscience 114:1091-1101.

Zhang JW, Deb S, Gottschall PE (2000) Regional and age-related expression of gelatinases in the brains of young and old rats after treatment with kainic acid. Neurosci Lett 295:9-12.

ABOUT THE AUTHOR

Joanne Mayer received her Bachelor of Science degree in Cell and Molecular Biology at the University of Florida in 2000. Upon completion of her undergraduate degree, Joanne worked under Dr. Marieta B. Heaton at the McKnight Brain Institute at the University of Florida, studying the molecular mechanisms underlying the nervous system anomalies produced by developmental alcohol exposure, which can lead to the fetal alcohol syndrome. After entering the graduate program in 2002, Joanne received her Master of Science degree in pharmacology from the University of South Florida in 2004 and has worked under the tutelage of Dr. Paul E. Gottschall investigating how insoluble substrates of the extracellular matrix of the nervous system influence neural plasticity *in vivo*. She successfully defended her doctoral dissertation in March of 2007 at the University of South Florida.